Electroabsorption measurements of conjugated organic materials

Pomfret, Stephen J.

Electroabsorption Measurements of Conjugated Organic Materials

by

Stephen J. Pomfret

A thesis submitted to the Faculty of Science,
Durham University, For the degree of Doctor of Philosophy.

Department of Physics,
University of Durham,
November 1995.

Electroabsorption Measurements of Conjugated Organic Materials

Stephen John Pomfret: Submitted for degree of PhD, 1995

Abstract

This thesis reports the results of electroabsorption measurements undertaken on three materials that are all, to some degree, conjugated: polymeric and oligomeric emeraldine base, and polysquaraine. The aim of these experiments has been to investigate the nature of the optical excitations occuring within the materials.

Electroabsorption (EA) spectroscopy involves the measurement of the change in absorption coefficient of a material with the application of an external field. The fields required are high and the resulting signals small, hence to perform such experiments a dedicated spectrometer was constructed. To achieve high sensitivity lock-in amplification techniques were used, and the sample kept at low temperatures. Such techniques resulted in the spectrometer being able to resolve changes in absorption of the order 1 in $5x10^7$.

The sample configuration consisted of thin films of the materials which were spun coated onto sapphire substrates, with interdigitated gold electrodes deposited on top. This configuration allowed the absorption of the material to be measured while alternating fields of up to 200 $kVcm^{-1}$ were applied.

The EA data of the oligomeric and polymeric emeraldine base are seen to closely resemble each other - indicating that the same photoexcitation processes are occurring. Using existing theories the spatial extent of the 2 eV excitation is calculated as ~0.4 nm, i.e. greater than one phenyl ring repeat unit. This is consistent with previously suggested models of 2 eV photoexcitation in emeraldine base. Similar calculations suggest a spatial extent of the 4 eV transition of ~0.25 nm, i.e. restricted to one phenyl ring. A feature in the EA spectra of the oligomeric emeraldine base has been observed at 1.35 eV - below the onset of linear absorption, and it is suggested that this may be evidence of a normally one photon forbidden transition becoming allowed in the presence of an external field.

Due to the fully conjugated nature of polysquaraine a different model has been used to interpret the EA spectrum. An energy level scheme for the material is suggested, including the possible location of a normally one photon forbidden transition at 1.75 eV.

Declaration

The material contained in this thesis has not been submitted for the examination for any other degree, or part thereof at the University of Durham or any other institution. The material contained in this thesis is the work of the author except where formally acknowledged by reference.

Acknowledgements

I would like to thank Dr. Andy Monkman for arranging this project, and for the patience and encouragement he has shown in the past few years.

Thanks to BICC and the DRA for being generous with both time and equipment.

Norman and Davey deserve a special mention for generally showing me the ropes, and keeping the whole system well oiled.

Thanks are also due to all the members of the workshops - both in physics and engineering - without whom all the gadgets, thingumies and whadyamacallits would never have been conjoured into existance.

Without the materials synthesised by Dr. Phil Adams and Dr. Eymard Rebourt there would have been nothing for me to study - thank you. Special thanks to Phil 'the chemist' for being patient with a physicist.

Thanks also go to my Mum and Dad who have always supported me. The biggest thanks of all go to Debbie, who has been with me through the bleakest of times - and generally put up with me being a pain in the butt.

Dedication

To Mr. Gregory the Surgeon

and

Sandra the Physio

Contents

Chapter 1

Introduction

Much attention is being focused upon the physical properties of conjugated polymers. A combination of unusual optical and electrical properties combined with ease of manufacture and processability has ensured that both academic and industrial institutions have realised the wealth of possible applications of such materials. Apart from the much publicised polymer LEDs, there have been advances in the use of polymers for electrical shielding, optical third harmonic generation, rechargeable batteries and gas sensing applications.

This thesis concentrates on the optical properties of three materials - polymeric and oligomeric emeraldine base, and polysquaraine. It describes the investigation of electroabsorption responses in thin films of these materials. Electroabsorption spectroscopy is the study of the change in absorption coefficient under the application of an external field. The fields required to cause measurable perturbations in such systems are large - of the order of 100 $kVcm^{-1}$ - and even with such large fields the resulting perturbations are small. The combination of the requirements of high voltages and the detection of small signals meant that a dedicated spectrometer had to be designed and constructed.

From the data acquired from such experiments certain theories may be employed to deduce information about the nature of the photoexcited states of materials.

Chapter two gives a brief overview of the basic concepts of the field of conjugated polymers. Initially it concentrates on the simplest of π-conjugated

polymers - polyacetylene. Due to its relative simplicity it has been extensively theoretically modelled in an effort to understand the mechanisms involved in optical and electrical excitations within the material. Many of these models, however, are based on a 'perfect' system, neglecting the effects of disorder and chemical impurities. Later work has shown that the effects of disorder may, in fact, be dominant in certain polymeric systems. Such effects are discussed, including the suggestion that excitons may be the dominant photoexcited species in a large group of polymers.

Chapter three introduces the concept of electroabsorption spectroscopy. It begins with a brief history of the use of the technique, from its first use with inorganic materials to its modern-day use with organics. Various theories are presented as to the origin of the variation in absorption coefficient, and as to the information that can be gained from its interpretation.

Chapter four contains a review of the relevant previous research undertaken on the materials investigated in this thesis. Due to the fact that the polyaniline family of polymers (of which emeraldine base is a member) was first synthesised over 100 years ago, this material has been extensively studied - especially so in the last fifteen years, during which interest in conjugated polymers has blossomed. Theoretical modelling of any polymer is a large task, hence most approaches to modelling concentrate on extrapolating results of calculations on oligomers. This has been the case for the semi-conjugated polymer emeraldine base, with four and five ring repeat unit oligomers being used to model the polymer. A phenyl capped oligomer of emeraldine base has been included in these electroabsorption studies so that the results can be compared with those of the polymer, and in doing so see if such theoretical extrapolation techniques are valid for this material.

Polysquaraine, however, is a relatively new material, having been specifically designed and synthesised with the aim of producing a fully conjugated polymer with a low energy optical band gap. Chapter 4 contains a brief description of the theory

behind its production, and a review of its characterisation. Comparisons are drawn between emeraldine base and polysquaraine.

Chapter five describes the experimental techniques involved in the measurement of the electroabsorption response of these materials. Firstly, a brief explanation of the chemical synthesis of the materials is given, followed by a desription of the method of sample preparation. The design and construction of the electroabsorption spectrometer is explained. The small size of the signal being measured necessitated the use of lock in amplification techniques, along with many other noise reduction methods. The interpretation of electroabsorption data requires knowledge of the absorption coefficient spectrum of each material - the method of acquisition of this data is included in this chapter.

The results are presented and discussed in chapter 6. The theories presented in chapter 3 are used to interpret the data, with the choice of approach being governed by the suggested nature of the photoexcited states of the material - as discussed in chapter 4. The electroabsorption response of the polymeric and oligomeric emeraldine base are compared and contrasted, followed by a discussion of the results for polysquaraine.

Finally, a summary of the thesis is given in chapter 7.

Chapter 2

An Introduction To Some Relevant Concepts.

This chapter aims to put the work of this thesis in perspective in relation to the ever broadening field of organic electroactive materials. It begins with the simplest model compound of its type, *trans*-polyacetylene, with the purpose of describing the basic concepts of energy levels and optical transitions within a π-conjugated molecule. The following sections broaden these ideas to encompass more complicated systems, and introduce the deviation from idealised models caused by disorder.

2.1 *Trans*-polyacetylene - a Model Compound

Trans-polyacetylene is a fully π-conjugated polymer with an idealised chemical structure of the form shown in Fig. 2.1a. Three other structures shown are the other possible configurations of the polymer, of which *cis-cisoidal* (d) is considered unstable due to steric considerations.

The term 'π-conjugation' refers to the delocalisation of electrons along a chain of atoms arising from the nature of covalent bonding between them. Polyacetylene (PA), like most of the polymers of interest to physicists, comprises of a polymer backbone of purely carbon atoms. The configuration of the electrons in the outer shell of a carbon atom is s_1p_3. Mixing of these orbitals can form four sp_3 hybrids, allowing carbon to form four covalent bonds - bonds of this type are termed 'single' bonds, or alternativley 'sigma' (σ) bonds. If, however, three electrons form

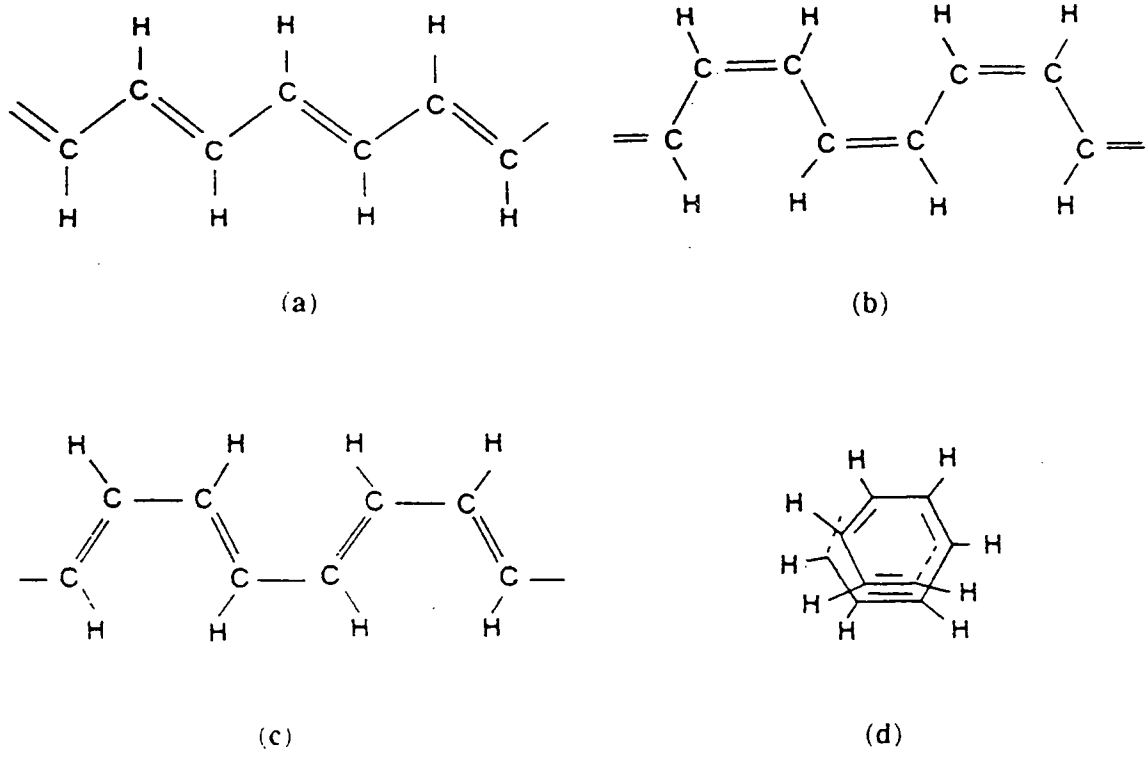

Fig. 2.1 Isomers of Polyacetylene, a) *trans-transoidal,* b) *cis-transoidal,* c) *trans-cisoidal,* d) *cis-cisoidal.* (after Yu[1]).

sp_2 hybridised states, then one p orbital remains unhybridised, and is termed a p_Z orbital. This is the configuration of the electrons in the outer shell of the carbon atoms in polyacetylene. The three sp_2 orbitals lie in a plane, each separated by 120°. Two of these form σ bonds with neighbouring carbon atoms, and the third forms a σ bond with a hydrogen atom, leaving the p_Z orbital at 90° to this plane, extending above and below. With the carbon atoms being so close to each other the p_Z orbitals of neighbouring atoms overlap forming another bond 'above' and 'below' the σ bond. This bond is termed a 'pi (π)' bond, and collectivley a σ and a π bond make a carbon 'double' bond, a schematic of which is shown in Fig.2.2. When many carbon atoms with this electronic configuration bond together the π bonding may become extended along the chain and the system is said to be π-conjugated (often just 'conjugated').

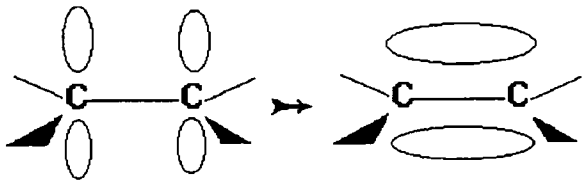

Fig.2.2 p_Z overlap to form a π-bond

Within such double bonds the σ bonds may be considered as simple harmonic oscillators (springs) joining the atoms, with the π electrons merely encompasing the system. Su, Schrieffer and Heeger [2, 3] devised a Hamiltonian describing such a system, having three separate contributions arising from π-electron interactions, electron phonon interactions, and phonons. This Hamiltonian has the form

$$H = H_{\pi} + H_{\pi-ph} + H_{ph}$$

and is termed the SSH (Su-Schreiffer-Heeger) Hamiltonian. It is used to describe how the distortion of the *trans*-polyacetylene chain away from its regular herring bone ground state geometry effects electronic properties. In the undistorted structure the CH units would be spaced at regular intervals 'a', measured parallel to the chain direction, so that the actual bond length would be $2a/\sqrt{3}$ (assuming 120° bond angles). The distortion is expressed in terms of the set of displacement parameters $\{u_n\}$, where u_n is the displacement of the n^{th} (CH) unit, again measured parallel to the chain direction. This situation is depicted in Fig.2.3.

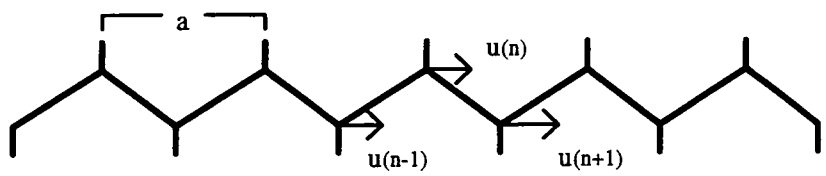

Fig. 2.3 Displacement parameter u as defined for *trans*-PA

In the SSH Hamiltonian

$$H_{\pi} = -t_0 \sum_{n,s} (c^{*}_{n+1,s} c_{n,s} + c^{*}_{n,s} c_{n+1,s})$$

with t_0 being the 'resonance' or 'transfer' integral of the undistorted lattice - it is a measure of the amount of overlap of neighbouring π-electron wavefunctions. $c^{*}_{n,s}$ and $c_{n,s}$ are respectively the creation and annihilation operators for π-electrons at

site n with spin s (=±1/2), hence this term describes the hopping of electrons from site n to n±1.

$$H_{\pi-ph} = \alpha \sum_{n,s} (u_{n+1} - u_n)(c^*_{n+1,s} c_{n.s} + c^*_{n,s} c_{n+1,s})$$

where α is a constant relating to the strength of the electron-phonon coupling (this is an approximation only valid for small u_n).

$$H_{ph} = \frac{K}{2} \sum_n (u_{n+1} - u_n)^2 + \frac{1}{2M} \sum_n p_n^2$$

where K is the lattice force constant, p_n is the momentum of the n^{th} (CH) unit and M is the mass of the (CH) unit [3]. The importance of this description of the electronic states in a conjugated system is that it implies a very strong correlation between the electronic and the physical configurations of the molecule, i.e. an extremely strong electron-phonon coupled system.

The most serious approximation of this model is the non-explicit treatment of Coulomb interactions between the π-electrons. Despite this seemingly large assumption, the model does result in some interesting predictions of the nature of the excited states in *trans*-PA. Only a brief outline of these calculations will be included here - there are many detailed reviews of their work to be found in the literature [4, 5].

At first sight the bond lengths between carbon atoms along a perfect PA backbone would be assumed to be all of equal length, with the π-electrons distributed evenly along the length of the chain. With further consideration, however, it emerges that a dimerisation of bond lengths enables a reduction of the

total energy of the electrons [2, 3] Direct evidence of this dimerisation has been observed using X-ray diffraction [6] and NMR [7] studies. This dimerisation is analogous to the Peierls instability for one dimensional metals, in which a static lattice deformation opens up a band gap at the Fermi level [8]. The conjugated π-electron band in the PA backbone is half filled (according to the Pauli exclusion principle - each p_z orbital contains only one of a possible two electrons: one spin up, one spin down). In the un-dimerised form *trans*-PA would therefore be a metal, having a finite density of states at the Fermi energy. This configuration is unstable with respect to a dimerised lattice, since the total energy of the occupied band states in the dimerised form is reduced by the presence of the band gap. A diagram depicting the manner in which energy can be reduced upon dimerisation is shown in Fig.2.4. The semi-conducting nature of *trans*-PA has been noted experimentally by Shirikawa [9], with optical absorption spectroscopy [10-12] and photoconductivity [13] measurements revealing a band gap of ~1.4-1.5 eV.

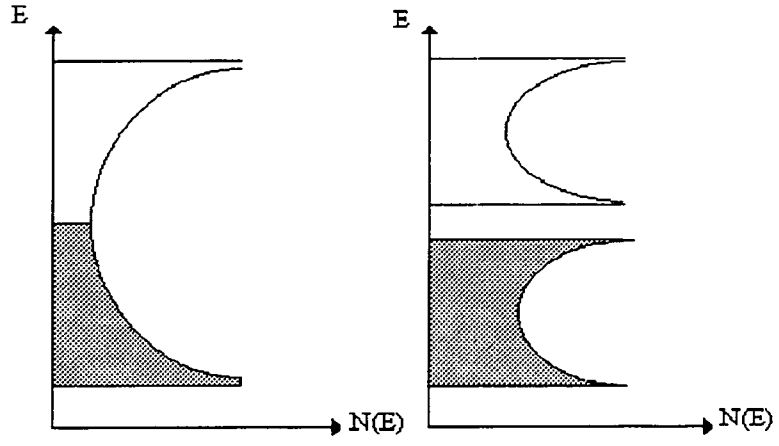

Fig.2.4 Peierls distortion of a half filled band. Left - showing electron occupation of un-dimerised lattice, and right - showing formation of band gap to reduce total energy of system.

The energy decrease available from such a distortion has been predicted to be dependent upon the number of repeat units in the conjugated system - i.e. the chain length of an ideal system. The value of band gap should therefore be observed to decrease with increasing length of polymer chain - especially when starting from short chain oligomers, as the value of the band gap is highly dependent upon chain length for short chain lengths. Such a phenomena has been observed experimentally by Hudson [14] and Brassett [15].

2.1.1 Bond Alternation Defects

If a chain has an odd number of carbon atoms, then, in order to satisfy boundary conditions, a bond alternation defect must occur somewhere along the chain. This takes the form of an antibonding p_Z orbital, and is often depicted in the form shown in Fig.2.5.

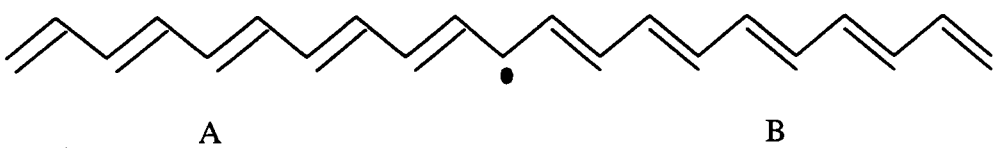

Fig.2.5 Bond alternation defect on a *trans*-PA chain

The defect separates two phases of the polymer, depicted as phase A and phase B. The only difference between the two ground state phases is the sense of the alternation of the double and single bonds, and as such they are degenerate in energy. Due to this degeneracy in energy there is no preference as to the position of the defect (provided it is not near a chain termination), and the defect is free to move along the chain. A useful way of representing this structure of the chain is

through the introduction of an order parameter ϕ_n defined by $\phi_n = (-1)^n\left(u_n/u_0\right)$, where u_0 is the amplitude of dislacement in the ground state. The two degenerate ground states then correspond to ϕ_n=-1 or +1 for all n. This order parameter is useful when visualising the processes involved during photoexcitations, as will be seen later.

The representation of the defect in Fig.2.5 is, in fact, rather simplistic. It depicts the defect as occuring on one site - phase A changing to phase B over the space of just one carbon atom. Calculations have shown [2, 3] that the phase change extends over approximatley 14 bonds, having a form more like that depicted in Fig.2.6. This defect/ phase change/kink is known as a 'soliton'.

Fig.2.6 A soliton as an extended state

Fig.2.7 shows where a soliton is predicted to lie within the band energy structure of *trans*-PA - half way between the valence and conduction bands [2, 3]. The neutral soliton contains one electron (the antibonding p_Z electron) and hence has spin 1/2. This spin-charge relationship is unusual, since usually only charged entities have spin.

Non-topological excitations that do not involve the reversal of bond alternation are also possible and are termed polarons. If on one chain a soliton changes the sense of bond alternation from A to B, then another soliton on the same chain that reverses this, and changes B to A, is termed an antisoliton. A polaron is effectively a bound soliton-antisoliton pair. The creation of a polaron depletes the

valence and conduction bands by one whole state each, creating two localised states symmetrically split about midgap, each being able to accomodate two electrons due

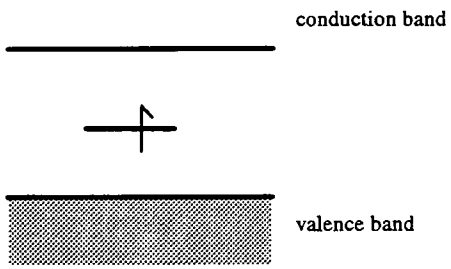

Fig.2.7 Location of soliton level in semi-conductor band picture

to spin degeneracy [16, 17]. Fig.2.8 shows the electronic structure of the positive polaron P^+. It should be noted that polaronic states obey the conventional spin-charge relationships.

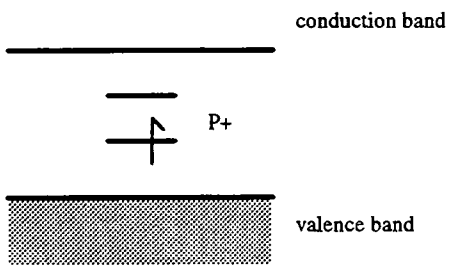

Fig.2.8 Location of a polaron level in the semi-conductor band picture

2.1.2 Photoexcitations in *trans*-polyacetylene

According to the Born-Oppenheimer approximation, the difference between the masses of electrons and nuclei is such that the two systems may be treated independently of one another. This leads to the Franck-Condon principle of electronic transitions, where it is assumed that such transitions occur so rapidly that

the nuclei can be assumed static. Thus, in *trans*-PA, when an electron is photoexcited it has been proposed that an electron-hole pair is produced in a perfectly dimerised lattice. After the photoproduction of the pair the lattice responds to the new electronic state by deforming to a more energetically favourable conformation, producing a soliton-antisoliton pair at mid gap [2, 3].

Numerical integrations of the SSH Hamiltonian for *trans*-PA have been performed by Su and Schrieffer [2, 3] which demonstrate how an electron-hole pair can generate such a soliton-antisoliton pair. A schematic of the process is shown in Fig.2.9: the left hand side of the diagram shows the response of the 1D lattice in terms of the order parameter ϕ_n, and the right hand side shows the corresponding changes in the spectrum of electronic levels. The first stage of the process is the promotion of an electron to the lowest unoccupied state at time t=0. If ϕ_n=+1 is the initial ground state, then within a single vibrational period (~ 10^{-13}s) the lattice deforms adiabatically, and simultaneously a pair of electronic states split off symmetrically from the valence and conduction bands. At times large compared with the vibrational period the localised defect develops into a charged soliton-antisoliton pair and the pair of electronic states, now at mid gap, become spatially localised at the instantaneous positions of the separating solitons. The calculations of Ball [18] show that the symmetry of the Hamiltonian forbids the production of a pair of neutral solitons.

So far the processes described have only involved the 1D case of single PA chains. Most systems, however, consist of many chains closely packed together allowing interactions between chains. If these interactions are sufficiently large it is possible for inter-chain photoexcitations to occur resulting in the electron and the hole being located on different chains. Su and Schrieffer [20] have demonstrated how an individual electron or hole could produce a polaron; a schematic of the process is shown in Fig.2.10. At time t=0 a single electron is added to a neutral

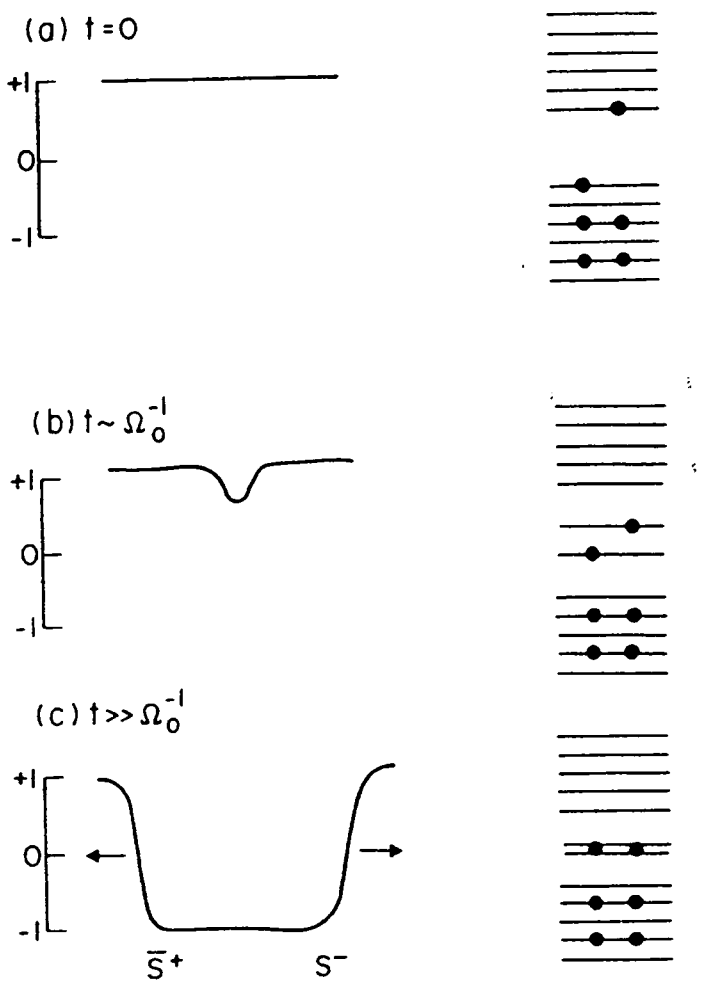

Fig. 2.9 Intra-chain photogeneration of spinless, charged solitons, a) at time t=0, b) $t \sim \Omega^{-1}$ (i.e. duration of vibration of lattice) and c) $t >> \Omega^{-1}$ - showing energy levels splitting from conduction and valence bands to form soliton state mid-gap. (after Orenstein [19]).

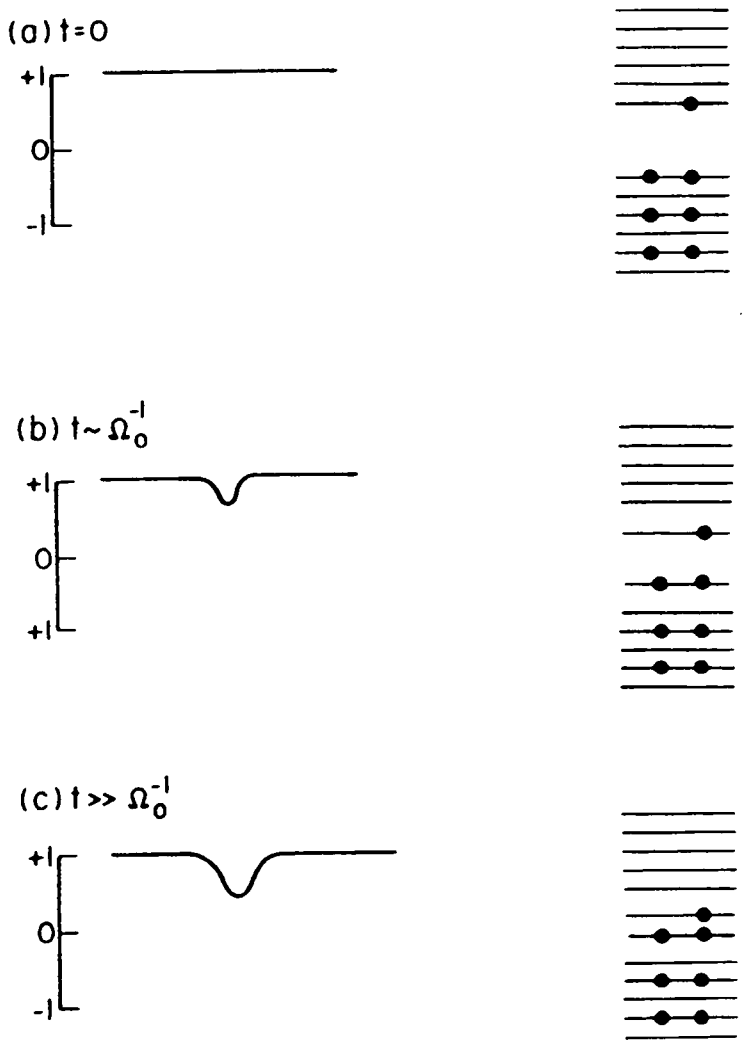

Fig. 2.10 Inter-chain photogeneration of polarons at times a) t=0, b) $t\sim\Omega^{-1}$, and c) $t>>\Omega^{-1}$, showing energy levels splitting off from conduction and valence bands to form level at mid-gap. (after Orenstein [19]).

trans-PA chain, and the lattice distorts in much the same way as before. In this case, however, a polaron is more energetically stable than a soliton-antisoliton pair. Thus inter-chain photoexcitation is expected to initially produce polarons.

Upon photoexcitation of such states, new optical transitions involving energies less than that of the band gap should become allowed. The new transitions that should theoretically become allowed after the photoexcitation of the various types of solitons and polarons are depicted in Fig.2.11. Such transitions have been observed [21-23] using the experimental technique of photoinduced absorption (PIA). This technique involves photoexciting a material at (or close to) its optical band gap (~ 1.4 eV for *trans*-PA), then using a second, variable wavelength light source to probe for new absorption features created by the initial photoexcitation. The interesting feature of these PIA studies is that although sub-band features were observed, they were not at mid gap (~0.7 eV), but rather two feactures, one at

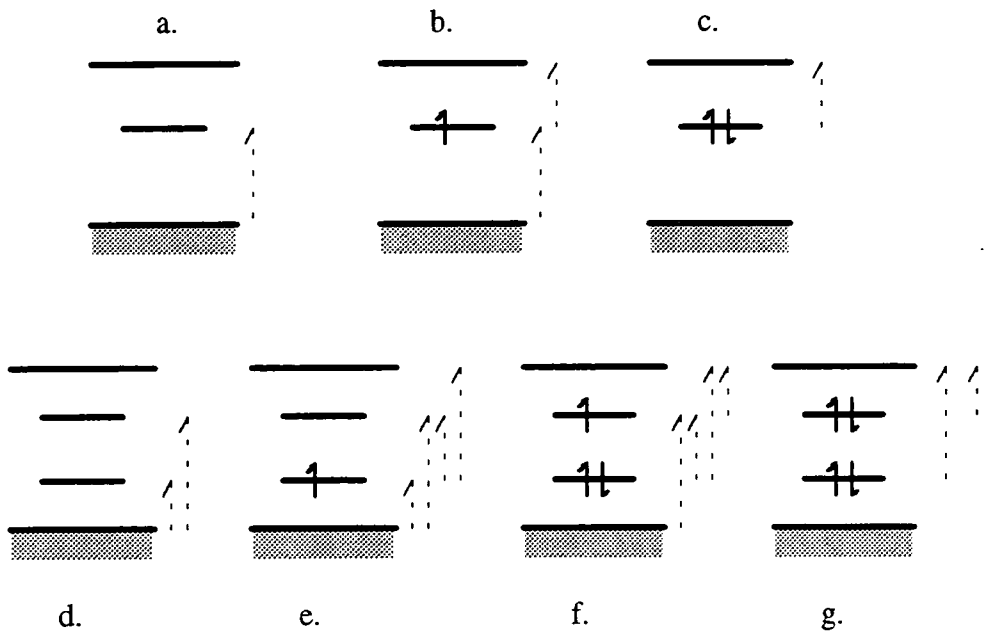

Fig.2.11 Schematic diagram of the possible optical transitions associated with positive, neutral and negative solitons (a, b, and c), positive bipolarons and polarons (d and e), and negative polarons and bipolarons (f and g).

0.45 eV and one at 1.35 eV [19, 22]. These two feactures have been assigned to charged and neutral solitons, respectively. The deviation of their positions away from mid gap has been attributed to the neglect of Coulomb interactions in the original SSH Hamiltonian, a topic which will be discussed later in this chapter.

The technique of photoinduced absorption is a very powerful experimental tool for probing the energy levels of excited states of a system, and has been used extensively with organic systems (see chapt. 4 for example). The time resolution of these experiments can also reveal important information about the material in question. Most PIA experiments involve the chopping of the pump beam with an optical chopper at frequencies around 100 Hz. This is slow in comparison with the excitation processes occuring within the system and is hence considered 'steady state' PIA - only observing the excited states well after the excitation process has occured. It is possible to perform time resolved PIA experiments, using a pulsed laser as the both pump and probe. This method allows investigation of the photoexcitation dynamics on a picosecond or femtosecond time scale. In this manner Shank *et al.* [24] revealed that the 1.35 eV photoexcitations in *trans*-PA are intrinsic to the polymer chains, rather than the possible alternative of the photoexcitations only occuring at defect sites.

2.2 Coulomb Interactions

The main assumption of the SSH model is the neglect of Coulomb interactions within the system. There have been many attempts to develop rigorous models including such interactions [4, 5] in an effort to account for the experimentally observed deviations from the predictions of the simple SSH model. These calculations agree on the dimerisation of *trans*-PA, and that solitons and polarons may be photoexcited within the material - though the energies predicted for

these states differ from those when Coulomb interactions are not included. Coulomb interactions are introduced into the SSH model as perturbations, and as pointed out by Campbell *et al.*, [25] the validity of treating such large effects as perturbations is dubious, and the debate looks set to continue [26-28].

If the Coulombic interactions in a system are large, then upon photoexcitation a bound electron-hole pair may be formed rather than the completely dissociated entity predicted in the SSH model. Such a pair is termed an exciton, and has an energy below that of the conduction band in the system - the energy reduction being due to the attractive Coulomb force between the electron and the hole. Excitons, unless trapped, are considered free to move through the system and hence transport energy; their movement does not result in the transport of charge as an exciton is electrically neutral. All excitons are unstable with respect to the ultimate recombination process in which the electron drops back into the hole.

There is abundant evidence that exciton formation is the primary photoexcitation in an important group of polymers, the polydiacetylenes (PDAs) [29, 30]. PDAs may be considered as a fully π-conjugated class of polymers, having the general form shown in Fig.2.12. They can be polymerised from monomer to

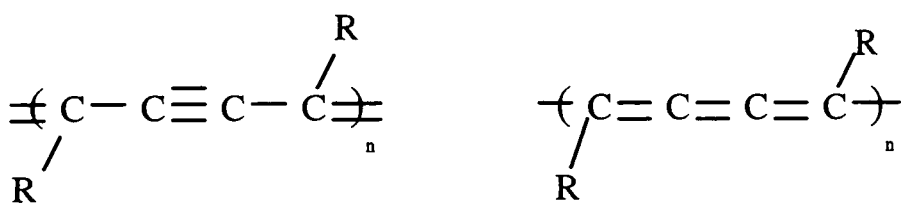

a. b.

Fig.2.12 The two general forms of polydiacetylene, a) acetylene form, b) butadiene form.

polymer while in the crystalline form (solid state polymerisation), resulting in the formation of a highly ordered conjugated polymer system. This alone makes PDAs very important, as it allows the study of conjugated systems relatively free from disorder. The electronic structure of PDAs, as investigated using electroabsorption techniques, will be discussed further in chapter 3. The various types of excitons and their related properties will be dicussed in more detail in the section 2.5.

2.3 Disorder in Conjugated Polymers

The systems considered in the previous sections have been that of idealised polymer chains. No system, however, is completely free from some form of imperfection or discontinuity - chain terminations (ends), for instance, are always present.

There are many types of disorder, though they usually result in the same effect - a reduction of the effective length over which conjugation extends, termed the 'conjugation length'. Within a real polymer chain the following forms of disorder must be taken into consideration:

a) defects in chemical structure - such as chain terminations, crosslinkages, structural impurities [31].

b) variations in configuration - departures from the ideal geometrical structure involving the disruption of double or triple bonds. Since it involves a change in the electriconic structure of the system, it is considered to be a change in the chemical structure.

c) variations in conformation - departures from the ideal geometrical structure involving rotation about single bonds. This does not involve the breaking of bonds, and is hence considered to be a change in the physical state of the molecule. This type of disorder is often temperature dependent [32], such as the phenyl ring rotations in polyaniline [33] and *cis* and *trans* isomerism in polyacetylene. Rotation of bonds may change the orientation of p_z orbitals and hence the degree of π-electron delocalisation - and hence the conjugation length - may be affected.

The number of defects present in a system is obviously important, as the more defects, the shorter the effective conjugation length. In the case of a polymer with a high degree of disorder, the semi-conductor band picture may break down; the short conjugated segments being more appropriately modelled by molecular states. To this end Eckhardt [34] suggested that *trans*-PA should be treated as a collection of short conjugated units with the lowest optical excitation being excitonic, rather than solitonic in nature. The question of whether conjugated polymers are best described in terms of excitons or band states is discussed in the section 2.5.

2.4 Non-degenerate Ground State Polymers

Solitons can only occur in systems which have two ground state configurations that are degenerate in energy. This is true for *trans*-PA, but not for most other conjugated polymer systems. The more general case is that a polymer exists in its lowest energy configuration 'A', and any change in this configuration - for instance upon photoexcitation - leads to the polymer being in a higher energy configuration ,'B'. If, then, a photoexcitation occurred that produced a bond alternation with configation A on one side and B on the other, the defect would tend

to migrate along the chain so as to leave the whole chain in the lower energy configuration, A.

However, if two such excitations were to occur close to each other with the higher energy configuration, B, trapped in between them (ABA), then the overall excitation would be stable with respect to its position on the chain. This type of excitation has already been described in section 2.1.1 for *trans*-PA - a polaron. An example of the chemical structure suggested for such an excited state in a non-degenerate ground state polymer, (*p*-phenylene) (PPP), is shown in Fig.2.13.

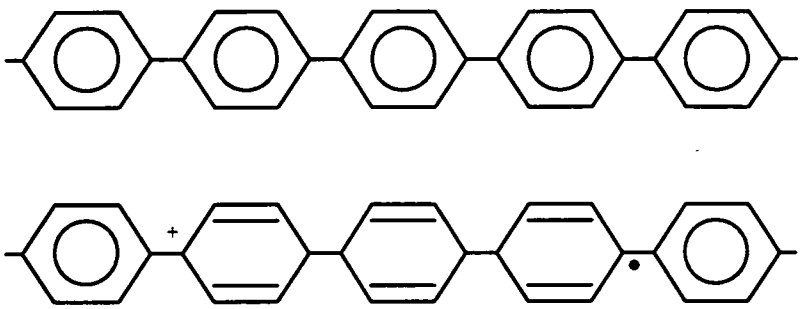

Fig.2.13 Schematic representation PPP (top), and of a positively charged polaron defect on a PPP chain (bottom) (after Chance, ref.[35]).

As for *trans*-PA, the formation of a polaron in a nondegenerate ground state system involves the raising of one energy level from the valence band and the lowering of one from the conduction band producing two levels within the band gap. These states may be located symmetrically about the mid-point of the gap, though the positions will differ for polymers with different symmetry.

2.5 Excitons in Organic Materials

Within previous sections *trans*-PA and other polymers have been described in terms of a semi-conductor band system using the SSH model. This model

neglects, amongst other things, electron-electron interactions - as pointed out in section 2.2. For some systems the inclusion of such interactions may result in excitons becoming the primary photoexcitations.

The SSH model requires a high degree of coupling between structural sub-units of the system. In systems where this is not the case the SSH model is not appropriate. In cases of weak intersite coupling a photoexcited electron will remain on the initial site of photoexcitation, bound to the resulting hole. Such a bound pair is termed a Frenkel exciton. The separation of the electron from the hole in such an exciton is small - less than the distance to the nearest neigbouring site, i.e. the interatomic distance in a normal crystal or the intermolecular distance in a molecular crystal. Such an exciton in a crystal lattice is depicted in Fig.2.14. The exciton may move through the system as a bound pair, transferring energy - but as with all excitons no charge is transferred. The electron in a Frenkel exciton may be considered as freely orbiting its respective hole, and as such the pair has no permanent dipole moment.

At the other extreme one can have excitons where the electron-hole separation distance is more than an order of magnitude larger than the site separation distance. This type of exciton is known as a Wannier (or sometimes Wannier-Mott) exciton, and is depicted in Fig.2.14. In such a situation the intervening medium between the electron and the hole may be approximated as a dielectric continuum, and hence the exciton can be seen as analogous to a large positronium atom. The Coulombic interaction between hole and electron is given by $-e/\varepsilon r$, (where r is the electron hole seperation distance) and optical transitions of such an excitation have been seen to resemble the Rydberg transitions in a hydrogen atom [36]. Such excitons occur mainly in inorganic systems where the interaction energy is great and the dielectric constant high. Even so, calculations by Bounds and

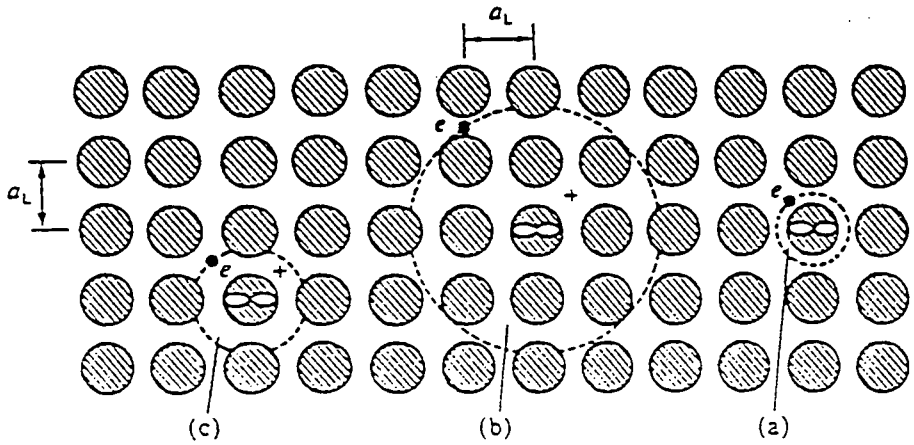

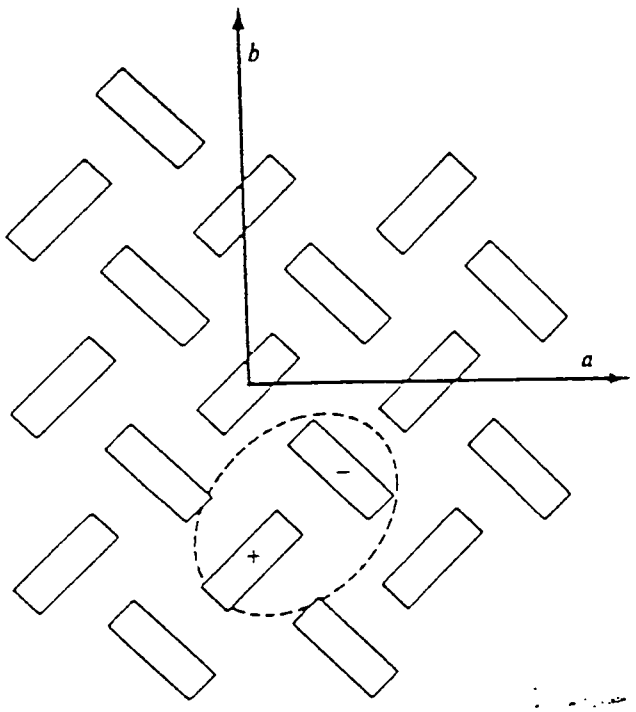

Top - Fig. 2.14 Schematic showing three types of exciton in a regular crystal with lattice spacing a_l, a) Frenkel exciton, b) Wannier exciton and c) charge transfer exciton (after Pope and Swenberg, ref[36]).

Bottom - Fig. 2.15 Schematic showing a charge transfer exciton as the lowest photoexcitation in crystalline anthracene.
(after Pope and Swenberg, ref[36]).

Siebrand [37] for the molecular crystal anthracene suggest that all but the lowest lying excited states in this organic material can be treated as Wannier excitons. Once again, with the electron freely orbiting the hole, these excitons have no permanent dipole moment.

Frenkel and Wannier excitons represent the two extremes with respect to charge separation distances within excitons. Between these two lies the intermediate case of the charge transfer (CT) exciton. The basic distinction of a CT exciton, as opposed to Frenkel and Wannier exciton, is that the electron is considered to be excited to a particular site rather than being free to 'orbit' the hole. This site is usually the nearest or next nearest neighbour. Such a transition results in a state with a permanent dipole moment being formed - as depicted in Fig.2.15 for the lowest photoexcitation in crystalline anthracene - in contrast to the non-polar Frenkel and Wannier excitons.

CT excitons occur mainly in heteromolecular structures such as charge transfer complexes, evidence of which is seen in, for instance, anthracene PMDA (pyromelitic dianlhydride). In such non-isotropic heteromolecular systems electron excitation is favoured from one constituent to the other (i.e. from donor to acceptor).

2.5.1 The Exciton Model of Conjugated Polymers

The question now arises as to which model should be used to desribe conjugated polymers; the semi-conductor band model or the exciton model. The problem is, as yet, unresolved.

Bassler *et al.* [28] have suggested that for a large group of conjugated polymer systems the semi-conductor band model is not appropriate. Instead, they suggest that the disorder inherent within most polymers shortened the conjugation length to such an extent that the SSH model breaks down. Instead of a semi-

conductor band model, the energy levels of the short conjugated chains are more appropriately described in terms of molecular states. Within these states the electron correlation effects are dominant over the electron-phonon interactions. To investigate the applicability of the exciton model to amorphous systems Bassler and co-workers investigated the conjugated polymer systems of poly(phenylphenylenevinylene) (PPPV) and poly(dodecylthiophene) (PDT). They use the results of absorption, luminescence, electroabsorption, and photoconductivity experiments for these materials to demonstrate that such a model is consistent with observed physical properties.

Firstly, a direct comparison is made between the absorption spectra of PPPV and related short chain oligomer compounds of varying chain length. The spectra indicate that the chromophores involved in the absorption process in PPPV are equivalent to oligomers containing around 10 repeat units. This implies that the average conjugation length within the polymer chain is only 10 repeat units long. Bassler *et al.* attribute this short conjugation length to disorder within the system - a similar proposition having been made by Eckhardt for *trans*-PA [34]. Since the size of the optical band gap depends upon conjugation length, the spread of conjugation lengths due to disorder causes the experimentally observed inhomogeneous broadening of the absorption peaks in the polymer. This broadening of absorption peaks in the polymer system compared to related short chain oligomers is observed for almost all conjugated organic systems, only being obscured when a more dominant broadening effect is present.

Bassler suggests that the absorption profile of such a system does not depict that of a semi-conductor band model, but more that of transitions to locally excited states of chromophores randomly distributed along the polymer chain. Further evidence to support this argument comes from the results of fluorescence

experiments [38-40], and the observed magnitude of the Stokes shift, as discussed below.

In a polymer system of the type suggested by Bassler [28], electronic coupling would exist between neighbouring sites on the chain and on neighbouring chains, allowing transfer of excited states through the system. It would be expected, therefore, that in a system of this kind the magnitude of the Stokes shift would be dependent upon the photoexcitation energy - for the following reason. If it is assumed that the coupling energy between sites allows transfer only to nearest neighbouring sites, then when an excitation occurs the excited state will migrate through the system until it reaches a site of minimum energy - all its neighbouring sites having higher energy values. It will be from this site that the excited state would radiatively recombine with energy ν_{loc} - this energy would be similar throughout the system. This being the case, photoexcited states of any energy above ν_{loc} should thermalise until they reach ν_{loc}, and then fluoresce with that energy. The Stokes shift - the difference between excitation energy and photoemitted energy - should therefore increase with increasing photoexcitation energy above ν_{loc}. For photoexcitations below ν_{loc} there should be no Stokes shift, since there is no method for non-radiative decay.

Such fluorescence experiments have been carried out for PPV [40], PPPV [38], and PDT [39], all had similar responses to that shown for PPV in Fig.2.16. In each case the emission energy is independent of the excitation energy as long as $\nu_{exc} \geq \nu_{loc}$. Below ν_{loc} the emission energy is dependent upon the excitation energy. ν_{loc} therefore indicates the energy threshold between states that participate in energy transport and those that do not.

This, however, is not conclusive proof that the system is excitonic, it merely indicates that the results are compatible with such a proposed model. The localisation energy ν_{loc} may also be interpreted as the energy that distinguishes

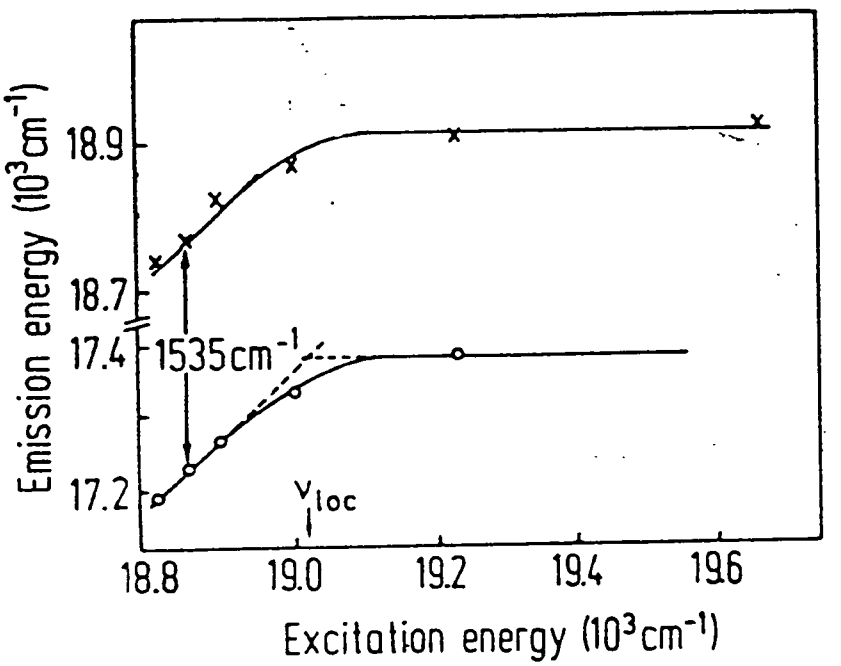

Fig. 2.16 Plot of emission vs. excitation energy for the 0-0 and 0-1 vibronic bands of a PPV film (after Bassler, ref[28]).

localised from delocalised states within a band model. More evidence is needed for the excitonic argument to be convincing - Bassler *et al.* [28] use the results of electroabsorption studies on thin films of the polymer as evidence that the systems are, indeed, excitonic in nature. As will be described in chapter 3, there are several ways to interpret the results of electroabsorption experiments. Using the assumption that excitons are the primary photoexcited species, from their results Bassler estimates the spatial extent of such excited states as being no more than 2-3 repeat units of the polymers. With the average conjugation length of 10 repeat units, this presents the picture of excitons moving coherently within a polymer segment, confined by topological faults.

The conclusion that the photoexcitations of PPPV and PDT are excitonic in origin and should be described in the above manner is then shown to be compatible with the results of photoconductivity (PC) investigations. In PDAs the onset of PC is found to occur some 0.4 eV above the exciton energy [29]. Excitons occurring in PDA exist for only short times on very ordered chain segments, so it is unlikely for them to escape geminate recombination. The exciton requires more energy to dissociate, and hence the onset of PC is at higher energies than the absorption. In PPPV, however, the onset of PC is found to occur at similar energies to the onset of absorption [28]. To explain this Bassler invokes disorder effects. If the system consists of an array of chromophores with different conjugation lengths - and hence different excitation energies, as well as different ionisation energies and electron affinities - an exciton created on a higher energy segment has the option to expand if the electron or the hole can jump to an adjacent, more extended chromophore with higher electron affinity/lower ionisation energy. In that case the expense of Coulombic binding energy can be more than compensated for by the gain in delocalisation energy, as illustrated in Fig.2.17. Even low energy excitons may escape geminate recombination through this disorder induced process, and hence the

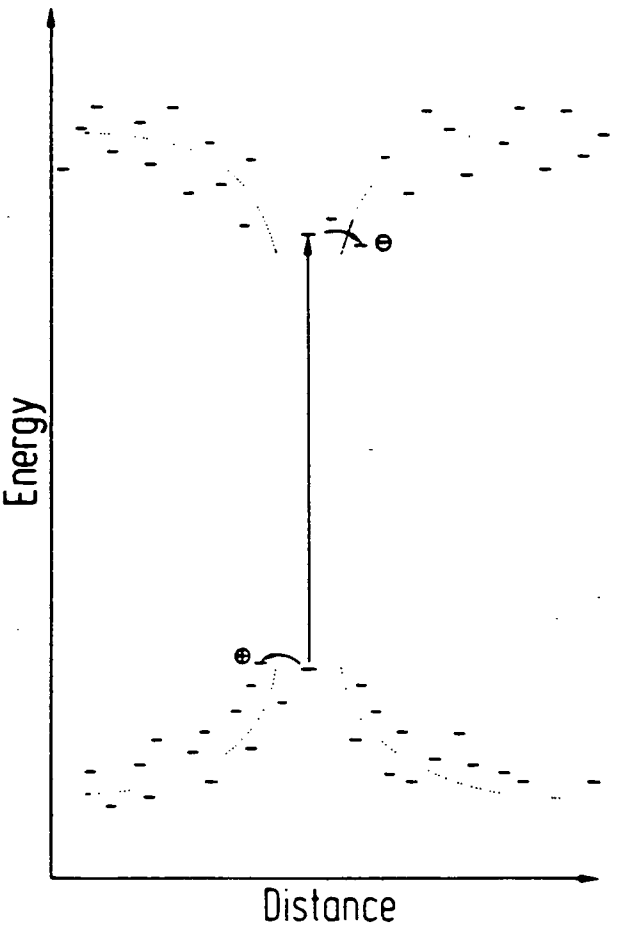

Fig. 2.17 Schematic view of the disorder-promoted expansion of a singlet-exciton into a Coulombically bound geminate e-h pair - each line represents an available site for the electron/hole to reside. (after Bassler, ref[28]).

onset of PC becomes approximately coincident with the onset of absorption.

The results of all these experiments are consistent with the idea of photoproduction of excitons within a diosdered polymer system, and hence Bassler *et al.* [28] suggest that such a model may be applicable to many amorphous polymers.

2.6 Summary

This chapter has introduced the basic idea of conjugation in polymer systems, concentrating mainly on the simplest of conjugated polymers, *trans*-polyacetylene. The semi-conductor band model was used to describe the energy levels of the electrons within the system and the extension of this using the SSH model has been briefly outlined, introducing the concept of solitons, polarons and bipolarons. The deficiencies of such a model have been indicated, including the neglect of electron-electron interactions and the possible effects that disorder may introduce. This leads to the question as to whether it would be better to consider many of π-conjugated polymers as having excitons as the primary photoexcitations, located on short conjugated sub-units of the polymer chain.

This thesis investigates the primary photoexcitations of three materials, polymeric and oligomeric emeraldine base, and polysquaraine, with the aim of further understanding the nature of the excited states produced. Combined with the results of previous investigations, it may be possible to gain a better insight into the photoexcitation processes occuring in these materials.

References

1. Yu, L., *Solitons and Polarons in Conducting Polymers*. 1988, Singapore: World Scientific Publishing Co. Pte. Ltd.
2. Su, W.P., J.R. Schrieffer, and A.J. Heeger, Phys. Rev. Lett, 1979. **42**: p. 1698.
3. Su, W.P., Phys. Rev. B, 1980. **22**: p. 2099.
4. Baeriswyl, B., D.K. Campbell, and S. Mazumdar, in *Conducting Polymers*, H. Keiss, Editor. 1991, Springer, New York.
5. Heeger, A.J., *et al.*, Rev. Mod. Phys, 1988. **60**: p. 781.
6. Fincher, C.R., *et al.*, Phys. Rev. Lett, 1982. **48**: p. 100.
7. Yannoni, C.S. and T.C. Clarke, Phys. Rev. Lett, 1983. **51**: p. 1191.
8. Peierls, R.E., *Quantum Theory of Solids*. 1955: Oxford University Press.
9. Shirakawa, H., Makromol. Chem, 1978. **179**: p. 1565.
10. Suzuki, H., *et al.*, Phys. Rev. Lett, 1980. **45**: p. 1209.
11. Etemad, S., A.J. Heeger, and A.G. MacDiarmid, Ann. Rev. Phys. Chem, 1982. **33**: p. 443.
12. Fincher, C.R., *et al.*, Phys. Rev. B, 1979. **20**: p. 1589.
13. Blanchet, G.B., C.R. Fincher, and A.J. Heeger, Phys. Rev. Lett, 1983. **51**: p. 2132.
14. Hudson, B.S. and B. Kohler, Ann. Rev. Phys. Chem, 1974. **25**: p. 437.
15. Brasset, To be published in Synth. Met, .
16. Fesser, K., A.R. Bishop, and D.K. Campell, Phys. Rev. B, 1983. **27**: p. 4804.
17. Campbell, D.K. and A.R. Bishop, Nucl. Phys. B, 1982. **200**: p. 297.

18. Ball, R., W.P. Su, and J.R. Schrieffer, J. Phys. (Paris) Colloq, 1983. **44**: p. C3-429.

19. Orenstein, J., *Handbook Of Conducting Polymers*, T.A. Skotheim, Editor. 1986, Marcel Decker, New York.

20. Su, W.P. and J.R. Schrieffer, Proc. Natl. Acad. Sci. USA, 1980. **77**: p. 5626.

21. Colaneri, N.F., *et al.*, Phys. Rev. B, 1988. **38**: p. 3960.

22. Orenstein, J., G.L. Baker, and Z. Vardeny, J. Phys. Colloq. C3, 1983. **44**: p. 407.

23. Vardeny, Z.V. and J. Truac, Phys. Rev. Lett, 1985. **54**: p. 1844.

24. Shank, C.V., *et al.*, Phys. Rev. Lett, 1982. **49**: p. 1660.

25. Campbell, D.K., D. Baeriswyl, and S. Mazumdar, Synth. Met, 1987. **17**: p. 197.

26. Abe, S., *et al.*, Phys. Rev. B, 1992. **45**: p. 9432.

27. Abe, S., J. Yu, and W.P. Su, Phys. Rev. B, 1992. **45**: p. 8262.

28. Bassler, H., *et al.*, Synth. Met., 1992. **49**: p. 341.

29. Lochner, K., *et al.*, Phys. Status Solidi (b), 1978. **88**: p. 653.

30. Sebastian, L. and G. Weiser, Chem. Phys, 1981. **62**: p. 447.

31. Rossi, G., Synth. Met, 1992. **49**: p. 221.

32. Salaneck, W.R., Contemp. Phys, 1989. **30**: p. 403.

33. Monkman, A.P., *et al.*, Mol. Cryst. Liq. Cryst., 1993. **236**: p. 189.

34. Eckhardt, H., J. Chem. Phys, 1983. **79**(4): p. 2085.

35. Chance, R., *et al.*, *Solitons, Polarons, and Bipolarons in Conjugated Polymers*, in *Handbook of Conducting Polymers.*, T.A. Skotheim, Editor. 1986, Marcel Dekker, Inc, New York.

36. Pope, M. and C.E. Swenberg, *Electronic Processes in Organic Crystals*. Monographs on the Physics and Chemistry of Materials. Vol. 39. 1982: Oxford University Press.

37. Bounds, P.J. and W. Siebrand, Chem. Phys. Lett, 1980. **75**: p. 144.

38. Mahrt, R.F., *et al.*, Makromol. Chem. Rapid Commun., 1990. **11**: p. 415.

39. Mahrt, R.F. and H. Bassler, Synth. Met, 1991. **45**: p. 107.

40. Rauscher, U., *et al.*, Phys. Rev. B, 1990. **42**: p. 9830.

Chapter 3

Theory of Electroabsorption Spectroscopy.

This chapter aims to give an overview of the theory behind electroabsorption spectroscopy. Detailed description of the actual techniques used within the experiment will be discussed later, in chapter 4.

3.1 An Overview of Modulation Spectroscopy

There are many various types of modulation spectroscopy, all of which have the aim of revealing more information about the energy level structure of materials than is available from linear absorption or reflection spectra. Measurements involve the monitoring of transmittance, or reflectance, of a sample in the presence of a periodic perturbation. The use of modulated perturbations allows phase sensitive detection methods to be used, and hence small induced changes may be detected - signals with resolution of the order 1 in 10^6 are regularly reported [1-7]. Broad structures present in the unperturbed spectra do no not mask these feactures, as it is only the difference spectra (spectrum with applied perturbation minus the spectrum withouth the applied pertubation) which are recorded.

The sample in question may be periodically altered in some physical way, such as the application of heat or pressure, or the measurement parameters themselves may be periodically adjusted. An example of the latter is wavelength modulation, in which the wavelength of the incident light is modulated. This is considered to be an 'inherent modulation', meaning that it is a variation of the measuring system rather than 'external modulation' - variation of the physical conditions of the sample.

The work presented within this thesis is concerned with electroabsorption (EA) spectroscopy. It is an external form of modulation spectroscopy - the electric field through the sample being the modulated parameter. The resulting change in absorption of the sample can give information concerning the energy level structure of the material. Closely related to EA is electroreflection (ER) spectroscopy, which, as its name implies, is the same technique apart from the fact that it is the reflectivity of the sample which is monitored. The choice of measuring EA as opposed to ER of any one material mostly depends on the nature of the samples. The measurement of the EA response of a material requires an optically thin sample, and so ER instead of EA would have to be used for the study of the electromodulated optical response of samples which by their nature cannot produced optically thin, i.e. free standing stretch aligned polymer films.

The first electro-modulation spectroscopy was performed by Seraphin in 1964 [8], reporting electroreflectance data for germanium. Following on from this there was rapid development of modulation techniques, and much research undertaken into probing the band structures of inorganic semiconductors [9, 10]. Subsequent work on organic materials has shown that, though similar in some crystalline cases, organic and inorganic systems have different electromodulation responses. This is hardly suprising, considering the difference in structure between regular, three dimensional crystalline inorganic semiconductors and the quasi one-dimensional, often disordered organic materials.

There have been several theories put forward to explain the observed electromodulated spectra observed in organic systems, each with its own set of approximations and assumptions. The rest of this chapter will attempt to outline both the theories for inorganic and organic materials, so as to put the discussion of the results of this thesis in context.

3.2 Electromodulation of Inorganic Systems

In 1958 Franz [11] and Keldysh [12] predicted that the application of a uniform electric field should induce optical absorption below the energy gap of an inorganic semiconductor. The effect, which came to be known as the 'Franz-Keldysh effect', was based upon the concept of holes and electrons being able to tunnel through the energy gap in the presence of an applied electric field by the process of photon-assisted tunneling. Above the gap a series of oscillations (the Franz-Keldysh oscillations) were also predicted. These predictions were confirmed in electroabsorption and electroreflection experiments in the mid-60's [8, 13-16]. Further calculations by Aspnes and Rowe [17, 18] indicated that full quantum mechanical expressions for the electric field induced broadening reduced to a simple form when only low fields are applied to the system. Resulting from their calculations there appeared three distinct regimes of applied field strength [19]:

a) the low field limit; a full quantum mechanical treatment of the electric field induced changes in the band structure was unnecassery to provide a good fit to the experimental results. Only a first order perturbation treatment was required, which resulted in a third order differential of absorption lineshape. This low field regime has been widely investigated, and led to electric field modulation spectroscopy becoming known as 'third derivative spectroscopy'.

The physical mechanism responsible for the electric field modulation is the coupling of the external field to the electrons within the crystal, causing them to accelerate through the lattice. The quantum mechanical perturbation calculation for this low field regime includes the term $H' = -e\vec{E} \bullet \vec{x}$ (electric field E in direction x) to account for the application of the uniform electric field in the Hamiltonian ($H = H_0 + H'$). This term is not lattice periodic and therefore destroys the

translational invariance of the Hamiltonian in the field direction (x). This results in the one-electron Bloch states of adjacent momentum (k) becoming mixed, and hence non-vertical optical transitions become allowed. Physically, this means that an electron accelerates and occupies a large number of k states before undergoing a collision process. It is this acceleration that leads to the third derivative lineshape behaviour in inorganic semiconductors.

b) intermediate field; the Franz-Keldysh effect - oscillations become apparent above the band gap (Franz-Keldysh oscillations). Even though this is the intermediate field case, it was often termed 'high field', as it was often difficult to achieve experimentally the fields necessary to leave this regime and enter the true high field regime described below. This intermediate regime is the one described by Franz and Keldysh using full quantum mechanical descriptions - rather than just a first order perturbation approach - of an electron being accelerated in a crystal band structure.

c) high field limit; the Stark effect. The applied fields necessary to acheive this regime are very high ($\sim 10^7$ Vcm^{-1}) and are not normally achieved. The field gradient across a unit cell of the crystal is so large that the band structure of the material is altered and the selection rules for optical transitions are modified.

The effects of impurity levels and strongly bound excitons in electromodulated spectroscopy of inorganic systems have also been considered. The picture of an electron being accelerated in an external field cannot be used in these cases, and hence more involved theoretical approaches are required. For localised states the problem has often been analysed in terms of the Stark effect. Reviews of electromodulation spectroscopy of localised excitations have been presented by Luty

[20], Dow [21], and Grassano [22]. Some of these theories, such as the use of the Stark effect, have been utilised in the consideration of electroabsorption response of polymer systems - as will be outlined in the next section.

3.3 Electromodulation of Organic Systems

It is obvious that unless an extremely ordered crystal of an organic system can be synthesised, the Franz-Keldysh approach used for crystalline inorganic semiconductors cannot be used for organic systems. EA experiments have revealed feactures in some PDAs [23] that have been attributed to the Franz-Keldysh effect, but this is confined to exceptionally high quality single crystals and in general a new approach must be sought to interpret the electromodulation spectra of the disordered polymer systems.

The field gradients present in an inorganic material are small and the bandwidths large due to the long range order and symmetry of the system, and hence an external applied electric field does not have to be large to cause a measurable perturbation to the system. In organic systems however, the internal field gradients are large and the bandwidths small, and hence much larger external electric fields need to be applied before any perturbation of the system may be observed. It is for this reason that electroabsorption responses in organics were not detected until much later than inorganic materials.

In the early '80's electroabsorption and electroreflectance techniques were applied to molecular crystals and organic polymers with conjugated π-electron systems [7, 24-26]. The extended electronic order and large bandwidths of these delocalised π-electron systems are sensitive to the applied electric fields as the

potential drop across these states forms a significant perturbation to the average internal fields.

Some of the first EA experiments performed by Sebastian and Weiser were on films of solid pentacene and tetracene [7]. An example of their EA spectra for pentacene is given in Fig.3.1. From this data they concluded that the photoexcited states were a combination of charge transfer and Frenkel excitons. The argument they used is as follows.

The absorption spectrum of a molecular system responds to the application of an electric field via the field induced change in absorption $\Delta E(F)$ of the transition energy. If E(0) is the transition energy in zero applied field, then

$$\Delta E(F) = E(F) - E(0) = -(\mathbf{m_f} - \mathbf{m_i}) \bullet \mathbf{F} - \tfrac{1}{2}\mathbf{F} \bullet \Delta p \mathbf{F} \qquad \text{eqn. 3.1}$$

where $\mathbf{m_i}$ is the dipole moment of the ground state, $\mathbf{m_f}$ the dipole moment of the excited state, and Δp is the change in the polarisability upon photoexcitation. For apolar molecules, such as tetracene and pentacene, $\mathbf{m_i}$=0. Using the idea of charge transfer occuring upon photoexcitation the dipole moment of the final state ($\mathbf{m_f}$) is equal to q**r**, where q is the charge transferred (which is assumed to be one electron, and hence q=-1), and **r** is the separation distance.

The change in absorption coefficient as a function of ΔE may be expressed as a McLaurin series truncated at the second term

$$\Delta\alpha = \frac{\partial\alpha}{\partial E}\Delta E + \frac{\partial^2\alpha}{\partial E^2}(\Delta E)^2 \qquad \text{eqn. 3.2}$$

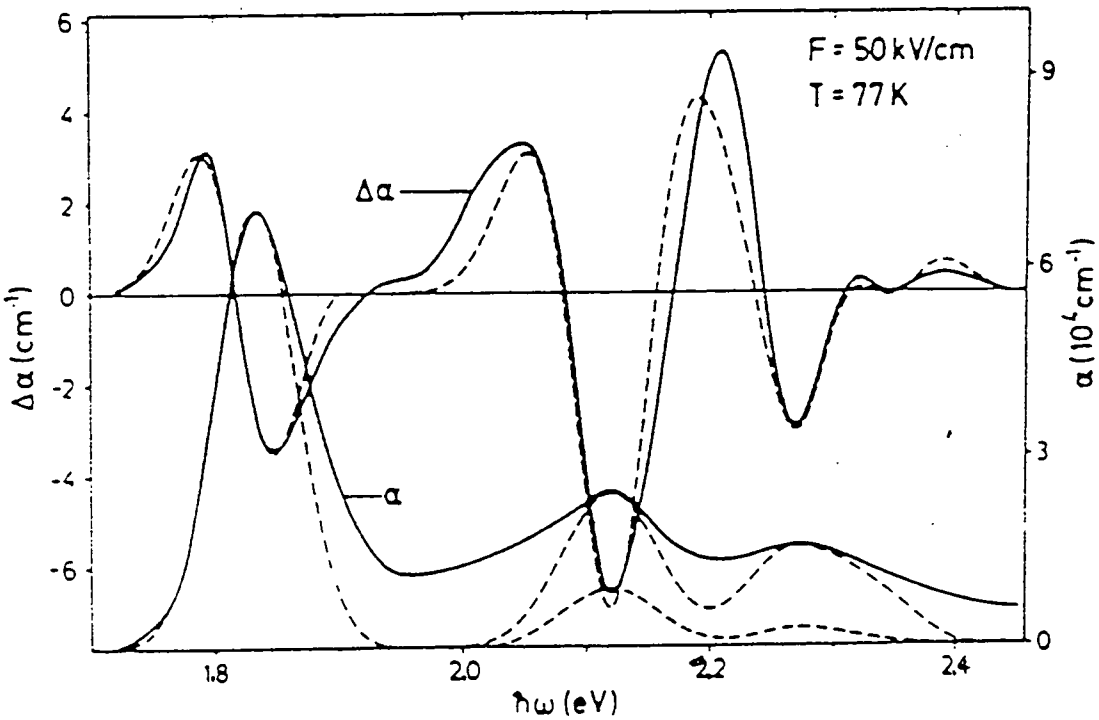

Fig. 3.1 Absorption (α) and EA ($\Delta\alpha$) for pentacene, at a temperature of 77 K and an applied field of 50 kV/cm. Solid lines represent experimental results, dashed lines represent the fit from theoretical modelling. (after Sebastian, ref[7])

Combining eqn. 3.1 and eqn. 3.2 gives the change in $\Delta\alpha$ as a function of the modulating electric field. Sebastian points out two cases of importance - the production of excited states with and without a dipole moment.

A Frenkel exciton is small and may be considered to be a freely orbiting electron hole pair - and hence overall neutral. Photoproduction of such a state, or any centrosymmetric state, results in $\langle \mathbf{m_f}.\mathbf{F} \rangle = 0$, with the consequence that the only contribution to ΔE comes from the change in polarisability. Truncating eqn. 3.2 at the first term gives

$$\Delta\alpha = \tfrac{1}{2}\Delta\bar{p}F^2\frac{\partial\alpha}{\partial E} \qquad \text{eqn. 3.3}$$

where $\Delta\bar{p}$ is the average over the change in components of the polarisability tensor. Eqn. 3.3 describes the Stark effect. This eff0ect is always present, since the polarisability of a molecule changes as a result of the change in electron distribution upon electronic excitation.

When a charge, q, is transferred a distance, r, upon photoexcitation the predicted EA is different. The final state now has a dipole moment $\mathbf{m_f} \approx q\mathbf{r}$, and $\Delta E \approx -\mathbf{m_f}.\mathbf{F}$, (the contribution from Δp being small in comparison). Isotropic averaging over the randomly oriented charge transfer dipoles gives

$$(\Delta E)^2 = \tfrac{1}{3}(qrF)^2 \qquad \text{eqn. 3.4}$$

and

$$\Delta\alpha = \tfrac{1}{6}(qrF)^2 \frac{\partial^2\alpha}{\partial E^2} \qquad \text{eqn. 3.5}$$

In summary, Sebastian *et al.* [7] predict that with the application of an external field a red shift of absorption peaks due to the Stark effect will occur if the photoexcited states are overall neutral. This results in an EA signal with the lineshape of the first derivative of absorption, i.e $\partial\alpha/\partial E$. If, however, the photoexcited state has a dipole moment then the applied field is predicted to broaden and suppress the absorption peak resulting in an EA spectra with the lineshape of the second derivative of absorption, i.e. $\partial^2\alpha/\partial E^2$. Both responses are predicted to have a quadratic dependence upon applied field. Sebastian and Weiser interpreted the EA spectrum for pentacene, presented in Fig 3.1, in this manner and concluded that the band edge excitation at 1.8 eV is due to a Stark shift of Frenkel excitons, whereas the features at higher energies are attributed to charge transfer excitons. Using the above equations it was also possible for Sebastian and Weiser to calculate values of the change in polarisability, Δp, and charge seperation distance, r, for excited states within pentacene and tetracene.

It has been found that for some materials a combination of both first and second derivative lineshapes provides the best fit to the experimental EA data. This has been interpreted simply as a combination of the two processes described above happening simultaneously, with neither dominating [27].

An alternative suggestion for the origin of second derivative lineshape of EA for disorded polymers is that of lifetime broadening of the excited state due to the application of the external field [4]. Horvath and Weiser [27] dismiss this idea,

using the argument that if it were the case, then the same physical processes and hence the same second derivative lineshape should be observed in crystalline samples.They point out that PDAs, and even weakly bound excitons in semiconductor systems such as CdS [28], respond to applied fields primarily with a first order lineshape - indicative of a quadratic Stark shift.

Recent work by Horvath and Weiser [27] has shown that materials which are theoretically predicted to have centrosymmetric, and hence neutral excited states, may have EA spectra corresponding to lineshapes of the second derivative of absorption, apparently in contradiction to this earlier argument concerning charge transfer excitons. They consider that the disorder present within an amorphous material may produce non-uniform internal fields that in turn may cause idealy non-polar states to become polarised. This idea is important in the discussion of the EA of emeraldine base, as will be discussed later in this thesis.

Sebastian and Weiser also carried out electroreflectance studies on various PDAs [25]. The EA signals in these compounds were around two orders of magnitude larger than those of pentacene and tetracene. Using their previous method to analyse the data produced polarisabilities and separation distances of the charges so large that they were considered incompatible with the polymer systems. In an effort to reconcile the results with theory they introduced a new dimension to their model. As before, they proposed that the photoinduced species is a charge transfer exciton. PDAs are centro-symmetric, and so the charge is transferred in no preferential direction - it can be excited equally well to the 'left' as to the 'right', as depicted in Fig.3.2. In the presence of an applied field, however, the charge will be excited in a preferential direction - 'down field'. This preference was designated δ, and incorporated into their previous calculations. It turned out that δ had much the

same effect as the polarisability, p, though on a larger scale, and seemed to adequately explain the experimental results.

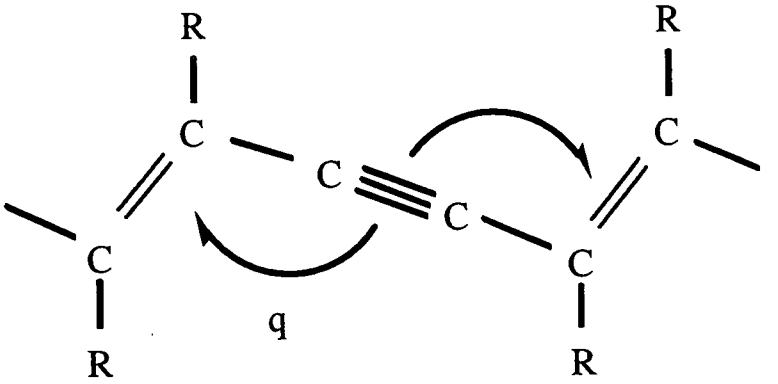

Fig.3.2 Repeat unit of PDA and schematic charge transfer with excitation (after Sebastian, ref.[25]).

The theories presented so far (apart from the dismissed 'line broadening' suggestion) have been concerned with the applied electric field interacting with photoexcited states that have involved the displacement of charge (whether symmetrically or asymmetrically) being described in terms of the Stark effect.

A slightly different approach has been taken by Guo *et al.* [29] and Kawabe *et al.* [30, 31] in an attempt to explain the effects of an external electric field upon the photoexcitations in PDAs. As mentioned previously, PDAs are important in this field since their optical properties are determined by their high degree of structural order. Polarised absorption and electroabsorption investigations of crystalline PDAs [7, 25, 32] have shown that the conjugated π-electrons may be considered as almost ideal 1-dimensional systems extending along the polymer chains. From studying the response of systems relatively free from disorder, a higher degree of understanding may be attained about the physical processes involved. Using this knowledge

attempts can be made to model the more complicated disordered systems, assuming that the same physical processes are involved.

Guo *et al.* [29] undertook a detailed theoretical and experimental study of the EA response of PDAs in response to the publication of several conflicting theories on the subject. Their investigations concentrated on the PDA poly[1,6-di(N-carbozolyl-2,4-hexadiyne] (DCH-PDA), the absorption and EA spectra of which are shown in Fig.3.3. In agreement with previous work they conclude that the linear absorption and the EA response originates from the PDA backbone. Also in agreement with previous work they assign the main low energy EA peak to a Stark shift of an exciton. The necessity for an alternative approach to the analysis of the EA data for PDAs originates from the higher energy EA feacture, observed around 2.4 eV, which is consistently observed above the exciton peak in a region where linear absorption is negligible.

Sebastian and Weiser, who noted the occurrance of this peak in 1981 [25], ascribed it to a transfer of oscillator strength to a normally forbidden transition at the band edge. Later work by Tokura *et al.* [32] and Hasegawa *et al.* [33], however, proposed that this EA feacture was due to a normally dipole forbidden state becoming weakly allowed in the presence of a symmetry breaking external field. Guo suggested that this could not be the case, due to the oscillatory nature of the signal around zero, evident in Fig.3.3, which is not consistent with a transfer of oscillator strength to a new state. The EA signal associated with a transferral of oscillator strength to a new state would have no negative portion at the energy of the new state, but would involve the loss of oscillator strength from the nearest normally allowed state.

Guo attempted to resolve the disagreement by carrying out a detailed theoretical investigation of the processes involved in two photon absorption, third harmonic generation and electroabsorption in PDAs [29]. He concluded that the

high energy EA feacture is due to the conduction band threshold, as explained below.

Eigenstates of linear conjugated polyenes and polymers with a center of inversion, such as PDAs, are classified as A_g if they are symmetric with respect to the inversion center, and B_u if they are asymmetric. Each state is further characterised by a quantum number describing its relative ordering in terms of energy, thus $1A_g$ is the ground state. Dipole allowed transitions may only occur between A_g and B_u states, making excitation from the ground state to an A_g state one-photon forbidden, but two photon allowed. The system can be significantly altered in the presence of a weak static applied electric field, F, (weak relative to the internal fields of the system). The A_g and B_u states can become mixed according to

$$|n\rangle = |n^{(0)}\rangle + \sum_{n \neq m} \frac{\langle n^{(0)}|H_f|m^{(0)}\rangle}{E_n^{(0)} - E_m^{(0)}} |m^{(0)}\rangle \qquad \text{eqn. 3.6}$$

where H_f is the perturbation introduced by the applied field F. The unperturbed energies and wavefunctions are denoted by $E_n^{(0)}$ and $|n^{(0)}\rangle$, while $|n\rangle$ refers to the perturbed wavefunction and $|m^{(0)}\rangle$ is the unperturbed nearest neighbouring level. The degree of mixing, and hence the degree of perturbation, is thus dependent upon the separation of the energies of the states involved, $(E_n^{(0)} - E_m^{(0)})$. Applying an external field may cause the shifting of energy levels (the Stark shift), and may also cause a transfer of oscillator strength from normally one-photon dipole allowed transitions to previously one-photon forbidden transitions. Assuming a symmetric ($1A_g$) ground state, this implies transitions to higher lying A_g states may become weakly allowed if there is an appropriate B_u state energetically close to the upper A_g state.

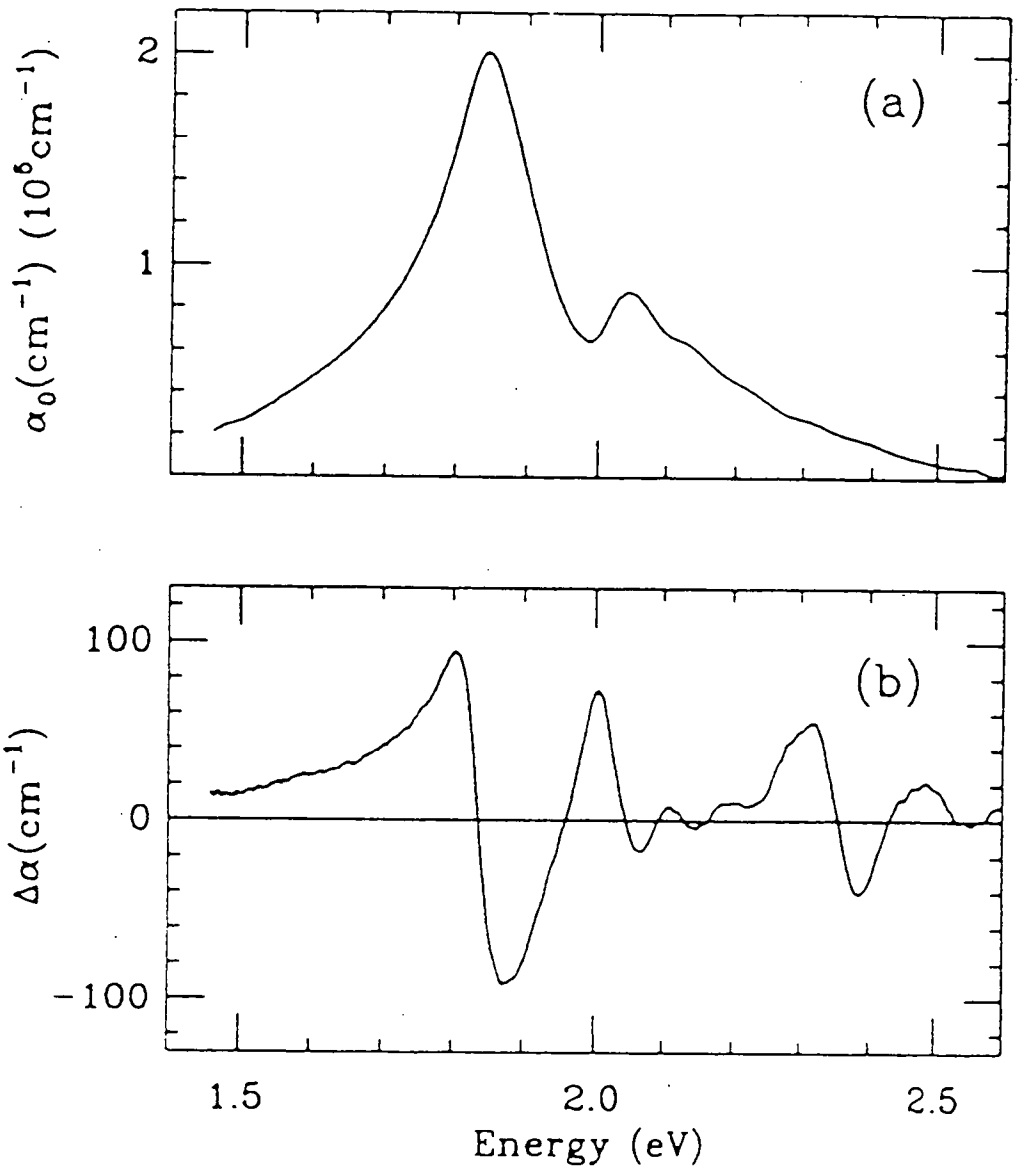

Fig. 3.3 Absorption (top) and EA (bottom) spectra of DCH-PDA (after Guo, ref[29]).

Using the above model Guo *et al.* [29] propose the high energy EA feacture is due to an increase in the oscillator strength of the A_g states at the band edge, with an accompanying decrease in probability of transitions to the B_u states in the same energy range. Based on these results, and those of third harmonic generation experiments, they propose an energy level scheme for PDAs of the form shown in Fig.3.4.

This model has been extended to other, more disordered polymeric systems, including polyacetylene (PA) [34], poly(phenylene acetylene) (PPA) and polydiethyl silane (PDES) [35] by Jeglinsky and Vardeny. The EA spectra of these polymers have many similar generic feactures; a peak at or near the optical band edge, followed by a trough, returning to zero. To illustrate the form of such spectra, the EA responses of PPA and PDES are given in Fig.3.5.

The initial peak (a) may have the lineshape of the first or second derivative of the linear absorption, but is often found to depart from this lineshape before the negative peak. Both these cases are recognised in Fig.3.5, with PPA being related to the first derivative and PDES to the second derivative of their linear absorption spectra. Jeglinsky [35] suggests that the difference between polymers with the different lineshape may be due to the positioning of the nearest one-photon forbidden ($2A_g$) state with relation to the lowest normally allowed ($1B_u$) state. He suggests that if there is no near neighbouring state, then the resulting EA spectrum will have a first derivative lineshape as for PPA, consistent with the peak being Stark shifted. The presence of an A_g state just below the $1B_u$ state, however, causes the predominant perturbation to be a transferral of oscillator strength to this lower lying state, resulting in a second derivative lineshape of the EA spectrum, as for PDES. The feactures marked (b) are proposed to be evidence of previously dipole

forbidden mA_g states (labelled 'mA_g' due to their exact positioning in the energy level ordering being unknown) becoming allowed in the presence of the applied field.

To provide further evidence for this energy level configuration, Jeglinski [35] subtracts the absorption first derivative lineshape, the lineshape expected if the Stark shift were the only process occuring, from the EA spectra of each material, the results of which are shown in Fig.3.6. These spectra should indicate the energies to and from which oscillator strength has been transferred. As a method of verifying the validity of these subtractions, the integral of the transfer of oscillator strength over the energy range of their spectra had to be assumed to be zero, i.e. it was assumed that no states of energies outside the range of their spectra were involved in transferral of oscillator strength. For PPA (Fig.3.6a) it can be seen that oscillator strength has been lost from the $1B_u$ exciton at 2.5 eV - marked (a) - and gained by some feature at (b) 3.2 eV, which they assign to an mA_g state. There is also a feature at (c) 3.8 eV for which they have no suggestion.

The picture is somewhat different for PDES (Fig.3.6b). The loss of oscillator strength at (a) is once again assigned to a $1B_u$ exciton, perhaps with evidence of a vibronic sideband, and (b) again assigned to an mA_g state. The difference occurs below the $1B_u$ state, at (d), where there appears to be a gain in osciillator strength. It is this which they assign to a transferral of oscillator strength to a $2A_g$ state - the state that initially caused the second derivative lineshape of the EA spectrum. The positioning of this state also ties in with the fact that luminescence has not been observed in PDES - such a state just below the opticlal gap provides an alternative, non-radiative route for relaxation of the excited state.

It appears, therefore, that the theory proposed by Guo *et al.* [29] for interpreting the EA results of highly ordered PDAs can be extended to much more disordered π-conjugated systems, and provide a model that is consistent with experimental results.

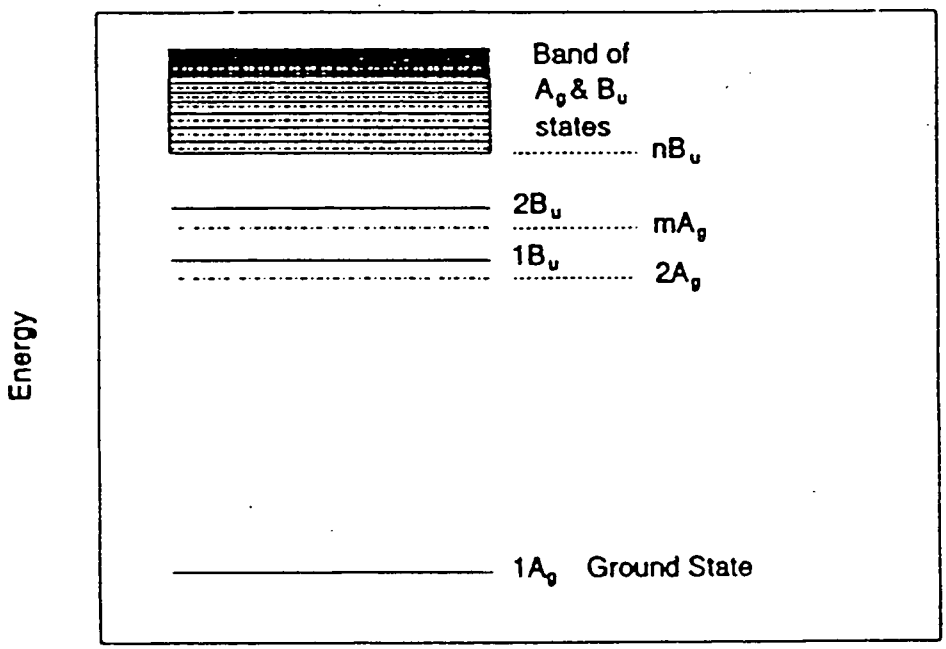

Fig. 3.4 Proposed energy level scheme for PDAs
(after Guo, ref[29]).

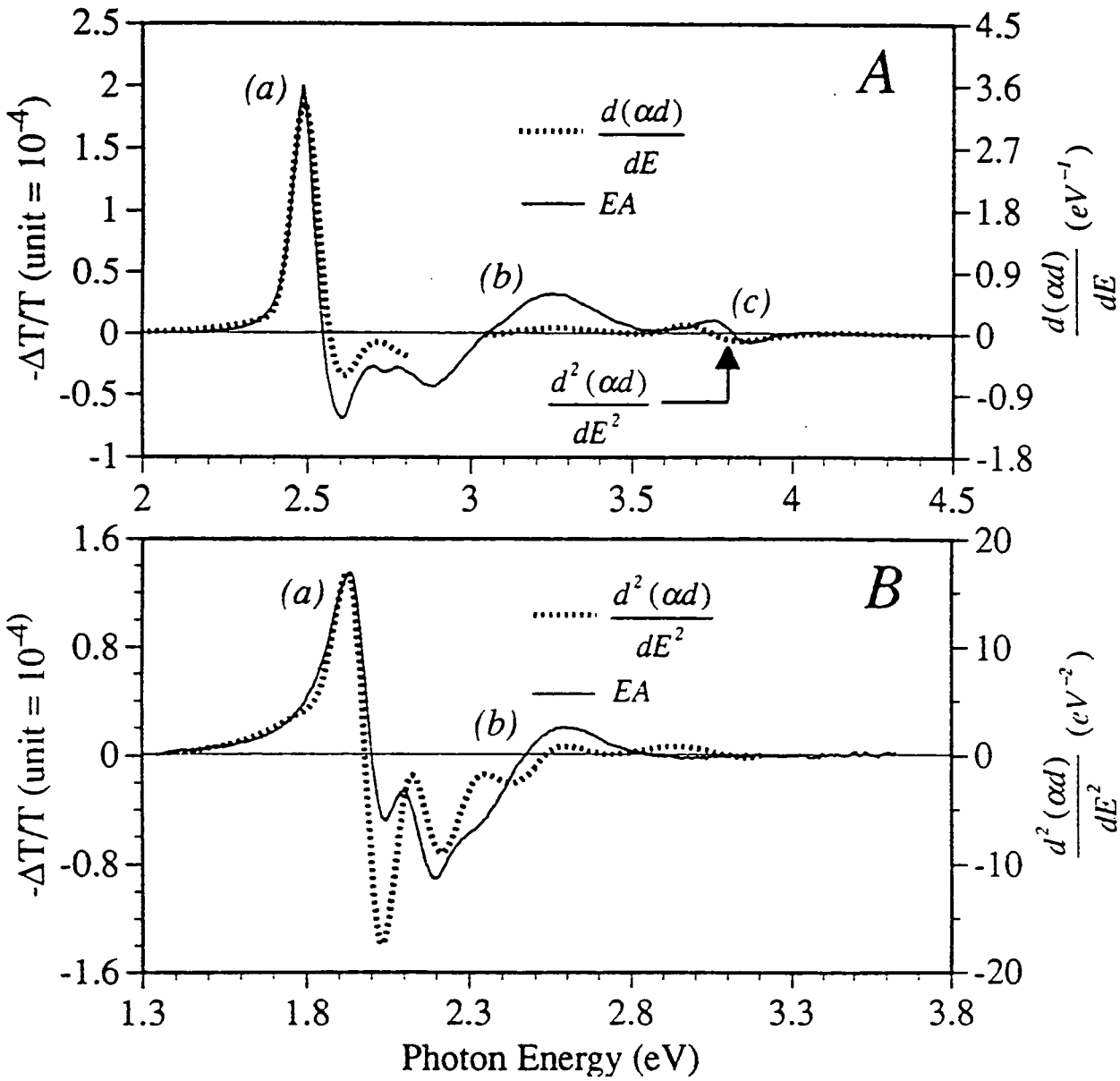

Fig. 3.5 EA spectra of a) PPA and b) PDES, along with the closest matching derivative of their absorption spectra (after Jeglinsky, ref[35]).

It has become apparent from various EA studies [32, 36-38] that if the incident optical field is polarised, the relative orientation of the optical field to the applied electric field can reveal further information about the material in question. The technique of electroabsorption spectroscopy involves the mixing of two independently polarised electric fields, the quasi-dc applied electric filed and the optical field. If the whole optical probe is polarised, then the polarisation dependence of the EA response may be investigated. As mentioned previously, the polarisation dependence of the EA signal of PDAs has helped show that the π-electron systems in such materials are quasi 1D, being oriented along the back-bone of the system. Polarisation dependencies have also been shown to occur in stretch oriented polymer films, as reported by Hagler *et al.* for PPV [36], and also for unoriented films [38].

Horvath *et al.* [37] have desribed the polarisation dependence of the EA response of poly-(phenylphenylenevinylene) (PPPV) and poly-(dodecylthiophene) (PDT). They consider the photoexcitations to occur on ordered subunits of the polymer chain, and that the transition dipole moment lies along the backbone of the chain. In an unoriented film these transition dipole moments will be randomly oriented, and they have shown that in such a system a ratio of the EA response of 3:1 should be found for the two cases of the fields being parallel and perpendicular. Polarisation dependent spectra for PPPV and PDT show this ratio of 3:1, adding weight to their argument. This is constant over the whole spectral range, indicating that the whole spectrum has a common origin

Hagler [38], however, has subsequentley suggested that the approach of Horvath *et al.* is rather simplistic. By considering the field amplitudes, rather than intensities, and taking into account the two dominant transition dipole moments $\langle 1B_u|r|G\rangle$ and $\langle mA_g|r|1B_u\rangle$ (G is ground state) Hagler predicts ratios of EA response

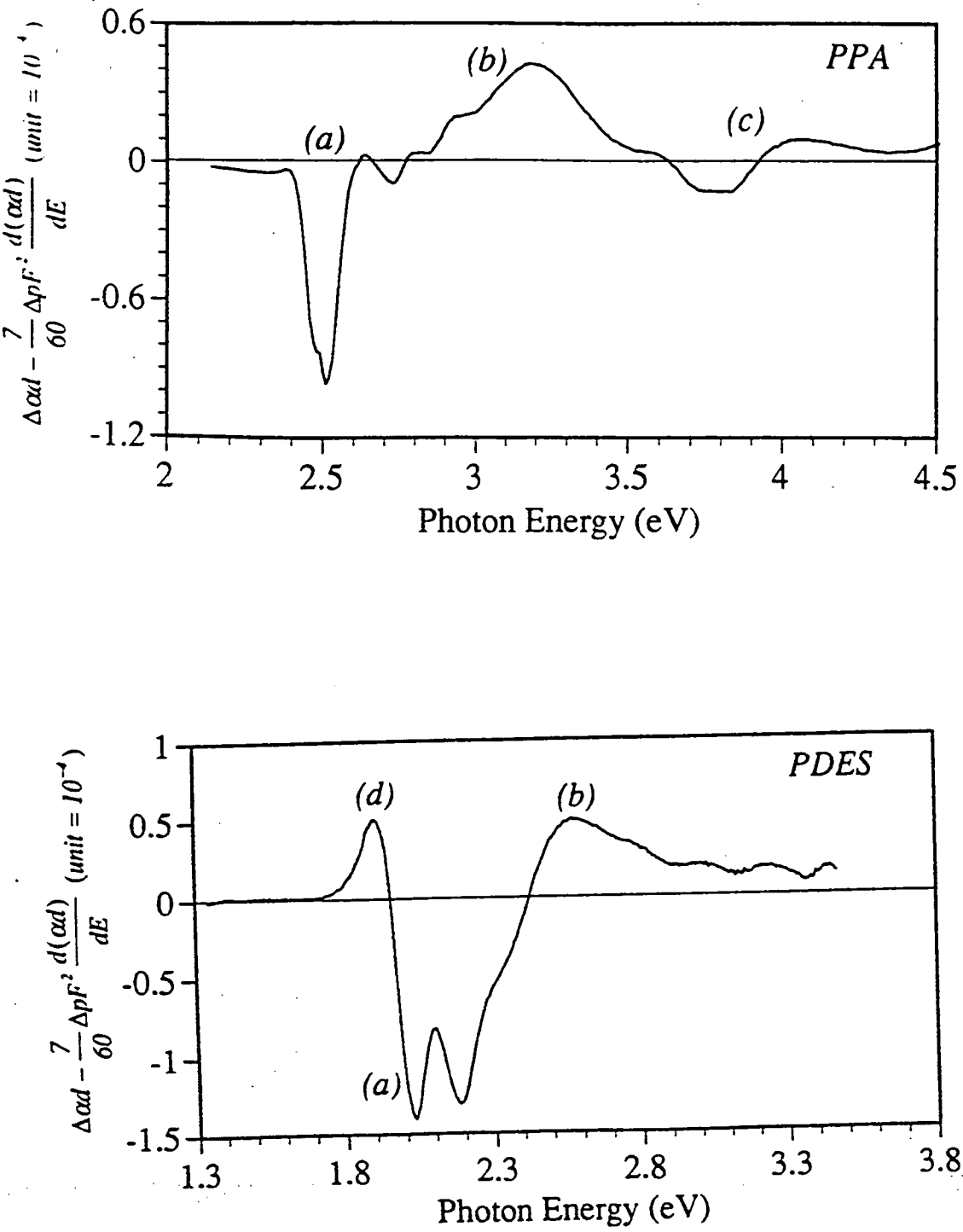

Fig. 3.6 Difference between EA and first derivative for
PPA (top), and PDES (bottom)
(after Jeglinsky, ref[35]).

ranging from 3:1 to 1:3 for the polarisation dependencies. The value is dependent upon the angle between the transition dipole moments involved.

This chapter has given a brief overview of the current theories concerning electroabsorption spectroscopy in organic materials. It is obvious that the choice of method of analysing the EA data of any one material is, to some extent, up to the judgement of the individual. The choice must be guided by taking into consideration the morphology of the sample, the nature of the chemical composition, and any theoretical predictions as to the nature of the excited states. The early model of Sebastian and Weiser [7] would still seem to be more appropriate for localised exciton states, whereas the more recent model presented by Guo *et al.* [29] is more appropriate for fully π-conjugated systems described by molecular states.

References

1. Botta, C., G. Zhuo, O.M. Gelsen, D.D.C. Bradley, and A. Musco, Synth. Met, 1993. **55-57**: p. 85.
2. Gelsen, O.M., D.D.C. Bradley, H. Murata, T. Tsutsui, S. Saito, J. Ruhe, and G. Wegner, Synth. Met, 1991(41-43): p. 875.
3. Gelsen, O.M., D.D.C. Bradley, H. Murata, N. Takada, T. Tsutsui, and S. Saito, J. Appl. Phys, 1992. **71**: p. 1064.
4. Phillips, S.D., *et al.*, Phys. Rev. B, 1989. **40**(14): p. 9751.
5. Worland, R.S., *Electroabsorption in Conjugated Polymers*, PhD Thesis. 1989, Santa Barbra: California. p. 255.
6. Worland, R., S.D. Phillips, W.C. Walker, and A.J. Heeger, Synth. Met, 1989. **28**: p. D663.
7. Sebastian, L., G. Weiser, and H. Bassler, Chem. Phys, 1981. **61**: p. 125.
8. Seraphin, B.O. in *Proc. 7th Intern. Conf. Physics of Semiconductors*. 1964. Paris: Dunod, Paris.
9. Hamakawa, Y. and T. Nishino, in *Optical Properties of Solids*, B.O. Seraphin, Editor. 1980, North Holland Publ. Co., New York.
10. Aspnes, D.E., in *Handbook on Semiconductors*, T.S. Moss, Editor. 1980, North-Holland Publ. Co.
11. Franz, W., Z. Naturforsch Teil, 1958. **A13**: p. 484.
12. Keldysh, L.V., Zh. Eksp. Teor. Fiz, 1958. **34**(54): p. 1138.
13. Seraphin, B.O. and N. Bottka, Phys. Rev, 1965. **139**(A): p. 560.
14. Seraphin, B.O., R.B. Hess, and N. Bottka, J. App. Phys, 1965. **36**: p. 2242.
15. Frova, A. and P. Handler, Appl. Phys. Lett., 1964. **5**: p. 11.
16. Frova, A. and P. Handler, Phys. Rev, 1965. **135**(A): p. 1856.
17. Aspnes, D.E. and J.E. Rowe, Solid. Stat. Comm., 1970. **8**: p. 1145.

18. Aspnes, D.E. and J.E. Rowe, Phys. Rev. B, 1972. **5**(10): p. 4022.

19. Aspnes, D.E. . in *Proc. 11th Int. Conf. on the Physics of Semiconductors*. 1972. Warsaw: Polish Scientific Publishers, Warsaw.

20. Luty, F., Surf. Sci, 1973. **37**: p. 120.

21. Dow, J.D., in *Optical Properties of Solids*, B.O. Seraphin, Editor. 1976, North-Holland Publ. Co., New York. Chp. 2.

22. Grassano, U.M., Nuovo Cimento, 1977. **39**: p. 368.

23. Weiser, G., Phys. Rev. B, 1992. **45**(24): p. 14076.

24. Sebastian, L., G. Weiser, G. Peter, and H. Bassler, Chem. Phys, 1983. **75**: p. 103.

25. Sebastian, L. and G. Weiser, Chem. Phys, 1981. **62**: p. 447.

26. Sebastian, L. and G. Weiser, Chem. Phys. Lett, 1979. **64**(2): p. 396.

27. Horvath, A. and G. Weiser, Mol. Cryst. Liq. Cryst, 1994. **256**: p. 79.

28. Lange, H. and E. Gutsche, Phys. Sta. Sol., 1969. **32**: p. 293.

29. Guo, D., S. Mazumdar, S.N. Dixit, F. Kajzar, F. Jarka, Y. Kawabe, and N. Peyghambarian, Phys. Rev. B., 1993. **48**(3): p. 1433.

30. Kawabe, Y., F. Jarka, N. Peygambarian, D. Guo, S. Mazumdar, S.N. Dixit, and F. Kayzar, 1991. **44**(12): p. 6530.

31. Kawabe, Y., F. Jarka, N. Peyghambrarian, D. Guo, S. Mazumdar, S.N. Dixit, and F. Kajzar, Synth. Met, 1992. **49-50**: p. 517.

32. Tokura, Y., Y. Oowaki, T. Koda, and R.H. Baughman, Chem. Phys., 1984. **88**: p. 437.

33. Hasegawa, T., K. Ishikawa, T. Koda, K. Takeda, H. Kobayashi, and K. Kubodera, Synth. Met, 1991. **41-43**: p. 3151.

34. Jeglinski, S. and Z.V. Vardeny, Synth. Met, 1992. **49-50**: p. 509.

35. Jeglinski, S.A., Z.V. Vardeny, Y. Ding, and T. Barton, Mol. Cryst. Liq. Cryst., 1994. **256**: p. 87.

36. Hagler, T., K. Pakbaz, and A.J. Heeger, Phys. Rev. B, 1994. **49**(16): p. 10968.

37. Horvath, A., H. Bassler, and G. Weiser, Phys. Stat. Sol. (b), 1992. **173**: p. 755.

38. Hagler, T., Cem. Phys. Lett., 1994. **218**: p. 195.

Chapter 4

Review of Materials.

The three materials used in the electroabsorption investigations of this thesis will be reviewed; polyaniline - concentrating on the polymeric and oligomeric forms of emeraldine base - and a recently developed fully conjugated polymer, polysquaraine.

4.1 Emeraldine Base

Emeraldine base (EB) is the half oxidised form of the polyaniline family of polymers. A schematic of its chemical structure is depicted in Fig.4.1 alongside the other two oxidation states, leucoemeraldine base (LB) and pernigraniline base (PNB).

Polyaniline is the oldest known synthetic organic polymer, having first been discovered by Letherby [1] as a result of the anodic oxidation of aniline. The product formed was a dark green precipitate that came to be known as aniline black. Soon after, Green and Woodhead [2, 3] determined that the polymer existed in distinct oxidation states. Following its discovery there was very little research into the material, other than that of the dye industry, until the mid '60s and early '70s when work by Josefowitz *et al.* [4-6] led to a more detailed understanding of the polymer. In particular, the conductive nature of the protonated emeraldine oxidation state was discovered (although the structure of this conductive form was still unknown) , and its possible use in electrolyte rechargeable batteries reported [4-7].

The discovery of an electrically conductive form of polyaniline, and further reports of an electrochromic response [8], resulted in a high degree of research

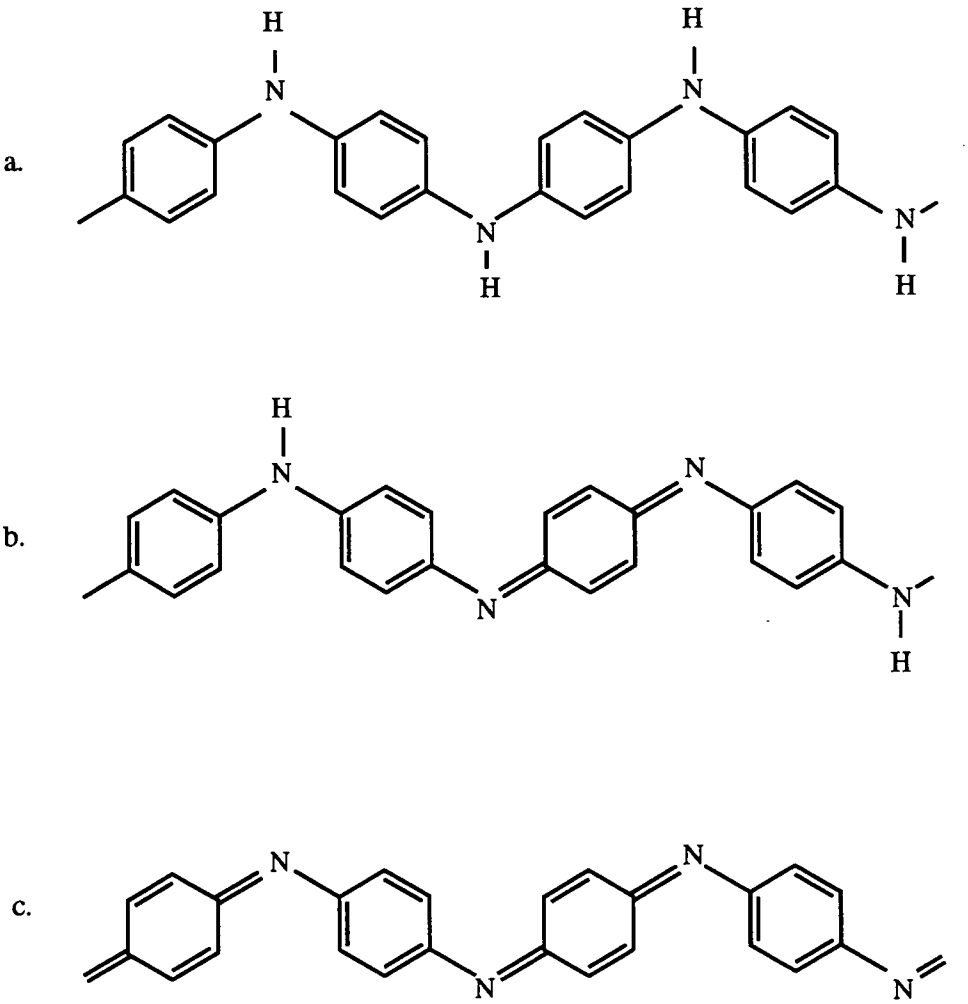

Fig. 4.1 Chemical structure of the three main oxidation states of polyaniline, a) leucoemeraldine base (LB), b) emeraldine base (EB), and c) pernigraniline base (PNB).

being undertaken into the polyaniline family. In particular, the groups of MacDiarmid [9-11] and Heeger [12-14] undertook detailed investigations into the electrical and optical nature of the polymer.

This large degree of interest is still very evident in academic and industrial institutions, and further applications are still being presented [15]. While there is interest in the emeraldine base, the primary photoexcitations of the material have not been fully characterised. The electroabsorption investigations reported in this thesis aim to expand the current knowledge concerning these photoexcitations.

4.1.1 Chemical and Geometric Structure

The deduction of the idealised chemical structures of the three base forms of polyaniline shown in Fig.4.1 have been achieved through comparison to model compounds [16, 17], elemental analysis [11], direct chemical synthesis models [18, 19], and infrared spectroscopy [20, 21]. There have also been investigations into the solution-state carbon-13 nuclear magnetic resonance of polyaniline [22], which have shown that the vast majority (>95%) of the material present in a sample of LB had the postulated structure (*para*-substituted phenyl rings linked by amine groups). By comparing the data for LB with those of EB it was shown that the two had the same skeletal structure, indicating that the structure for EB given in Fig.4.1 is indeed correct. The ^{13}C-NMR spectra for EB is considerably more complicated than that for LB, indicating that there is a number of conformations of the EB molecule. The authors attribute this to the presence of quinoid rings in the EB form which, due to their restricted rotational degree of freedom (as discussed later), cause certain conformations to become inequivalent. Some of these various conformations (often termed 'conformers') are shown in Fig.4.2. The authors also attribute the difference in the complexity of the spectra to the fact that the quinoid rings in EB are not

necessarily located every fourth ring, as indicated in the idealised structure, but may be distributed at varying intervals along the chain. This deviation from the ideal case allows further conformations to be formed from combinations of the various conformers shown in Fig.4.2.

The fully reduced form, LEB, is a white/grey solid that is relatively unstable in air. It is non-conjugated and an insulator. The proposed structure of the purple fully oxidised form, PNB, however, is fully conjugated. The symmetry of the chemical structure of PNB, depicted in Fig.4.1, means that it has two degenerate ground state configurations. This, in theory, makes PNB the 'big brother' of *trans*-PA and implies that it should be able to sustain the formation of solitons. Indeed, Coplin *et al.* [23] report that they have observed soliton feactures in photoinduced absorption studies of the material.

The third oxidation state of polyaniline is the half oxidised emeraldine base - an air stable, electrically insulating blue/purple solid. It is proposed to be semi-conjugated; the conjugation extending over the quinoid ring to the two neighbouring benzenoid rings through the imine nitrogen atoms. The polymeric form of EB is found to be soluble in N-methyl-2-pyrolidine (NMP) [24], m-cresol [25] and conc. sulpuric acid (H_2SO_4) [26]. From these solvents films of polyaniline may be cast and otherwise processed. The polyaniline films cast from NMP remain in the EB oxidation state, whereas the films cast from sulphuric acid are protonated to the emeraldine salt (ES) form (providing the acid is not too concentrated, as the lack of water prevents the acid from dissociating). It has been found that the NMP acts as a plasticiser [27], resulting in the films of EB being far more mechanically robust than those processed in the ES form - hence processing in the EB form is usually the preferred method. These films may then be converted to a conducting form using a protonic acid. The electrical properties of free standing films are still currently

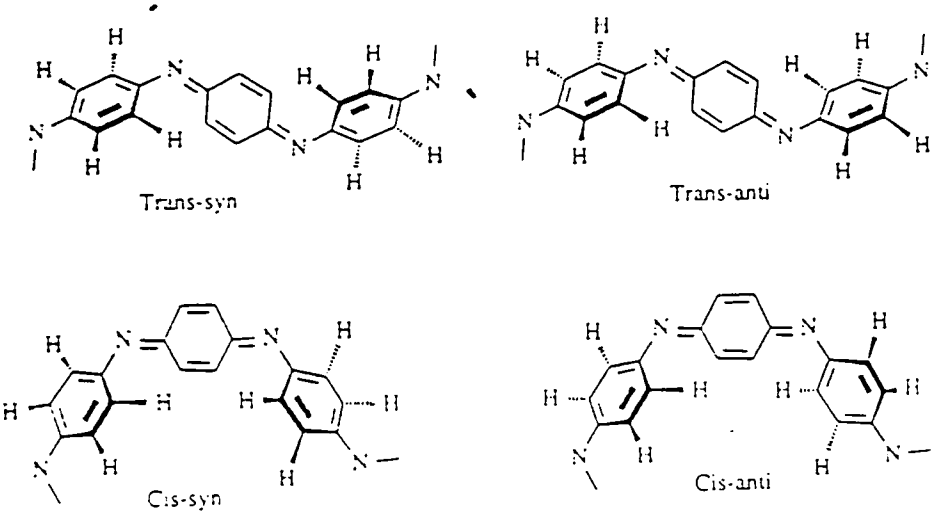

Fig. 4.2 Various conformations possible in EB
(after Kenwright, ref[22]).

being investigated, including stretch orientation of the films with the aim of increasing the conductivity along the stretch axis [27].

The chemical formula given in Fig.4.1 is actually rather simplistic as it presents only a two dimensional representation of the molecule. It is believed that the C_6 rings are forced to twist away from a planar configuration due to the steric hindrance of the hydrogen atoms attached to the ring units [22, 28-32]. The twisting of the rings effectivley reduces the amount of p_z orbital overlap, and hence the extent of π-electron delocalisation along the chain is reduced for EB and PNB. Theoretical investigations into the optimum geometry of the chains has been carried out by several groups, including those of Bredas [33], Epstein [30], and Duke [28, 29] - a balance between the steric hindrance driving the system away from planarity and the reduction of energy by electron delocalisation driving the system towards its planar form. Considerations of the effects of ring rotations with respect to the physical properties of PANi have also been reviewed by Monkman *et al.* [31] .The electronic states of EB will be discussed in the next section of this chapter.

4.1.2 Review of the Optical Properties of Emeraldine Base.

The main method of experimental investigation of the configuration of the elctronic levels of a material is by optical spectroscopy; linear absorption, photoinduced absorption (PIA), photoluminecsence (PL), photoconductivity (PC), and electroabsorption (EA). Relevant reported investigations of emeraldine base will be reviewed in this section, along with the interpretations of the results.

4.1.2.1 Linear Absorption.

The linear optical absorption spectra of EB as measured by Monkman *et al.* [34] is presented in Fig.4.3. All reports of the absorption spectra have the same general shape and peak positions, though the relative heights of the absorption peaks do vary between measurements. The differences that occur may be attributed to the different methods of preparation of the material, and further, the method of preparing the sample for optical spectroscopy.

There have been many theoretical investigations into the origin of these absorption features. The calculations involved in such investigations are complex and hence in practice only short chain oligomers are considered; the results are then extrapolated to the case of the polymeric system. These extrapolations would seem reasonable in the case of EB and LB as they are not fully conjugated; each sub-unit acts independently, much as the oligomeric equivalent. Methods used in calculating the properties of ES must be treated with a little more caution due to the proposed fully conjugated nature of the polymer.

The absorption spectra of such short chain oligomers have been compared with their associated polymeric systems [35, 36], and their similarity has been taken as evidence of the validity of such theoretical extrapolations. With the aim of further extending this comparison between oligomer and polymer for polyaniline, the phenyl capped tetramer [4-(phenylamino)phenyl]-1,4-benzenediamine, whose chemical structure is shown in Fig.4.4, has been included in these electroabsorption investigations. The result of such an experimental comparison should further test the extent to which the theoretical extrapolations are valid.

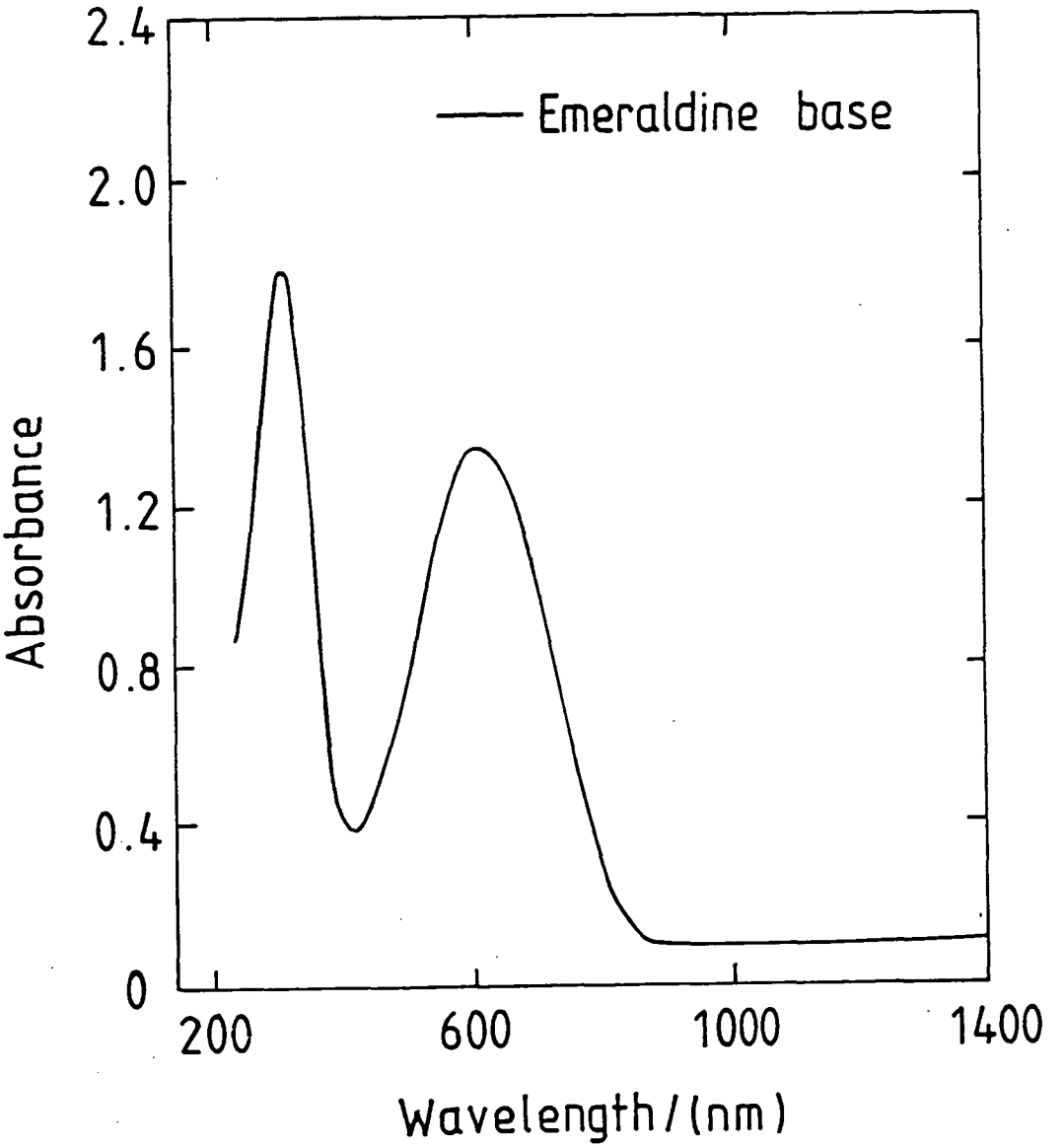

Fig. 4.3 Linear absorption spectrum of emeraldine base, (after Monkman *et al.*[34]).

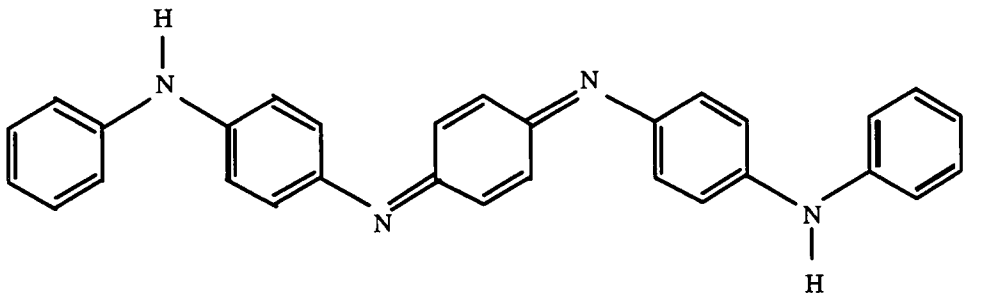

Fig.4.4 Chemical structure of phenyl capped tetramer.

Presented in Fig.4.5 are diagrams of the band structures of oligomeric LB, PNB and EB calculated by Bredas *et al.* [37] using a Valence Effective Hamiltonian (VEH) model. This model neglects electron correlation effects. The fully reduced LB is predicted to have a large optical gap of 3.8 eV, while the band gap of PNB is predicted to be as low as 1.4 eV.

The energy level structure presented for EB is slightly more complicated due to the fact that the unit cell is twice as large. This results in twice as many bands appearing in the structure, with a the resulting band gap of ca. 1.4 eV. This is not the experimentally observed value, implying that the VEH approach is not completely applicable to EB. The problem arises from the nature of the origin of the four bands labeled in the diagram, a, a', b and b'. The first three are located on the benzenoid rings, whereas b', the lowest unoccupied band, is located on the quinoid ring.

This difference in localisation was first identified by Duke *et al.* [28] .They based their discussion of the energy states on a localised orbital approach in terms of the $2p_{\pi}$ atomic orbitals. CNDO (complete neglect of differential overlap) calculations were used, which involve neglecting all interactions except those of nearest neighbours. Within this picture the 3.8 eV excitation of LEB is assigned to a

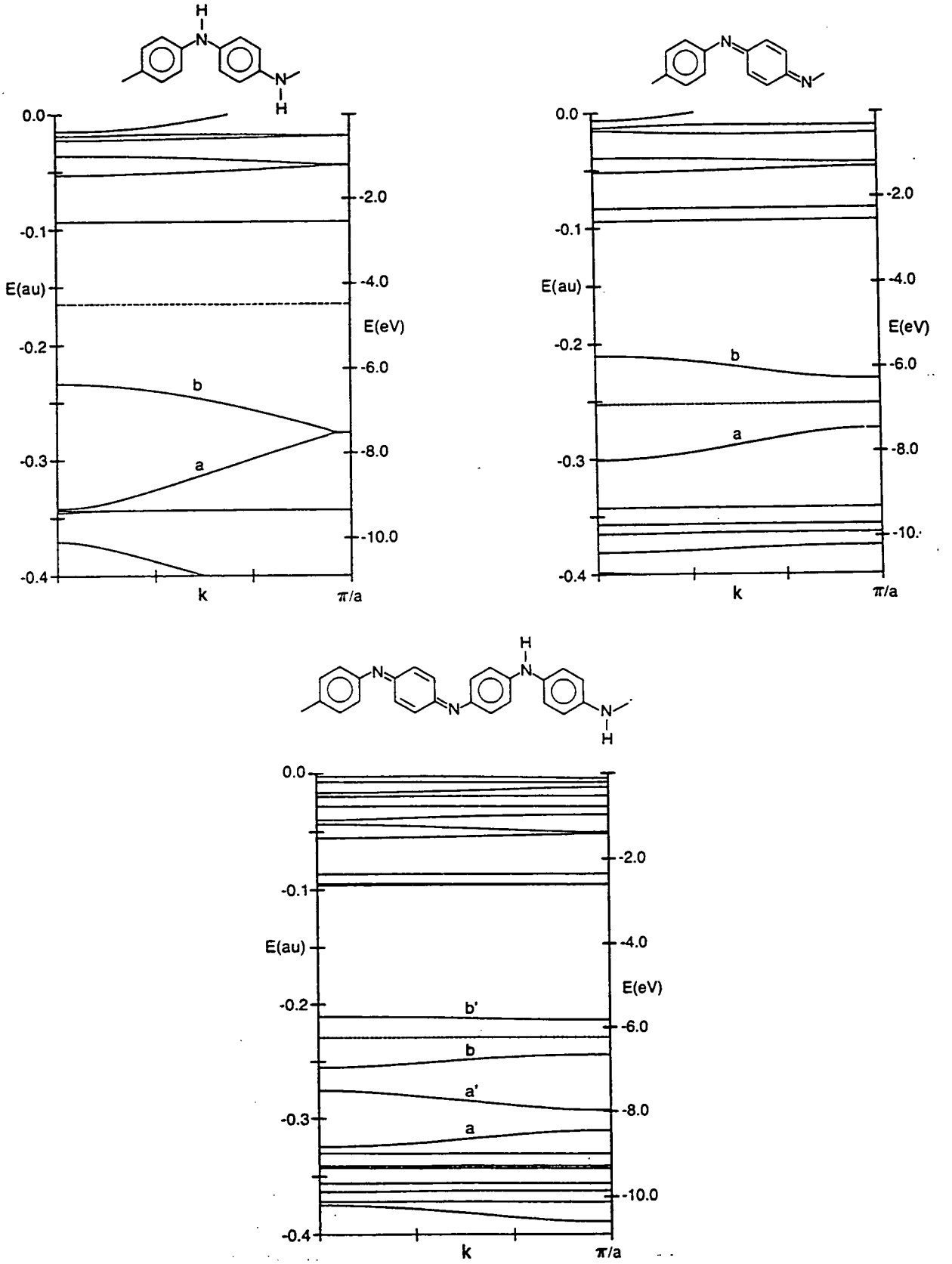

Fig. 4.5 Band structures calculated for the oligomers corresponding to top left - LB, top right - PNB, bottom - EB (after Boudreaux, ref[37]).

π-π* transition on a benzenoid ring. This assignation is confirmed by the presence of such an absorption from the highest occupied molecular orbital (HOMO) to the lowest unoccupied molecular orbital (LUMO) in the oligomers of aniline occurring at a similar energy. (Such transitions are not observed in benzene at these energies due to symmetry considerations). Using this model Duke proposes that the lowest optical excitation of EB should be due to the formation of a self trapped molecular exciton at ca. 2.2 eV. Upon photoexcitation an electron is predicted to be excited to the LUMO of the quinoid ring from the HOMO levels of the two neighbouring benzene rings, as depicted in Fig.4.6. The quinoid ring is then predicted to twist away from its ground state configuration by ca 90°, trapping the state while making it more stable.

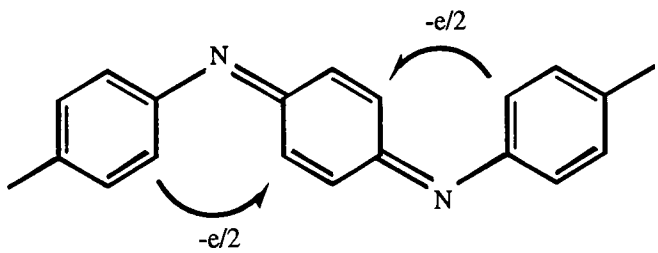

Fig.4.6 Schematic of proposed CT exciton formed upon 2 eV photoexcitation.

The large change in conformation of this ring effectively results in the trapping of the exciton on a particular site. This photoexcitation involves a degree of charge transfer and so is designated a charge transfer exciton, even though the final state is predicted to be symmetrical and hence possesses no permanent dipole moment. Later work by Stafstrom *et al.* [38] using various different theoretical models also predicts the formation of such an exciton upon 2 eV photoexcitation.

4.1.2.2 Photoinduced Absorption.

Photoinduced absorption involves photoexciting a material at (or close to) its optical band gap using a 'pump' beam, and then using a 'probe' beam to scan the spectrum and detect any variations in the absorption coefficient caused by the initial photoexcitation. In practice the pump beam is usually a laser so as to acheive high light intensities, which is then chopped to facilitate the use of lockin techniques.

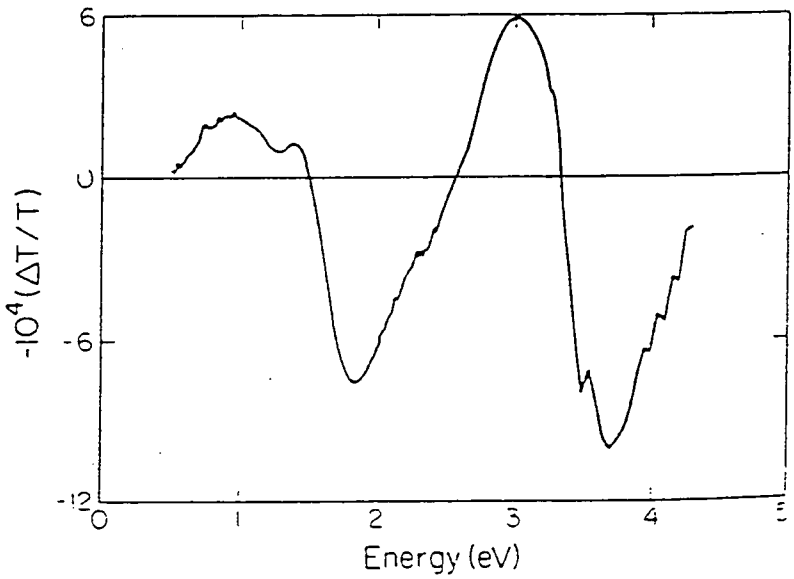

Fig.4.7 Photoinduced absorption spectrum for EB.

The first report of PIA for EB was by Roe *et al.* in '88 [39], the results of which are shown in Fig.4.7. The sample was pumped at 2.54 eV, i.e. into the 'exciton' absorption band. Photoinduced absorptions are seen at 0.9, 1.4 and 3.0 eV, and bleachings at 1.8 and 3.7 eV. From the dependence of the various peaks upon light intensity and chopper frequency, and by analogy with the absorption spectrum of ES, Roe proposed a unimolecular origin for the lower bleaching, and bimolecular processes for the other feactures. They assign the 1.4 and 3.0 eV feactures as being new optically allowed transitions due to the initial pump beam photoproducing

positive polarons, P^+. These polarons are formed upon the decay of an exciton to a pair of positive and negative polarons, P^+ and P^-. The 1.8 eV feacture is assigned to the filling of the molecular exciton states by the pumping laser photons, and the 3.7 eV feacture to the depopulation of the π levels required for the production of the aforementioned polarons. They have no suggestion as to the origin of the 0.9 eV feacture.

An alternative explanation for the results which Roe does not rule out is that the features are due to the formation of a triplet manifold of exciton states.

Stafstrom *et al.* [38] extended their calculations of linear absorption to include the PIA results of Roe, and also tend to assign the features to polaron and bipolaron formation, although they too cannot rule out the formation of triplet excitons. Nor could their calculations explain the feature at 0.9 eV.

EB has also been investigated using the technique of photoinduced infrared absorption (PIIRA). McCall *et al.* [40] use their results from this method to estimate the effective mass of the proposed photogenerated polaron, with the result $M_{pol} \sim 60m_e$. They propose that this high effective mass is due to the polaron being associated with changes in the phenyl ring torsion angles - ring flipping - as mentioned previously. The photogenerated species are observed as having long lifetimes - up to 2 hours when measured at 80 K, becoming shorter with increasing temperature. Again this is consistent with the idea of the polaron being associated with ring flipping, as the low temperatures may be considered as 'freezing out' the rotational degrees of freedom and 'freezing in' any photoproduced ring torsional polarons. Monkman *et al.* [31] report a phase transition in EB at ~190 K, which they assign to the temperature below which ring rotational degrees of freedom are restricted.

Kim *et al.*[12] also performed PIIRA spectroscopy investigations on EB, and found different responses when pumping into the 2 eV and the 4 eV absorption

bands. Drawing comparisons between the doping induced IR modes and the photoinduced IR modes upon 2 eV pumping Kim suggests that the 2 eV absorption results not in the exciton proposed by Duke [28, 29], but rather an n-π^* transition [12, 13] - analogous to the process that occurs upon protonic doping of EB. An n-π^* transition involves the promotion of a lone pair electron from an imine nitrogen atom adjacent to a quinoid ring to the anti-bonding π^* orbital of that ring, as depicted in Fig.4.8. Kim points out that for reasons of symmetry the system must be highly disorded for this excitation to be allowed.

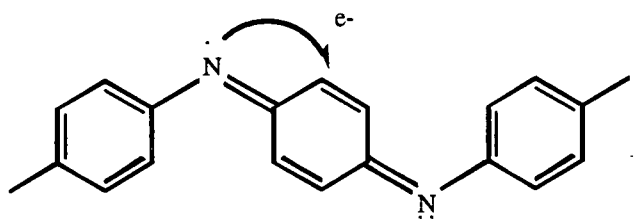

Fig.4.8 Schematic of suggested n-π^* transition in emeraldine base.

It is this requirement for disorder that led Phillips *et al.* [14] to contest this assignation of the 2 eV absorption feacture. The preparation route of the EB samples used by Phillips in optical investigations of the polymer resulted in films of semi-crystalline morphology. In comparing the relative amplitude of the absorption peaks with those of previously reported amorphous films and finding them similar, Phillips concluded that disorder played no part in the absorption profile of the 2 eV absorption peak. This, he argues, rules out the possibility of the 2 eV absorption being due to a disorder allowed photoexcitation, such as an n-π^* transition.

In 1990 McCall *et al.* [41] presented an extensive report on spectroscopy and defect states in polyaniline, concentrating on absorption and PIA of LB and EB.

They report their first PIA spectra for optical pumping into the 4 eV absorption band, and contrasting with the results if Kim *et al.* report that there is no significant difference from 2 eV pumping. From this, and other results, they propose a comprehensive model for the photoexcitation processes that occur within the LB and EB forms of polyaniline. The schematic representation of the five main excited states proposed are presented in Fig.4.9 depicting the hole polaron, the electron polaron, the negative polaron trapped at a quinoid, a hole polaron trapped near a quinoid, and the exciton. The exciton they propose is of the same form as that of Duke.

Once again it must be remembered that these are merely schematic representations of the configurations; it is expected that the charges involved will be more delocalised than indicated on the diagram. Theoretical calculations propose ring torsion angle distortions and bond length alterations associated with the excitations, in the manner outlined previously.

The proposed photoexcitations and relaxations for LB and EB in terms of the excited states are depicted schematically in Fig.4.10. The decay processes for excitations above the band gap in EB are predicted to be very similar as those for LB, though no luminescence is observed in EB due to the quinoid sites providing non-radiative routes of relaxation. The X* state marked in these diagrams indicates an excited exciton state, whereas X^+ represents a stabilised, longer lived exciton state - i.e. an exciton after the self trapping process has occurred.

Sariciftci *et al.* [42] have since carried out further PIA experiments upon polyaniline samples that have been cast from *m*-cresol, which, they claim, gave EB samples of higher quality. Using this EB higher resolution PIA spectra were obtained, distinctly resolving the peaks at 1.47 and 0.9 eV as well as the bleaching at 0.87 eV while pumping into the 2 eV absorption band. These results are in agreement with the first reports of PIA by Roe. They still stress, however, that the

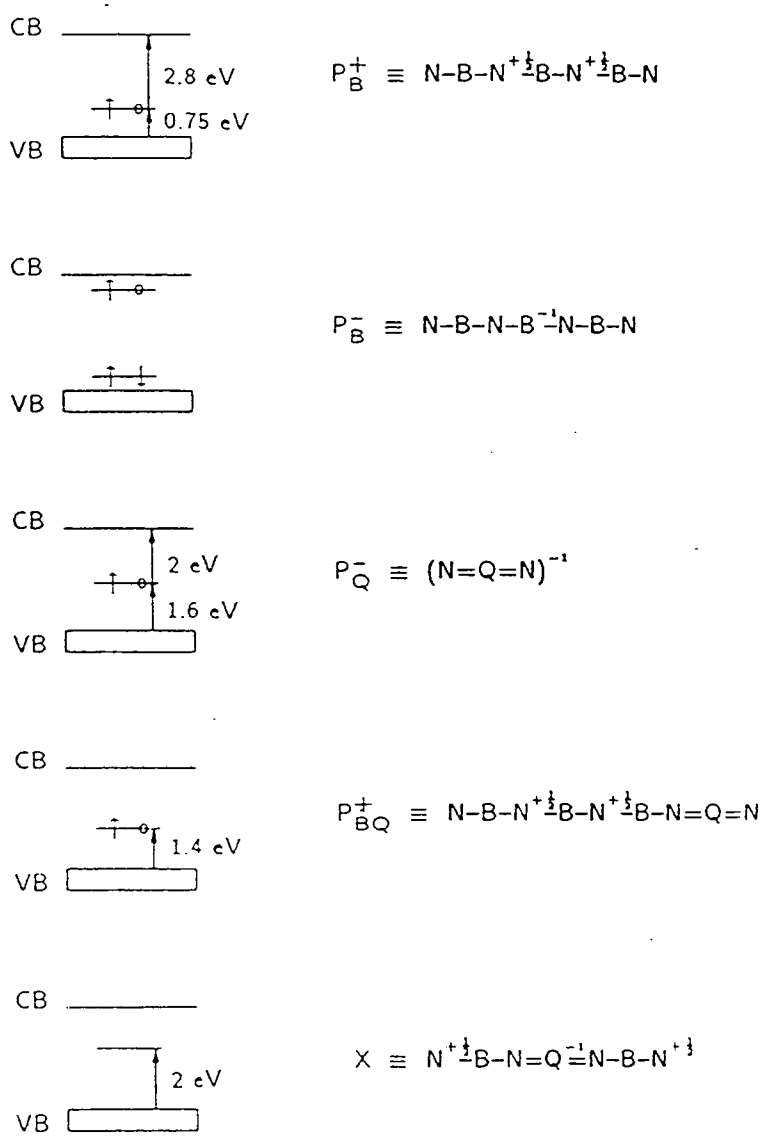

Fig. 4.9 The five main excited states of polyaniline,
as suggested by McCall, ref[41].
(Key: B-benzene ring, Q-quinoid ring, N-nitrogen, X-exciton).

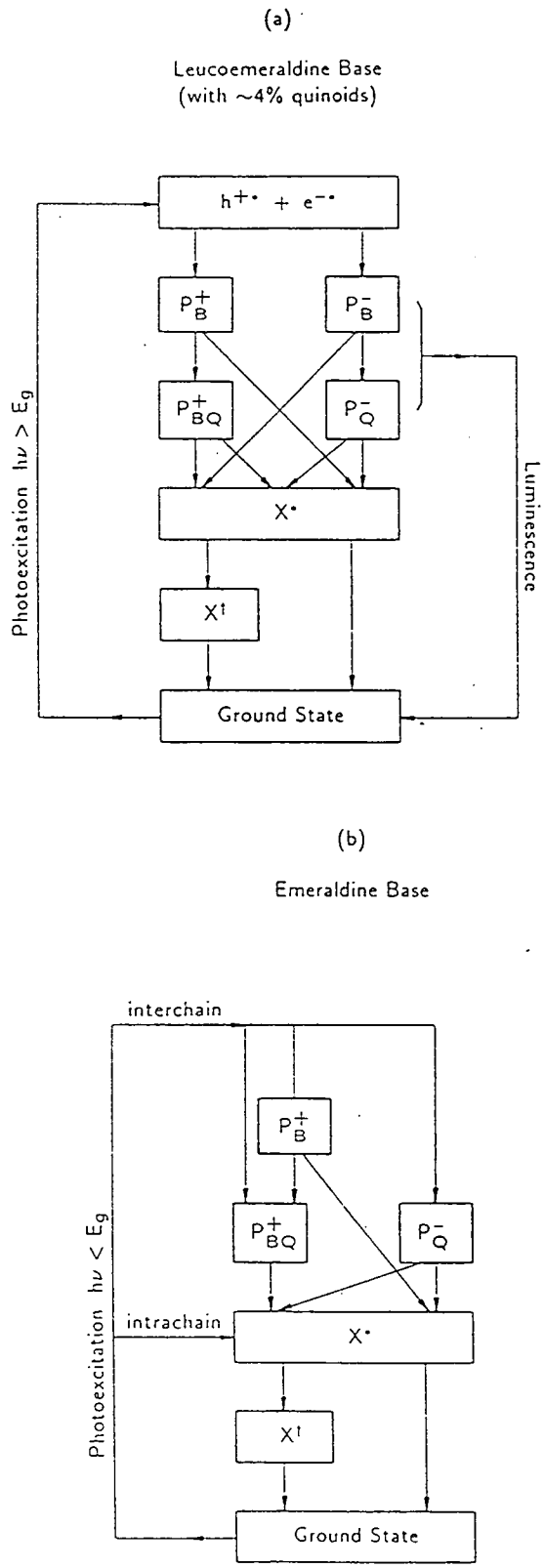

Fig. 4.10 Schematic of the relaxation routes of photoexcitations a) above the optical gap of LB, and b) just below the optical gap of EB - after McCall, ref[41].

occurrence of long lived triplet exciton states cannot be ruled out as being the origin of these photoinduced feactures.

4.1.2.3 Photoconductivity.

There have also been investigations into the photoconductive (PC) properties of EB [14, 43]. As its name implies, PC spectroscopy is the observation of the variation of the conductivity of a sample upon illumination with light of a specific wavelength. The PC reports of EB are fairly consistent; very small PC for the 4 eV absorption, with even less for the 2 eV peak. The variations are so small that some groups have attributed their origin to heating effects. Such low PC signals have been attributed to the low mobility of any carriers produced due to their association with ring torsion defects. The smaller signals associated with the 2 eV absorption are attributed to the fact that the excitons that are photoproduced are energetically trapped, and even when free must dissociate before being able to transfer charge.

4.1.3 Ring Rotations in Polyaniline.

Some of the first considerations of phenyl ring containing polymers simply applied the SSH Hamiltonian to the system in question, the results of which had varying degrees of accuracy. More recent approaches have included the role of phenyl ring torsion angle in determining the nature of the ground and excited states. This has been especially relevant in the case of polyaniline since the presence of nitrogen atoms between the phenyl rings means that the rings have a relatively large degree of rotational freedom. The ring torsion angle is of great importance in the determination of the electronic levels of any ring-containing π-conjugated system. As the angle between rings increases, the degree of π orbital overlap decreases, and

hence alters the electronic structure of the system. Delocalisation of the electrons in a system affords a reduction in the potential energy and so, if there were no other factors involved, all the rings in a ring-containing polymer would lie in the same plane so as to increase π orbital overlap, and hence decrease the total energy of the system. This, however, is not the case for polyaniline as there is substantial steric repulsion that favours ring conformations out of the nitrogen plane. Several groups have carried out theoretical studies to investigate the effect of ring torsion angle upon the electronic states of the simplest forms of polyaniline - LB and PNB [28-30, 33].

The most extensive of these investigations has been carried out by Ginder and Epstein [30], who introduced a ring torsion order parameter with which they modelled the physical properties of the LB and PNB molecules. They calculated a minimum in potential energy as having a structure of alternate rings being twisted away from the plane of the nitrogens by $\approx 56°$ and $\approx -56°$ respectively. In such a conformation, both LB and PNB have two degenerate ground states, and as such should be able to support the fromation of solitons. Indeed, there have been reports of experimental evidence to imply the existence of solitons in PNB [23].

The modelling of the ring rotations in EB, however, is made more complicated by the nature of the nitrogen-ring bonding. The formation of a double bond between the nitrogens and the respective quinoid rings reduces the degree of freedom with which this ring can rotate away from the nitrogen plane, and hence a simple alternating ring torsion angle model cannot be employed. The significance of the ring rotations in the electronic structure of EB is, however, evident in the proposed exciton model of the 2 eV absorption, as described in the previous section.

The ring torsion approach to modelling the excited states of LB and PNB also predicts the formation of polaron states on the chain; an excitation that results in a change in ring torsion angle may affect the extent of π-electron overlap and

hence create a state at mid gap. The effective mass of such a state would be large and the mobility low due to its association with a large chain deformation. This is in good agreement with the experimentally derived large effective mass M_{pol}~$60m_e$ mentioned earlier.

From this evidence it would seem that ring rotations play an important role in determining the physical properties of polyaniline. The existence of the long lived excited states that have been attributed to hindered ring rotations has even led to the suggestion that polyaniline may used as an optical storage medium at some time in the future [15].

4.1.4 Emeraldine Salt.

Emeraldine salt is the protonated form of EB, and has been receiving a great deal of attention since the discovery of its high degree of electrical conductivity [44].

Upon doping of EB using a protonic acid - hydrochloric acid for example - the emeraldine salt (ES) form of polyaniline is formed. This form of polyaniline is proposed to be fully conjugated, and the conductivity has been noted to increase by a factor of 10^{11}, reaching 1 Scm^{-1} [44].

In 1987 Stafstrom *et al.* [44] proposed that doping of EB leads to the segregation of unprotonated and fully protonated domains. Within the fully protonated domains it is proposed that bipolarons are formed initially, which then separate to form two polarons - as depicted in Fig.411. The polarons are predicted to stabelise in the form of a lattice, and it is proposed that this polaron lattice is the origin of the metallic characteristics of ES. A diagram of the band structure calculated for ES is shown in Fig.4.12. It shows the half filled polaron band, with a finite density of states at the Fermi energy indicating metallic behaviour in these fully

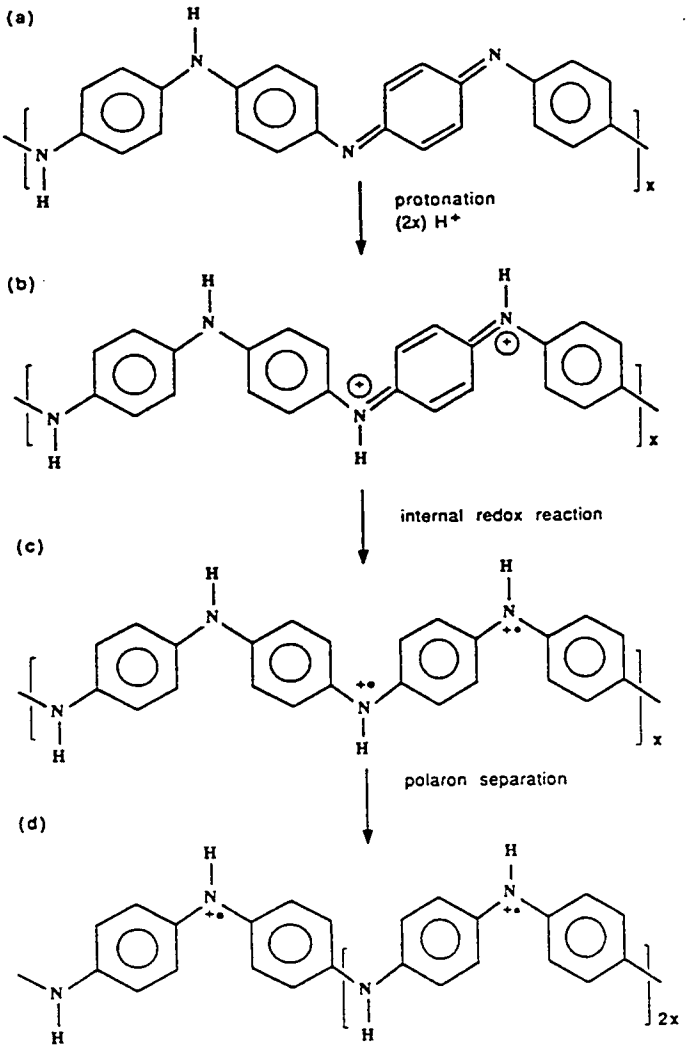

Fig. 4.11 Protonation leading to the formation of a polaron lattice in ES (after Stafstrom, ref[44]).

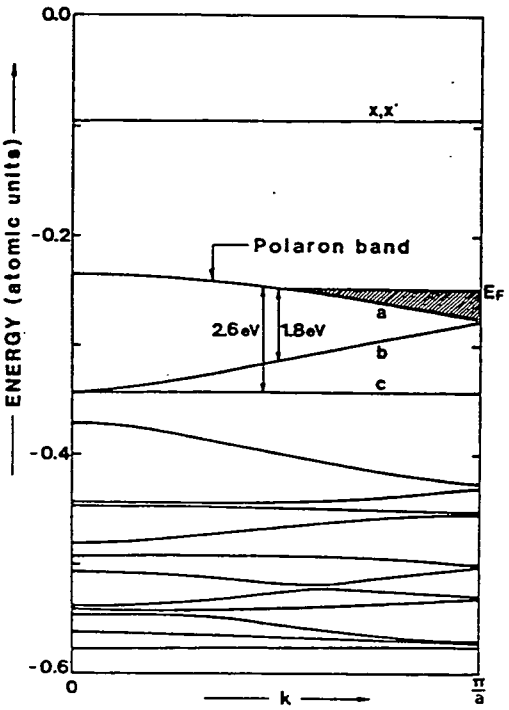

Fig 4.12 Energy level structure calculated for ES - showing 'metallic' polaron band (after Stafstrom, ref[44]).

protonated regions. Within this model the resulting conductivity values measured for ES are predicted to be limited by percolation effects between the protonated and unprotonated regions of the system.

4.1.5 Summary.

An overview of the chemical structure and physical properties of polyaniline has been presented. There seems to be general agreement over the photoexcitations in EB; the 3.8 eV absorption is associated with a π-π^* transition located on a benzenoid ring, and the 2 eV absorption with a charge transfer exciton associated with a ring rotation [28]. The n-π^* transition proposed by Kim [12, 13] has been dismissed by some, though there is no conclusive proof either way. After photoexcitation, the excited states are proposed to decay back to the ground state via some combination of exciton or polaron formation. Unlike LB, EB is not observed to photoluminesce due to the high concentration of quinoid rings.

4.2 Polysquaraine

The band gap of most conjugated polymers is generally rather large, usually between 1.5 and 4.0 eV. Having a band gap smaller than this would be advantageous as the reduced optical gap could allow such polymers to be utilised as infra red detectors and sensors.

With this in mind Havinga *et al.* [45, 46] set out to develop new families of low energy band gap conjugated polymers - polysquaraines and polycroconaines. The novel idea behind their development is the concept that the space charge effects produced upon the formation of a chain of regularly alternating donor and acceptor moieties will reduce the energy gap. If the donor and acceptor regions are extended the system can be considered similar to an inorganic n-i-p-i super lattice structure. The actual band gap is not changed at any point, but a small gap, E_g, is found if the spatial alternation of the level of the bands is taken into account - as depicted in Fig.4.13. If the HOMO levels of the donor and the LUMO levels of the acceptor are energetically close a small effective band gap E_g will result. In order to achieve strong band curvature strong donors and acceptors are required such that there is appreciable charge transfer in the ground state of the material. To this end squaric acid and croconic acid have been used as the acceptor-like moieties, with an ample choice of donor moieties available. The idealised structure of the particular polysquaraine studied in this thesis is shown in Fig.4.14.

There are analogies to be drawn between emeraldine base and polysquaraine. Both may be decribed as 'AB' type polymers, indicating a regular alternation of two different structures within the polymer chain. This is obvious for polysquaraine, as it has been designed with this structure in mind. From the structure of EB depicted in Fig.4.1 it is clear that EB may be described as an AB polymer in two ways. As with all oxidation states of PANi it may be described as a regular alternation of phenyl

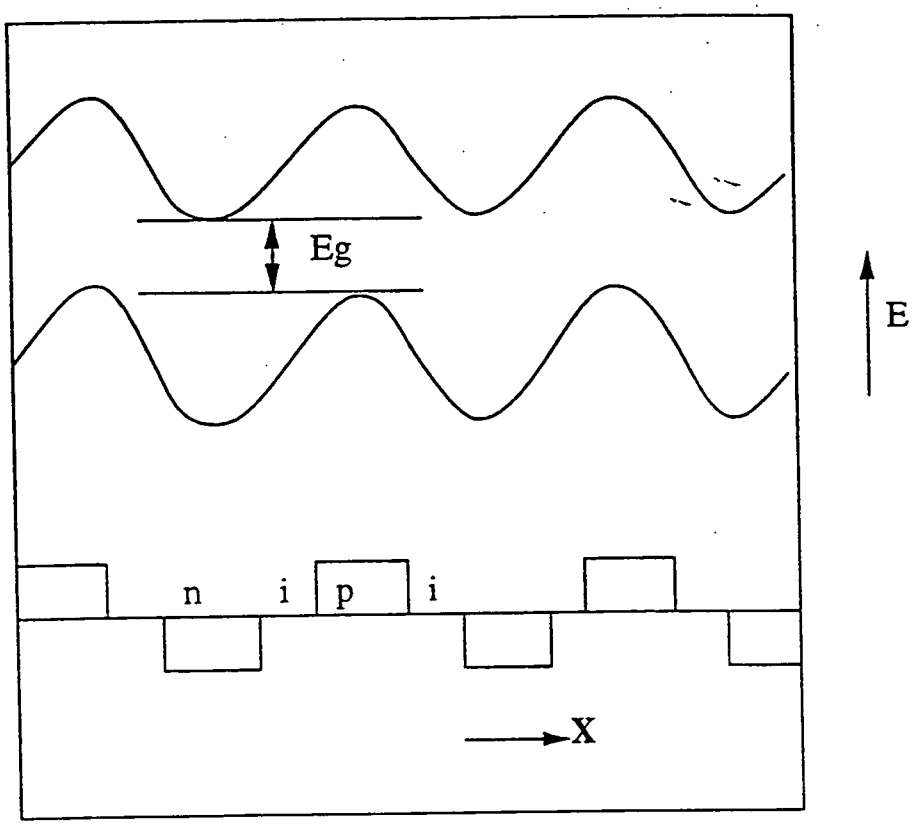

Fig. 4.13 Band structure of an n-i-p-i quantum well structure - a model for polysquaraine.

rings and nitrogen atoms. EB may also be considered as an alternation of three benzenoid rings with their associated amines, and quinoid rings with their associated imines. In this context the 2 eV exciton proposed by Duke [28] may be thought of as occuring from donor (A) to acceptor (B), allowing EB to be thought of as having some degree of charge transfer characteristics - analogous to polysquaraine. One of the main differences between the two polymers is the fact that EB is semi-conjugated, while polysquaraine is proposed to be fully conjugated - a fact that should result in a marked difference in the EA response of the two materials.

Polysquaraine is relatively new and hence there has been little work reported in the literature. The absorption spectrum of the material taken during the initial characterisation, Fig.4.15, indicates an optical band gap of around 1.3 eV. This is slightly smaller than that for polyacetylene at 1.4 eV, indicating that the donor-acceptor concept does in fact produce a small optical gap. Gel permeation chromatography (GPC) studies have indicated that the chain length of the material is around 15 - 20 donor-acceptor repeat units [45,46]. The material is air stable, making it easy to work with - though it does seem to deteriorate with time when exposed to light. Being soluble in chloroform meant that optically thin films were easily prepared.

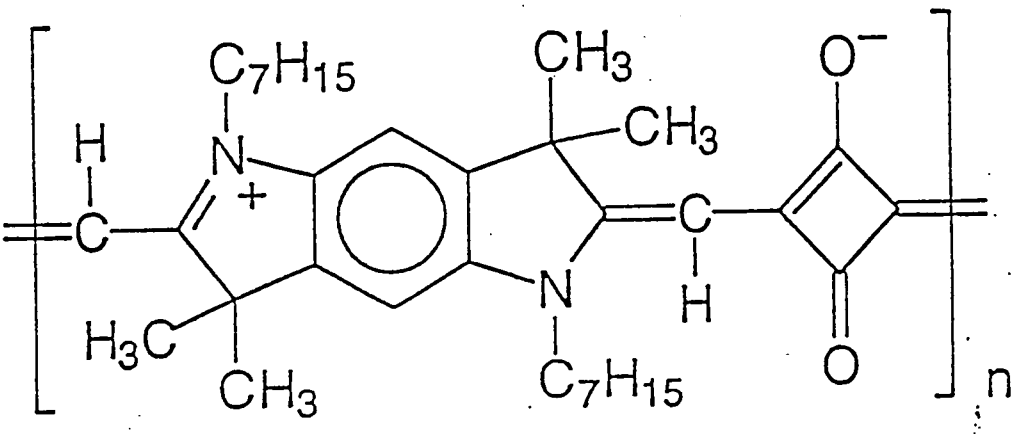

Fig. 4.14 Chemical structure of polysquaraine.

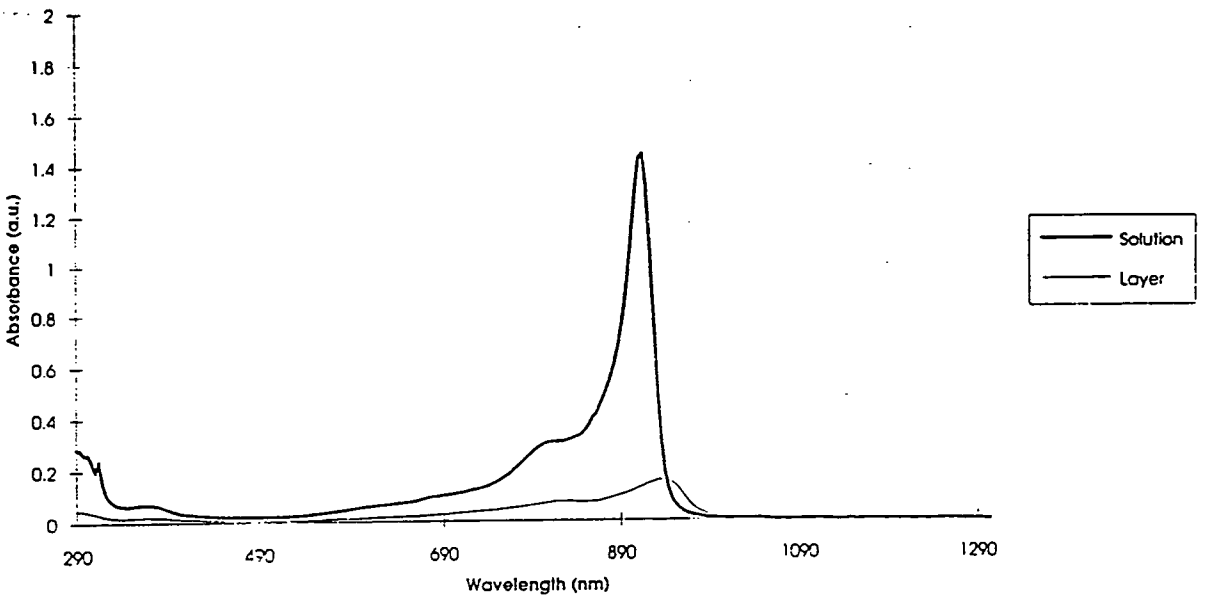

Fig. 4.15 Absorption spectrum of polysquaraine,
data from E. E. Havinga , Einhoven.

References

1. Letherby, H., J. Chem. Soc, 1862. **15**: p. 161.
2. Green, A.G. and A.E. Woodhead, J. Chem. Soc. Trans, 1910. **97**: p. 2388.
3. Grenn, A.G. and A.E. Woodhead, J. Chem. Soc. Trans, 1910. **101**: p. 1117.
4. Constantini, P., G. Belorgey, M. Jozefowicz, and R. Buvet, Comm. Symp. Int. Chim. Macromol. IUPAC. Prague, 1965: p. A481.
5. Doriomedoff, M., F.H. Cristofini, R. DeSurville, M. Jozefowicz, L.T. Yu, and R. Buvet, J. Chim. Phys, 1971. **68**: p. 1055.
6. Jocefowicz, M., L.T. Yu, G. Belorgey, and R. Buvet, J. Polym. Sci, 1967. **16**: p. 2931.
7. Nakajuma, T. and T. Kawagoe, Synth. Met, 1989. **28**: p. C629.
8. Diaz, A.F. and J.A. Logan, J. Electroanal. Chem, 1980. **11**: p. 11.
9. MacDiarmid, A.G., J.-C. Chiang, M. Halpern, W.S. Huang, S.L. Mu, N.L.D. Somasisi, W. Wu, and S.I. Yaniger, Mol. Cryst. Liq. Cryst, 1985. **121**: p. 173.
10. MacDiarmid, A.G., N.L.D. Somasisi, W.R. Salaneck, I. Lunsdtrom, B. Liedberg, M. Hasan, R. Erlandsson, and P. Konrasson, . Springer Series in Solid State Sciences. Vol. 63. 1985, Berlin: Springer.
11. MacDiarmid, A.G., J.-C. Chiang, A.F. Richter, N.L.D. Somasisi, and A.J. Epstein, *Conducting Polymers*, L. Acaer, Editor. 1987, D. Reidel Pub. Co. p. 105.
12. Kim, Y.H., C. Foster, J. Chiang, and A.J. Heeger, Synth. Met., 1989. **29**: p. E285.
13. Kim, Y.H., S.D. Phillips, M.J. Nowak, D. Spiegel, C.M. Foster, G. Yu, J.C. Chiang, and A.J. Heeger, Synth. Met., 1989. **29**: p. E291.

14. Phillips, S.D., G. Yu, C. Y, and A.J. Heeger, Phys. Rev. B, 1989. **39**(15): p. 10702.

15. Epstein, A.J. and A.G. MacDiarmid, Synth. Met, 1995. **69**: p. 179.

16. Baughman, R.H., J.F. Wolf, E. Eckhardt, and L.W. Schaklette, Synth. Met, 1988. **25**: p. 121.

17. Schaklette, L.W., J.F. Wolf, S. Gould, and R.H. Baughman, J. Chem. Phys, 1988. **88**: p. 3955.

18. Vachon, D.J., R.O. Angus Jr, F.L. Lu, M. Nowak, H. Schaffer, F. Wudl, and A.J. Heeger, Synth. Met, 1987. **18**: p. 297.

19. Wudl, F., R.O. Angus Jr, F.L. Lu, P.M. Allemand, D.J. Vachon, M. Nowak, Z.X. Liu, and A.J. Heeger, J. Am. Chem. Soc, 1987. **109**: p. 3677.

20. Ohsaka, T., Y. Ohnuki, N. Oyama, G. Katagiri, and K. Kamisaka, J. Electroanal. Chem, 1984. **161**: p. 399.

21. Furakawa, Y., F. Ueda, H. Y, I. Harada, T. Nakajuma, and T. Kawayoe, Macromolecules, 1989. **21**: p. 1297.

22. Kenwright, A.M., W.J. Feast, P.N. Adams, A.J. Milton, A.P. Monkman, and B.J. Say, Polymer, 1992. **33**(20): p. 4292.

23. Coplin, K.A., J.M. Leng, R.P. McCall , and A.J. Epstein, Synth. Met, 1993. **55-57**: p. 7.

24. Angelopolous, M., G.E. Asturias, S.P. Emer, A. Ray, E.M. Scher, A.G. MacDiarmid, M. Akhtar, Z. Kiss, and A.J. Epstein, Mol. Cryst. Liq. Cryst, 1988. **160**: p. 151.

25. Cao, Y., P. Smith, and A.J. Heeger, Synth. Met, 1992. **48**: p. 91.

26. Andreatta, A., Y. Cao, J.-C. Chiang, A.J. Heeger, and P. Smith, Synth. Met, 1988. **26**: p. 383.

27. Milton, A.J., *Structural Properties of Polyaniline Films*, PhD Thesis. 1993, Durham University: Durham.

28. Duke, C.B., E.M. Conwel, and A. Paton, Chem. Phys. Lett, 1986. **131**(1-2): p. 82.

29. Duke, C.B., A. Paton, E.M. Conwell, W.R. Salaneck, and I. Lundstrom, J. Chem. Phys, 1987. **86**(6): p. 3414.

30. Ginder, J.M. and A.J. Epstein, Phys. Rev. B, 1990. **41**(15): p. 10674.

31. Monkman, A.P., P.N. Adams, A. Milton, M. Scully, S.J. Pomfret, and A.M. Kenwright, Mol. Cryst. Liq. Cryst., 1993. **236**: p. 189.

32. Sjogren, B. and S. Stafstrom, J. Chem. Phys, 1987. **88**(6): p. 3840.

33. Stafstrom, S. and J.L. Bredas, Synth. Met, 1986. **14**: p. 297.

34. Monkman, A.P. and P.N. Adams, Synth. Met, 1991. **40**: p. 87.

35. Rodrigue, D., M. Domingue, J. Riga, and J.J. Verbist, Synth. Met, 1993. **55-57**: p. 4802.

36. Javadi, H.H.S., S.P. Treat, J.M. Ginder, J.F. Wolf, and A.J. Epstein, J. Phys. Chem. Solids., 1990. **51**(2): p. 107.

37. Boudreaux, D.S., R.R. Chance, J.F. Wolf, L.W. Shacklette, J.L. Bredas, B. Themas, J.M. Andre, and R. Silbey, J. Chem. Phys, 1986. **85**(8): p. 4584.

38. Stafstrom, S., B. Sjorgen, and J.L. Bredas, Synth. Met., 1989. **29**: p. E219.

39. Roe, M.G., J.M. Ginder, P.E. Wigen, A.J. Epstein, M. Angelopoulos, and A.G. MacDiarmid, Phys. Rev. Lett, 1988. **60**(26): p. 2789.

40. McCall, R.P., M.G. Roe, J.M. Ginder, T. Kusumoto, A.J. Epstein, G.E. Asturias, E.M. Scherr, and A.G. MacDiarmid, Synth. Met., 1989. **29**: p. E433.

41. McCall, R.P., J.M. Ginder, J.M. Leng, H.J. Ye, S.K. Monahar, J.G. Masters, G.E. Asturias, A.G. MacDiarmid, and A.J. Epstein, Phys. Rev. B, 1990. **41**(8): p. 5202.

42. Sariciftci, N.S., L. Smilowitz, Y. Cao, and A.J. Heeger, J. Chem. Phys, 1993. **98**(4): p. 2664.

43. McCall, R.P., J.M. Ginder, M.G. Roe, G.M. Asturias, E.M. Scherr, A.G. MacDiarmid, and A.J. Epstein, Phys. Rev. B, 1989. **39**(14): p. 10174.

44. Stafstrom, S., J.L. Bredas, A.J. Epstein, H.S. Woo, D.B. Tanner, W.S. Huang, and A.G. MacDiarmid, Phys. Rev. Lett, 1987. **59**(13): p. 1464.

45. Havinga, E.E., W.T. Hoeve, and H. Wynberg, Synth. Met, 1993. **55**(1): p. 299.

46. Havinga, E.E., W.T. Hoeve, and H. Wynberg, Polym. Bull., 1992. **49**(1-2): p. 119.

Chapter 5.

Experimental Procedures

This chapter contains three main sections describing the experimental techniques involved in the measurement of electroabsorption signals. The first section describes the preparation of the samples; cleaning of substrates, preparation and spinning of polymer solutions, and deposition of electrodes. Section two is concerned with the EA spectrometer itself - its design and construction. Following this there is a brief description of the methods used for measuring the thickness and absorption spectra of the films, as this data is required in the analysis of the EA spectra.

5.1 Sample Preparation

5.1.1 Chemical Synthesis

The chemical synthesis of the polymeric and oligomeric forms of emeraldine base will be briefly outlined here, as they were synthesised in Durham. The chemical synthesis route of the polysquaraine will not be included, as it was synthesised in the Philips laboratories, Einhoven - a description of the preparation route may be found in the literature [1, 2].

5.1.1.1 Polyemeraldine Base

12.96 g (0.100 mol) of aniline hydrochloride were disolved in 150 ml of distilled water and stirred in a jacketed reaction vessel at a temperature of 0 °C. 28.5 g (0.125 mol) of ammonium persulphate were then dissolved in 80 ml of distilled water and this solution added dropwise to the reaction mixture over a period of 4 h. After stirring for a total of 24 h the reaction mixture was filtered under vaccum and washed with 3x100 ml of water. The filter cake was then stirred in 33 % aqueous ammonia solution (to deprotonate the polyaniline) for 8 h before filtering, washing with 2x100 ml of water followed by 100 ml of isopropanol, and drying under vaccum at 60 °C to give the emeraldine base form of polyaniline in approximately 90 % yield.

The molecular weight of the polymer used exceeded a minimum value of about 30 000, as measured by gel permeation chromatography, using polyvinylpyridine as molecular weight standards in solutions containing 0.1 % lithium chloride in N-methyl-2-pyrrolidone. The use of solution state ^{13}C-NMR to further characterise the chemical structure of the material has been described in section 4.1.1.

5.1.1.2 Oligomeric Emeraldine Base

The structure of the oligomeric form of emeraldine base form of the oligomer [4-(phenylamino)phenyl]-1,4-phenyldiamine is shown in Fig. 4.4. It was first synthesised by Honzl in 1968 [3], and the preparation in Durham used a modified version of this preparation.

To produce the LB form of the oligomer the following synthesis route was used. 0.2 g of 2,5-Dioxo-1,4-cyclohexanedicarboxylic acid (1 mmol, 200 g/mol) and 0.55 g of N-phenyl-1,4-phenylenediamine from Aldrich (3 mmol, 184.24 g/mol) were mixed in 30 ml of degassed m-cresol. The mixture was heated to 80 °C in an

oil bath and refluxed for three days under nitrogen, followed by overnight exposure to air at room temperature. 100 ml of diethyl ether was then added, and a solid collected by filtration from the resulting mixture. Washing with diethyl ether afforded a pale blue-grey powder, which was recrystallised in dioxane. This LB oligomer was then converted to the EB oxidation state via oxidation with silver oxide. 150 mg of the LB oligomer (0.34 mmol, 442 g/mol) was added to 50 ml of THF at room temperature. 78 mg of silver(I) oxide Ag_2O (0.37 mmol, 231.74 g/mol) was added and the mixture left stirring for 48 hrs. The solution was then filtered and the THF removed by distillation. The residue was a blue solid, as expected for EB. The sample was characterised using FAB (fast atomic bombardment) mass spectroscopy (yielding m.w. 441), and IR absorption spectroscopy. The use of FAB, as opposed to EI (electronic impact) mass spectroscopy, allowed the EB form to be analysed without the sample being reduced back to the LB form.

5.1.2 Sample Construction

A diagram of the sample configuration used is shown in Fig. 5.1. The substrate of either glass or sapphire was coated with a thin film of the polymer, which in turn had a set of interdigitated electrodes deposited on top. Sapphire was used due to its high thermal conductivity combined with transparency in the UV - glass was used merely as a cheap alternative.

The first stage of preparation was the cleaning of the substrate to remove any grease or particles form its surface. This was achieved by placing substrates in an ultra-sonic bath, using cleaning solutions of first water and detergent, then water, then acetone - each for a duration of half an hour. The substrate was then dried of acetone using a nitrogen gun - a process that was found to prevent smears occuring.

The thin films of polymer were deposited on the substrates by spinning from solution - a detailed discussion of this topic may be found in ref.[4]. This process required the polymer to be homogenised in solution. For emeradine base and the tetramer the solvent used was N-methyl-2-pyrrolidine (NMP), and for polysquaraine, chloroform ($CHCl_3$). After preparing a solution of around 3 % by weight, it was homogenised using an Ultra-Turrax T25 homogeniser, then centrifuged at 4000 rpm for one hour. A few drops of solution were then pipetted onto the substrate on the spinner, and the spinning speed slowly increased until the surface tension of the film was overcome leaving a thin uniform film in the centre of the disc with a thicker ring around the edge. This thicker ridge was often removed using the corner of a paper towel to enable faster drying of the film. The films were better left to dry while still being being spun to prevent the migration of solution at the edge of the film back to the centre. The films containing NMP could take up to four hours to dry if left, and so drying was often assisted with judicious use of a hot air gun. The films of EB and tetramer produced in this way were uniform, without grains or pinholes.

The same preparation was used for the polysquaraines in chloroform - though even after this treatment the films still had a slightly granular appearance, as though many small crystallites had formed upon the evaporation of the solvent. Despite this, the majority of the film's composition was amorphous, and in the main, pinhole free.

The electrodes used for these investigations were interdigitated gold electrodes (as depicted in Fig. 5.1) with a finger spacing of 160 μm. The advantage

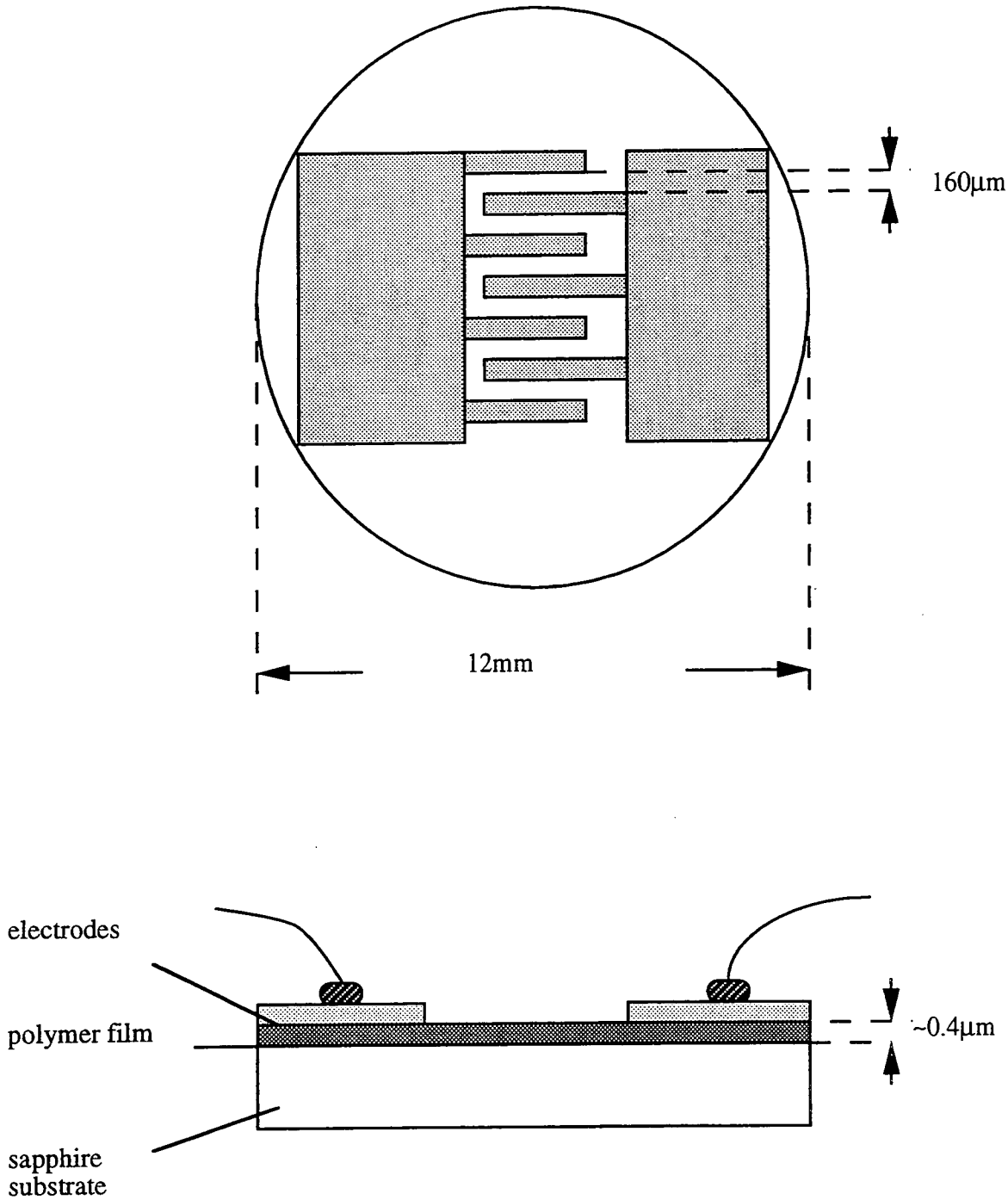

Fig. 5.1 Sample configuration

of using electrodes of this configuration, as opposed to just a single slit, is that the large light throughput results in a higher signal to noise ratio.

Originally these electrodes were deposited on the substrates via the process of chemical etching. This consisted of spinning a thin layer of photoresist on top of the substrate, then exposing the photoresist to UV negative image of the required electrodes. The photoresist image of the electrodes was removed using a suitable etching fluid. A thin layer of gold was deposited on the substrate using the technique of thermal evaporation deposition. The remaining photoresist was removed using an appropriate etching fluid, thus removing the gold that had been deposited on top of it and leaving an image of the electrodes on the substrate. Due to the narrow finger spacing required to achieve the high electric fields necessary in these experiments it took some time to perfect this technique. Once perfected on glass substrates the technique was used to form electrodes on sapphire. It was found, however, that the solvents used in the preparation of the polymer films tended to remove the electrodes from the polished sapphire surface. Attempts were made to improve the gold adhesion - including using a thin layer of chrome under the gold and chemically roughening the sapphire by slight etching with hydroflouric acid - with no positive results.

The problem of electrode adhesion was overcome by the acquisition of several sets of evaporation shadow masks in the form of the required electrodes. Using these masks it was possible to deposit the electrodes on the surface of the polymer films. It is possible that the heat involved in the deposition of the gold onto the polymer surface may have caused damage to the polymer. The only area that may have been effected, however, would be that *under* the electrodes. Since EA investigations are concerned with the optical properties of the polymer *between* the electrodes such damage would have been of no consequence.

Contacts were then made to the electrodes by bonding fine gauge wire to the the gold using silver loaded paint.

5.2 EA Spectrometer

The EA spectrometer consisted of a choice of appropriate light source and detector, a monochromator, a cryostat within which the sample was placed - all mounted on an optical bench. Electric fields were generated across the sample using an oscillator and amplifier. The EA signals were measured using lock-in techniques, with the whole experiment contolled by a PC allowing precision timing and remote data collection. A schematic of the apparatus is shown Fig.5.2.

There was a choice of two light sources. For work in the IR/VIS a fan cooled UV enhanced 100 W tungsten halogen filament lamp was employed. This lamp was powered by 12 V car batteries in order to reduce the electrical noise and possible lamp intensity variations that might occur if powered by a mains rectified dc source. For work in the VIS/UV a 250 W fan cooled xenon arc lamp was used: the high voltages required to power this lamp meant that it had the potential of being electrically noisy, so a mains isolator was used in an attempt to minimise any such noise.

To complement these light sources there was a choise of two photodetectors. For work in the IR a nitrogen cooled Laser Monitoring Systems In/As detector was available, while for the VIS/UV a UV enhanced SiTek silicon photodetector was used.

As shown in Fig.5.2 the light from the source was pre-monochromated, using a Bentham M300 monochromator which contained suitable filters to prevent

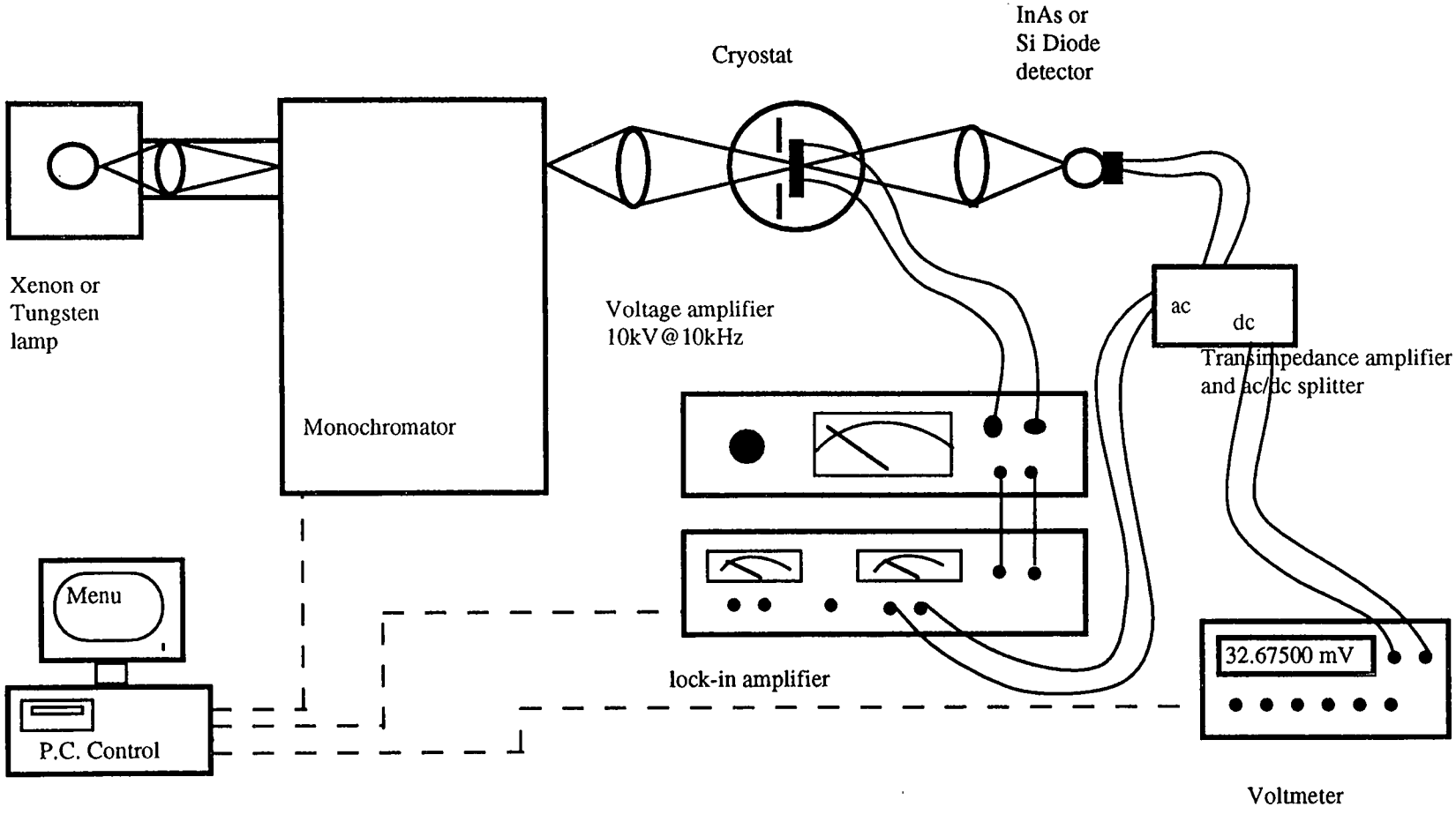

Fig. 5.2. Schematic of Electroabsorption spectrometer.

second order re-entry. The monochromated beam was then focussed down onto the sample using a quartz lens (f = 60 mm), and then further on to the detector using a second lens similar to the first.

The sample was kept under a vacuum of ~10^{-5} torr on a purpose built holder mounted on the cold finger of a Leybold helium fridge, allowing study in the range 10-300 K. The vacuum was maintaned with a turbo molecular pump, backed by a rotary pump. Most spectra were recorded at the 10K, the lowest temperature attainable with the system, to reduce thermal noise.

The large sinusoidal electric fields necessary for EA spectroscopy were attained by amplifying the output of the internal oscillator of the EG&G 5209 lock-in amplifier using a Trek 10/10 solid state amplifier. These high fields combined with the closely spaced electrodes allowed fields of up to 125 $kVcm^{-1}$ to be attained. Prior to the purchase of the Trek 10/10 amplifier attempts were made to attain the high fields required using a step up transformer. It soon became apparent, however, that the integrity of the sinsoidal voltage was lost during such large step up, and that an amplifier of some type was required. The Trek 10/10 was chosen because it exactly matched the needs of the experiment: the input voltage range (0-10 V) matched the output of the lock-in's internal amplifier (0-2 V), and with a fixed gain of 1000 the output matched the voltages required across the electrodes (0-2000 V). An output was available on the amplifier to check the integrity of the amplified signal on a CRO.

The current signal from either of the photodetectors was first converted to a voltage signal and amplified - using a low input impedance transimpedance amplifier - then split to allow simultaneous monitoring of the ac and dc components. The dc signal, T, was measured using a K195 DVM, while the ac component, ΔT, was analysed using the lock-in. The quotient of these two signals is the desired

perturbation due to the electric field, normalised to the transmission of the sample. The process of recording these two signals simultaneously had the effect of reducing possible causes of error in the data that existed if the spectra were recorded consecutively, such as variations in temperature of the sample, variations in intensity of the lamp, and exact positioning of the monochromator grating. Simultaneous measurement also reduced the amount of time taken in recording spectra: it was advantageous to take as short a time as possible on each spectrum as it was found that under such high fields many of the samples quickly de-natured. The exact process involved in the break down is unclear, though it may be that, under the influence of the high electric fields the gold electrodes tended to slowly migrate through the polymer until a short circuit was formed.

The polymers used in these experiments are considered to have been predominantly amorphous. Within an amorphous system the chains are randomly oriented, and hence when applying a sinusoidal voltage the electric field produced within the positive portion of the voltage biasing cycle has the same effect as the negative portion. The frequency of the EA response of such a system will therefore be at twice the frequency of the applied field. This was verified by the absence of any signal at the fundamental (applied) frequency (f). For this reason the lock-in was set to monitor the signals at 2f. Since the voltage source was sinusoidal (sin ωt) and the EA response is quadratic with applied field, the instantaneous change in transmission coefficient for an induced bleach is proportional to

$$F_0^2 \sin^2(\omega t) = \tfrac{1}{2} F_0^2[1-\cos(2\omega t)] \qquad \text{eqn. 5.1}$$

The lock-in reference was set to twice the fundamental, as mentioned above, and knowing

$$-\cos(2\omega t) = \sin\left(2\omega t - \pi/4\right) \qquad \text{eqn. 5.2}$$

meant that the dynamical component of the the lock-in had a phase change of $-\pi/4$ relative to the lock-in reference. Similarly, an induced increase in absorption would be expected to have a phase change of $\pi/4$ relative to the reference. The phase settings on the lock-in were performed manually, and reset for each spectrum. The values found for the phase change for induced absorptions were between 40° and 50° for each material relative to the applied voltage - consistent with the predicted values. While investigating the nature of the phase relationship between applied voltage and EA signal many inconsistencies became apparent. Upon further investigation - and lengthy consultation with the manufacturers - it was discovered that there was a hardware-software mismatch in the lock-in requiring the instalation of upgraded EPROMs. The fault was apparently inherent to all 5209s and 5210s of the period, so beware!

For each EA spectrum taken a value of time constant on the lock-in had to be chosen so as to provide a reasonably steady reading of the ac component of the signal. These values ranged from 0.3 s to 10 s depending on temperature, applied voltage, and sample. Voltage dependencies of the signal were measured manually, using longer time constants, (usually 30 s).

A great deal of time and effort was spent on reducing electrical noise within the system. All cables were shielded, with the earths connected in such a way as to prevent earth loops. All electrical equipment was also earthed, mostly via the optical

bench, again in such away as to prevent earth loops. Sensitive equipment was isolated from the mains using an active isolating transformer. As far as possible all electrically noisy equipment was kept physically separated from other equipment to prevent RF pickup. RF also caused problems when igniting the arc lamp; all other equipment had to be swithed off and inputs disconnected to prevent electrical damage, as was found to my cost.

The cryostat used throughout was a closed loop helium fridge, which necessitates the pumping of helium gas to and from the cryostat to the fridge unit. This pumping causes vibration of the cryostat, and hence of the sample, introducing yet another source of noise to the experimental system. In an effort to reduce this noise a special mount was constructed in which the cryostat could be firmly secured, and the mount bolted to the optics bench.

The combination of all these noise limiting feactures resulted in signal to noise ratio of EA signal of the order 5.10^7 - as is apparent in the EA spectrum of EB and of the phenyl capped tetramer in chapter 6.

When performing electroabsorption spectroscopy it is the change in optical transmission, ΔT, of the sample that is monitored, whereas the theories presented in chapter 3 talk of the change in absorption coefficient, $\Delta\alpha$. The following method and assumptions are used to convert from one to the other. When performing these EA measurements ΔT is normalised with respect to the normal transmission of the sample, T, giving the quotient $\Delta T/T$ - a value that is free of any spectral functions of the spectrometer. In considering the optical properties of the sample, the transmitted intensity, I_t, may be expressed in terms of sample thickness, d, absorption coefficient, α, and reflection coefficient, R, as

$$I_t = I_0(1-R)^2 e^{-\alpha d} \qquad \text{eqn. 5.3}$$

This expression assumes that the reflection coefficient at the front and back surfaces of the film are equal, and neglects multiple reflections within the sample. The effect of applying an external field, F, to the system may further be expressed as

$$\frac{\partial I_t}{\partial F} = -I_0 e^{-\alpha d}\left[d(1-R)^2 \frac{\partial \alpha}{\partial F} + 2(1-R)\frac{\partial R}{\partial F}\right] \qquad \text{eqn. 5.4}$$

Dividing by the unperturbed intensity yields

$$-\frac{\Delta I_t}{I_t} = -\frac{\Delta T}{T} = d\Delta\alpha + \frac{2}{1-R}\Delta R \qquad \text{eqn. 5.5}$$

For typical values of the optical constants [5] and film thicknesses the first term of eqn. 5.5 dominates, giving $\Delta T / T \approx -d\Delta\alpha$, thus allowing the EA results to be discussed in terms of the change of absorption coefficient.

5.3 Measurement of Absorption Coefficients

It is evident from earlier discussions that analysis of EA data requires the absolute absorption spectra of the materials in question. These absorption spectra were measured using a Perkin-Elmer Lamda-19 double beam spectrometer. Samples of different known thicknesses, on matched substrates, were placed in the path of the two beams. The resulting spectra taken with the samples in this configuration was due only to the thickness difference of the films.

In order to calculate the absorption coefficient spectrum from such an absorption spectrum it was necessary to determine the thickness of the polymer

films. Thickness measurements were made using an Alpha Step thickness gauge - a device that measures the movement of a finely balanced stylus as it is traversed across the surface of a sample. To measure the thickness of a film it was therefore necessary to score a 'trench' through the film, which was done using a razor blade. For the highly uniform films of emeraldine base only two sample thicknesses were measured (twice for each sample), and the absorption coefficient spectrum determined from the difference in absorption between these two samples. For a greater degree of accuracy more films could have been analysed, but since this work has been carried out previously for polyaniline, with consistent results, repeating the work did not seem necessary.

The films of polysquaraine were not as uniform as the films of polyaniline, and so a more involved method of determining the absorption coefficient was employed. Four films of varying thickness were spun onto matched substrates, and labelled S1...S4. The difference absorption spectra between all combinations of the films were measured in the manner explained above - S1 against S2, S3, S4 etc... The thickness of each film was determined using the Alpha Step thickness gauge. For each difference spectrum the value of the absorption at 1.4 eV was recorded, and knowing the approximate value of the difference in thickness of the two films, a value of the absorption coefficient at this energy could be calculated. The average value of absorption coefficient at 1.4 eV was then used to scale the whole absorption coefficient spectrum.

References

1. Havinga, E.E., W.T. Hoeve, and H. Wynberg, Polym. Bull., 1992. **49**(1-2): p. 119.
2. Havinga, E.E., W.T. Hoeve, and H. Wynberg, Synth. Met, 1993. **55**(1): p. 299.
3. Honzl, J. and M. Tlustakova, J. Polym. Sci, 1968. **22C**: p. 451.
4. Scully, M.S., *The Characterisation of Thin Films of Polyaniline for Gas Sensing*, M.Sc. Thesis. 1994, University of Durham.
5. Worland, R.S., *Electroabsorption in Conjugated Polymers*, PhD. Thesis 1989, Santa Barbra: California. p. 255.

Chapter 6

Results and Discussion

6.1 Emeraldine Base

The EA results for the polymeric and oligomeric forms of emeraldine base will first be presented separately, followed by a section in which the results are compared and contrasted.

6.1.1 Polymeric Emeraldine Base

6.1.1.1 Linear Absorption

The room temperature absorption coefficient spectrum of the polymeric form of emeraldine base is shown in Fig.6.1. It is in agreement with previously published spectra of the material [1, 2] - showing absorption peaks at 2.0 and 3.8 eV, with a further peak evident as a shoulder at 4.5 eV. Consistent with this previous data, the 3.8 eV absorption feature is around 1.4 times greater than that at 2 eV. As described in chapter 5, these absorption values were calculated by placing two films of different known thickness in a double beam spectrometer, thus allowing the resulting spectrum to be interpreted in terms of absorption per unit thickness. Table 6.1 lists the thickness measurements for two films that were used to calculate the above spectrum.

Absorption and EA spectra were initially taken at both room temperature and at 10 K. It was found that the low temperature absorption spectra had greatly reduced noise due to the reduced thermal activity, but had the same lineshape as the

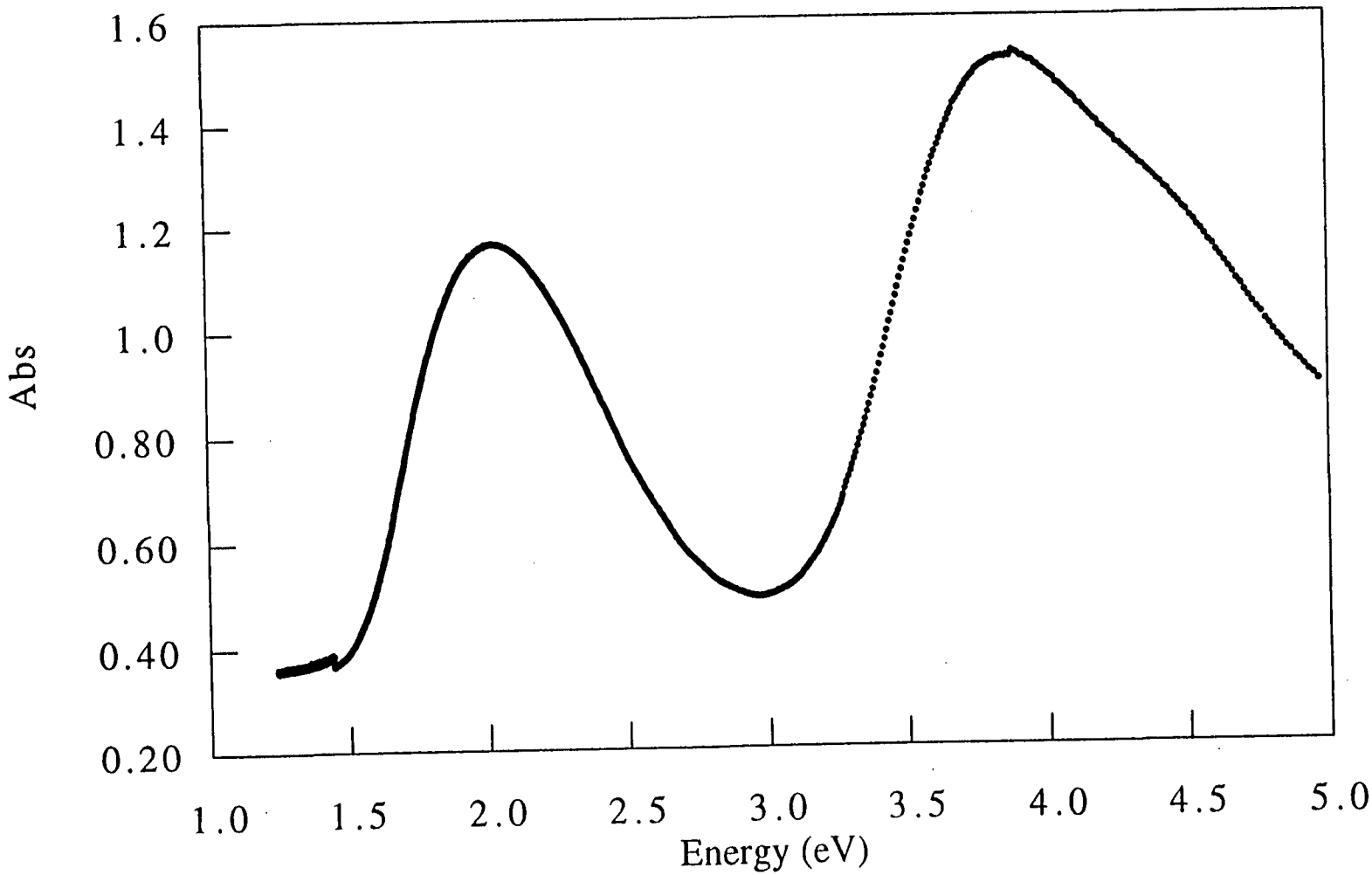

Fig. 6.1. Absorption spectrum of EB.

room temperature spectra. Absorption spectra of EB have been found to shift by approximately 0.08 eV without a change in lineshape from room temperature to 10 K, and it appeared that, within experimental error, the shift in EA peaks was of the same order of magnitude. At these low temperatures it was found that much higher fields could be applied to the samples before they broke down. This fact, along with the reduced noise and the fact that the lineshape was the same as that at room temperature, led to all the following spectra being taken at 10 K.

Sample	Thickness (μm)
S1	0.25 ± 0.02
	0.24 ± 0.02
S2	0.14 ± 0.02
	0.15 ± 0.02

Table 6.1 Thickness of EB spun films.

6.1.1.2 Electroabsorption

Fig.6.2 shows the EA response for EB at 10 K with an applied voltage of 87 $kVcm^{-1}$. The spectrum shows a positive peak at 1.58 eV, followed by a negative peak at 1.92 eV, returning to zero at around 2.3 eV. This part of the spectrum is associated with the 2 eV absorption. The EA spectrum then shows a peak at 3.3 eV, followed by a negative peak at 3.8 eV and positive peak at 4.3 eV, associated with the absorption at 3.8 eV.

The voltage dependence of the observed EA signal for 1.6 eV photoexcitation is shown in Fig.6.3. As can be seen, the EA signal has a quadratic

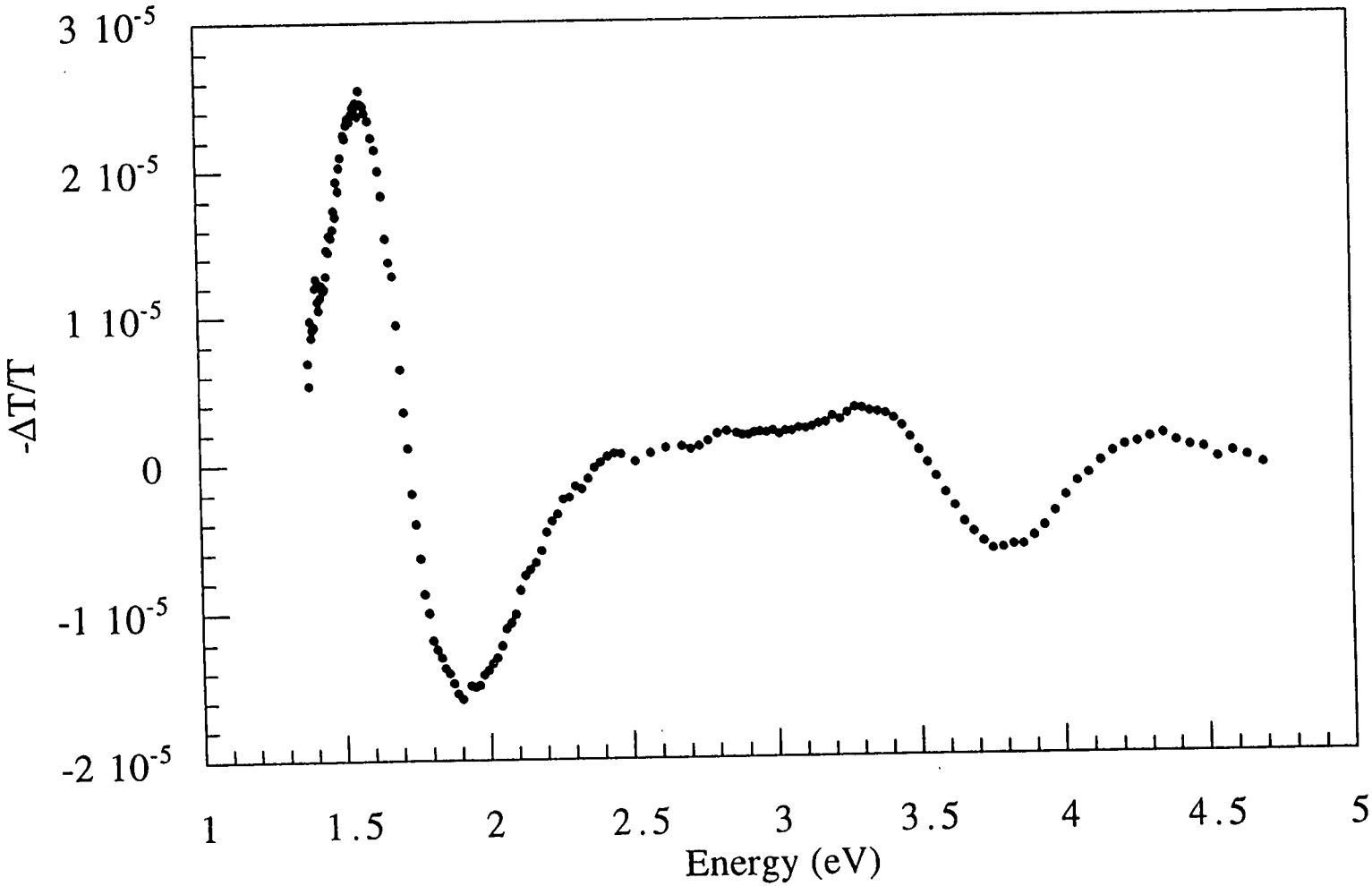

Fig. 6.2. EA of EB measured at a temperature of 10 K and an applied voltage of 87 kV/cm

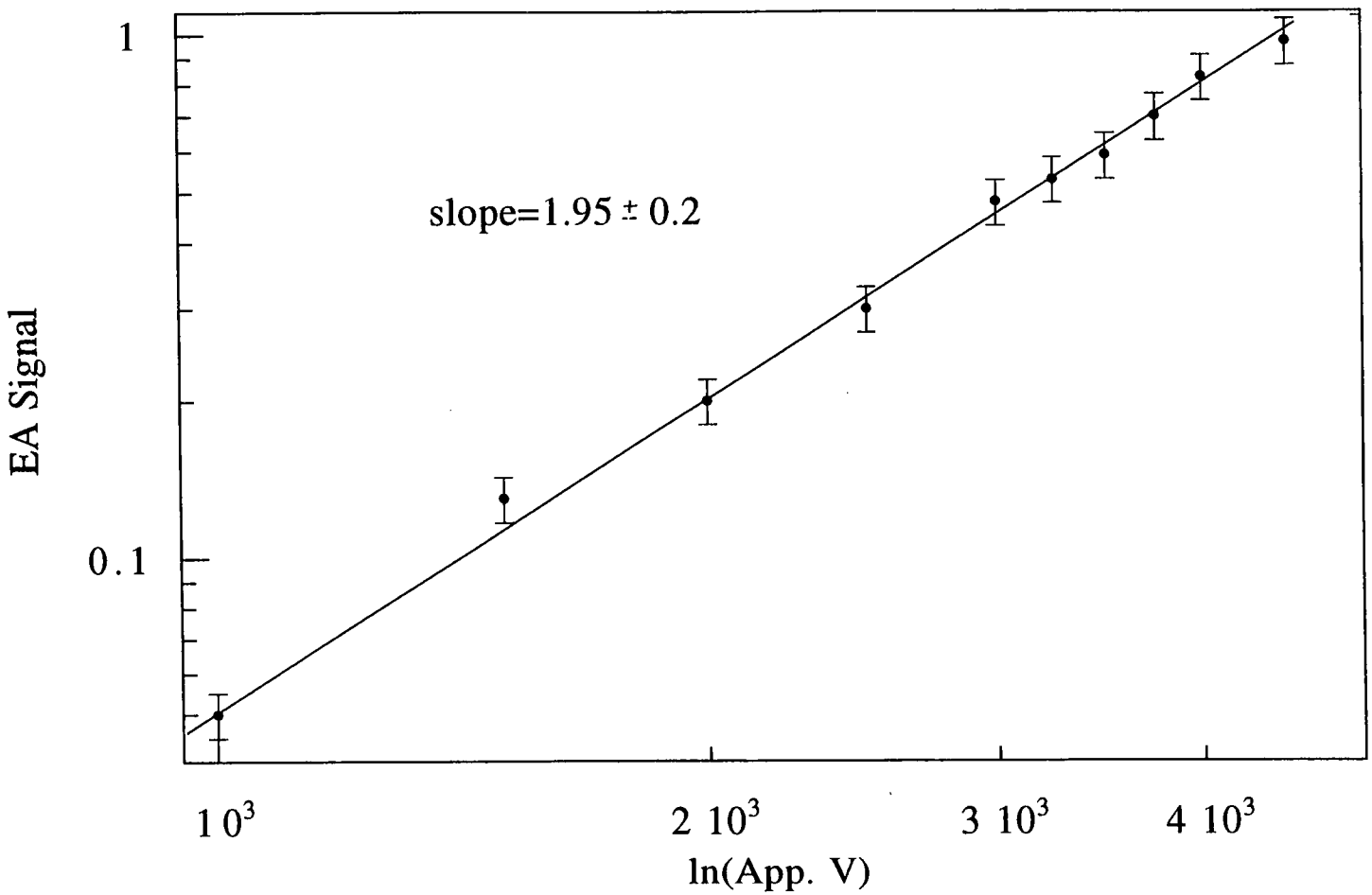

Fig. 6.3. Voltage dependence of EA signal for EB, measured at 1.6 eV

dependence upon applied electric field in agreement with the relevant theories presented in chapter 3. The whole spectrum has the same dependence, and hence varying the applied field does not change the lineshape of the EA response. Evidence of this is shown in Fig.6.4 which shows the EA response of the low energy peak of EB at various applied voltages.

As was explained in chapter 3, the lineshape of an EA spectrum is of importance when discussing the type of photoexcited states produced. Information may be gained from observing whether the EA lineshape most closely resembles the first or the second derivative of the normal absorption spectrum, or a mixture of the two. Figs.6.5 and 6.6 compare the EA spectrum with the first and second derivatives of the normal absorption. The derivative lineshapes have been scaled to match the EA lineshapes at 1.6 eV. It can be seen that the second derivative gives a good fit over the whole spectrum - no combination of the two lineshapes appeared to give a better fit, even when considering the responses associated with the two absorption peaks separately. The EA spectrum closely follows the second derivative lineshape up to 1.7 eV, where the two begin to separate and merely follow the same trend. The feature associated with the 3.8 eV absorption matches the second derivative lineshape, the size difference being due to the method of scaling mentioned above. The deviation from the derivative lineshape above the main absorption feature has been noted previously for other EA spectra of amorphous polymer films, notably for PPA and PDES as reported by Jeglinsky and Vardeny [3] as discussed in chapter 3. The exact reason for this type of deviation is as yet unclear. Combinations of first and second derivative lineshapes were tried, but none gave as good a fit as that shown in Fig.6.6.

The oscillations around 2.5 eV in the second derivative lineshape are thought to arise from intrinsic artifacts in the Lamda-19 spectrometer, rather than any evidence of structure in the absorption spectrum. Such oscillations were observed in

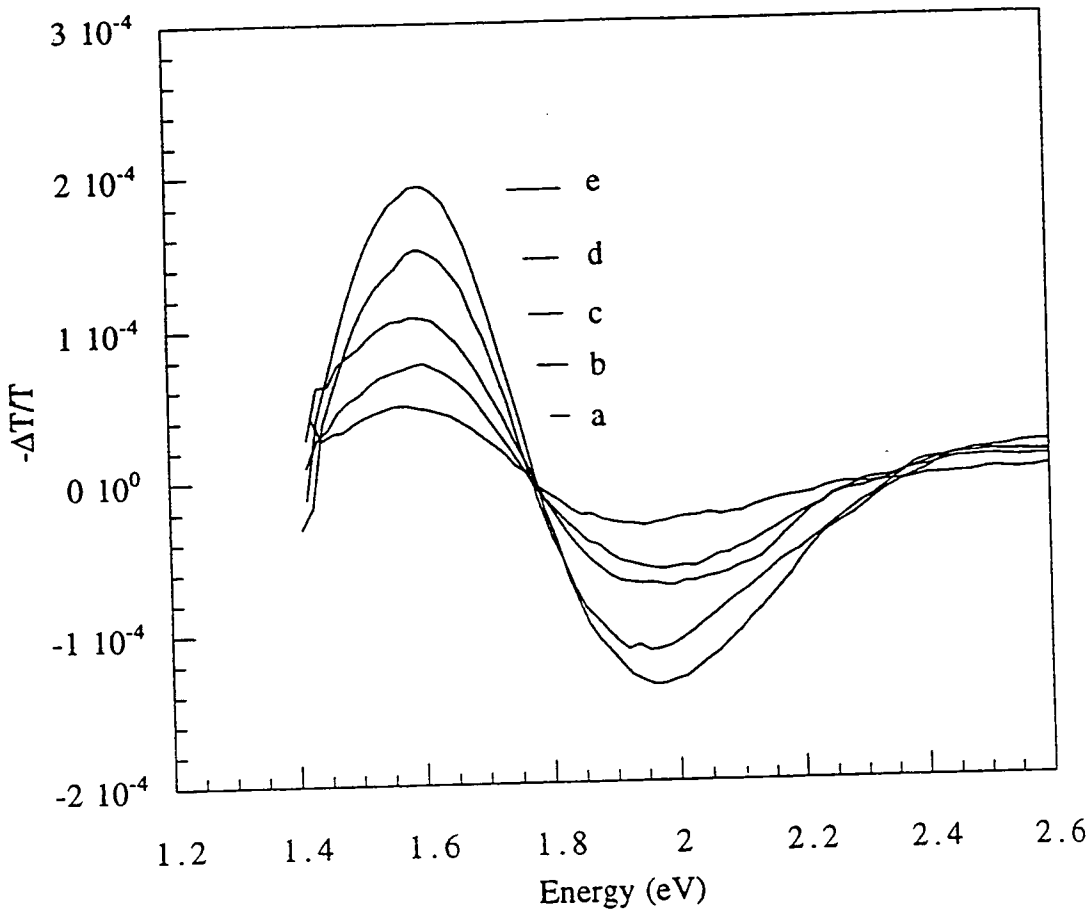

Fig. 6.4. EA of EB at a temperature of 20 K with applied voltage of a) 50, b) 62.5, c) 75, d) 87.5, e) 100 $kVcm^{-1}$.

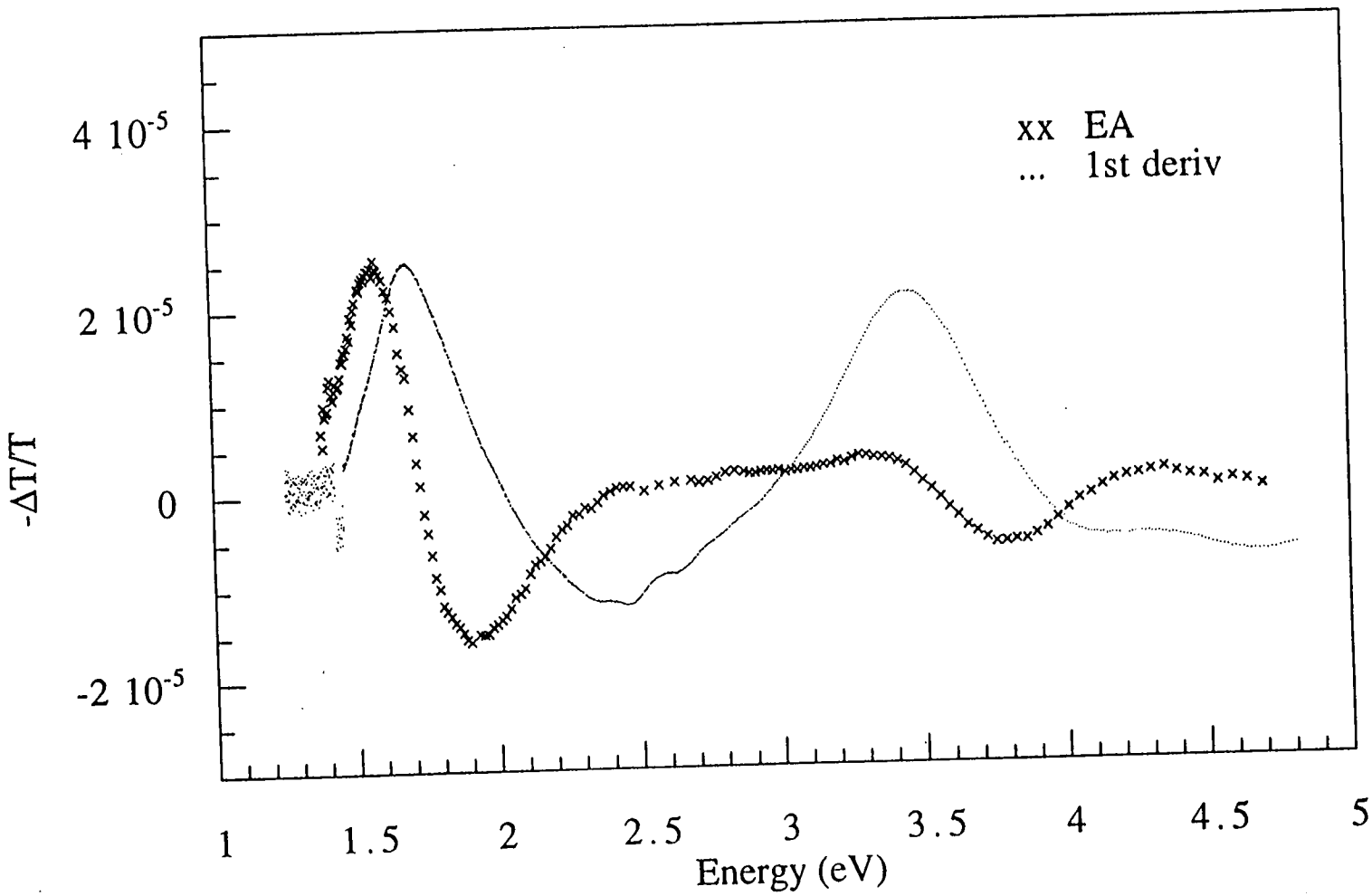

Fig. 6.5. EA of EB vs. 1st derivative of the linear absorption

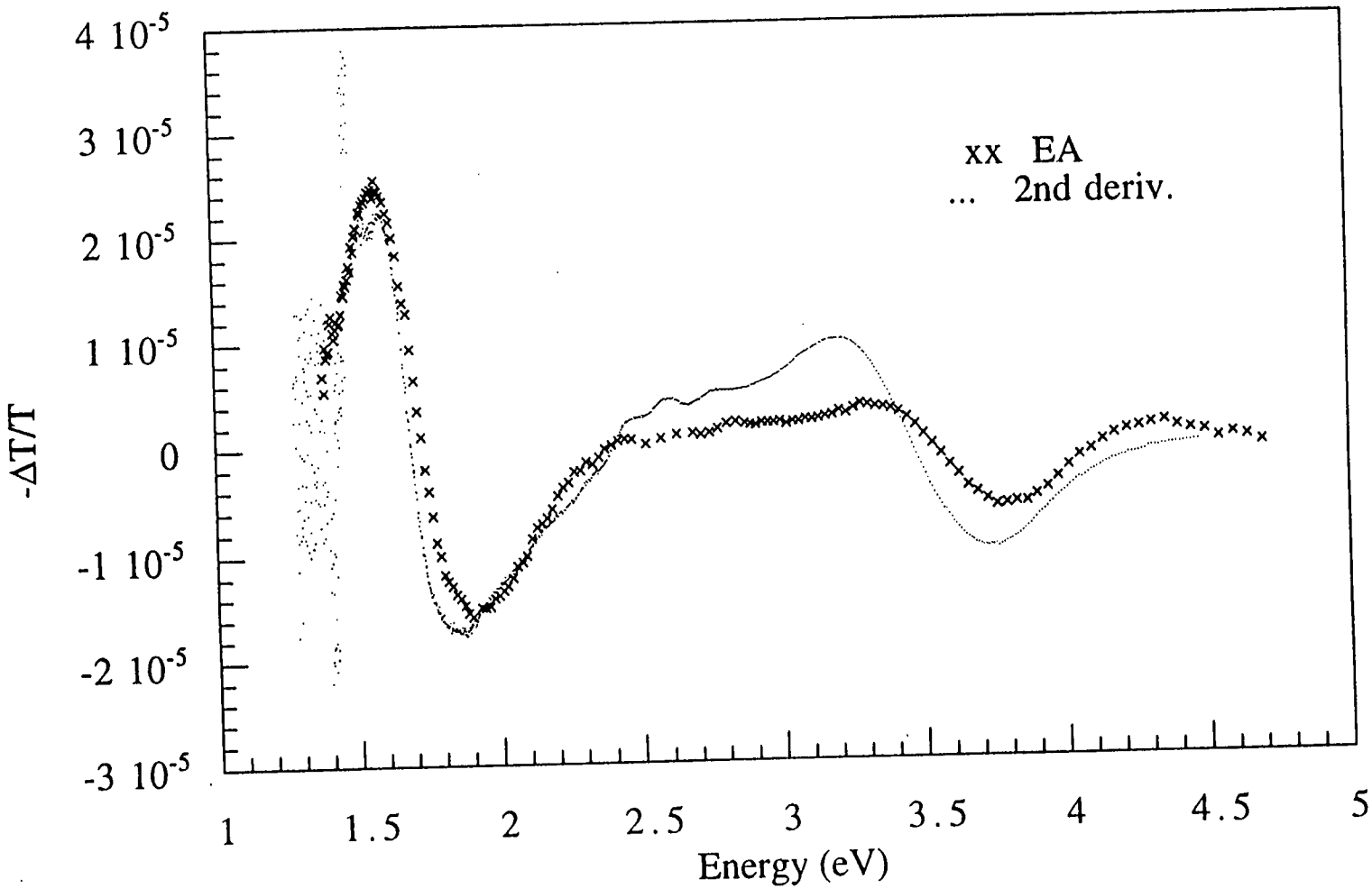

Fig. 6.6. EA of EB vs. 2nd derivative of linear absorption

many of the spectra taken with the spectrometer for many materials of various film thicknesses.

As mentioned in chapter 3, EA spectroscopy involves the mixing of two fields - the applied electric field and the optical field. The predicted ratio of the EA signal for the fields being parallel and perpendicular is proposed to have a value ranging from 3:1 to 1:3 [4]. Using a calcite crystal polariser positioned in the optical path after the monochromator, the polarisation of the EA signal of polymeric emeraldine base was measured, yielding the result of EA(parallel/perpendicular) = 2.3 - consistent with the predicted values.

6.1.1.3 Discussion

According to the theory of Sebastian and Weiser [5] a fit of second differential of normal absorption with the EA lineshape implies that the photoproduced states posses a permanent dipole moment. Of the two photoexcited states suggested by Kim *et al.* [6, 7] and Duke [8], only the n-π^* suggestion of Kim seems compatible with a second derivative lineshape as this involves the direct photoproduction of a permanent dipole, whereas the exciton suggested by Duke is symmetric and hence has no permanent dipole. It must be remembered, however, that the exciton proposed by Duke is *idealised* - the exciton being formed on a perfect polymer unit in a uniform potential. As has been pointed out in chapters 2 and 3, a real polymer system can be far from ideal due to the presence of disorder. Disorder may result in the occurrance of non-uniform electric fields within the system as well as causing conformations very different from those predicted for the ideal polymer chain. In these conditions it is possible that the ideal exciton proposed by Duke ends up asymmetric, and hence possessing a permanent dipole. This would

mean that the second order lineshape of the EA spectrum may be considered compatible with both proposed 2eV photoexcitations.

Using the method presented in chapter 3 (eqn. 3.5), and assuming the photoexcitation involves complete transferal of one electron (q=1), a rough estimate of the spatial extent of the photoexcited states can be made. For the 2 eV excitation this results in an electron-hole separation distance, r, of around 0.4 nm. Using this interpretation of this result implies that the 2 eV excited state is spatialy extended over a distance greater than just one ring.

This result must be treated with caution. It depends mostly upon the model used to interpret the results, and the assumption that the photoexcitation involves the complete transferal of one electron. It should also be noted that the proposed structure of the EB molecule has a herring bone arrangement, and that this structure brings neighbouring rings closer together than if the molecule were in a linear configuration. The use of this model therefore implies that the excited state is the charge transfer exciton suggested by Duke, rather than the n-π^* transition suggested by Kim.

The EA signal associated with the 3.8 eV absorption also has a second derivative lineshape, again implying the formation of an excited state with a permanent dipole moment. This seems inconsistent with the proposed theory presented in chapter 4 of a π-π^* transition on a benzenoid ring. Even so, calculating the spatial extent of the excited state, assuming the transferal of one electron (as for 2 eV excitation), yields a value of 0.25 nm, which is consistent with the photoproduction of an excited state contained within one ring unit. It may be, then, that the 3.8 eV absorption results in the production of some form of intraring exciton.

If, in fact, the 3.8 eV absorption produces a state with no charge transfer characteristics, an alternative process - such as lifetime broadening, or a transferal of

oscillator strength leading to broadening and suppression of the absorption peak - could also explain the second derivative lineshape of the the EA spectrum in this energy range.

During the experimentation undertaken on EB photoconductivity studies of EB were also performed in an attempt to spectrally resolve any photoconductive response. The results were consistent with those previously reported by other groups (see section 4.1.2.3) in being so small as to be indistinguishable from heating effects. This 'negative' result is, however, worth mentioning in relation to the EA data reported here. The lack of change in conductivity of the material upon photoexcitation of excited states implies that the excited species are either neutral or deeply trapped. For 2 eV excitation this is consistent with the idea of the formation of a trapped exciton. The absence of a photoconductive response for 3.8 eV excitation would be consistent with the formation of an intra-ring exciton.

6.1.2 Oligomeric Emeraldine Base

6.1.2.1 Linear Absorption

Sample	Thickness (μm)
S1	0.32 ± 0.02
	0.35 ± 0.02
S2	0.19 ± 0.02
	0.20 ± 0.02

Table 6.2 Thickness of OEB spun films.

The room temperature absorption spectrum of the oligomeric emeraldine base (OEB) is shown on Fig.6.7 showing absorption peaks at 2.1 and 4.0 eV. Table 6.2 lists the thickness measurements for two films of the oligomer used in determining the absorption coefficient values of the absorption spectrum.

6.1.2.2 Electroabsorption

The EA spectrum of OEB recorded at 10 K under an applied field of 44 $kVcm^{-1}$ is shown in Fig.6.8. The comparison of the lineshapes with the derivatives of the normal absorption are shown in Fig.6.9 and 6.10. It can be seen that the second derivative again gives the best fit to the EA data. As for PEB the derivative lineshape was scaled to match the EA data at 1.6 eV, resulting in the smaller response of the 4 eV photoexcitation being mismatched in size. The EA spectrum can be seen to follow the derivative lineshape up to 1.95 eV, after which the two merely follow the same trend.

The dependence of the EA signal on applied field for OEB, recorded at 10K and a photoexcitation energy of 1.6 eV, is shown in Fig.6.11. Once again the dependence is quadratic, in agreement with the theories presented in chapter 3.

6.1.2.3 Discussion

Assuming once again that the photoexcitations produce CT states, then the calculations of spatial extent of the states gives the results 0.4 nm for the 2 eV absorption, and 0.25 nm for the 4 eV absorption.

There is an interesting feature in this spectrum at 1.35 eV. This feature was reproducible between samples, and was dependent upon applied voltage. The exact

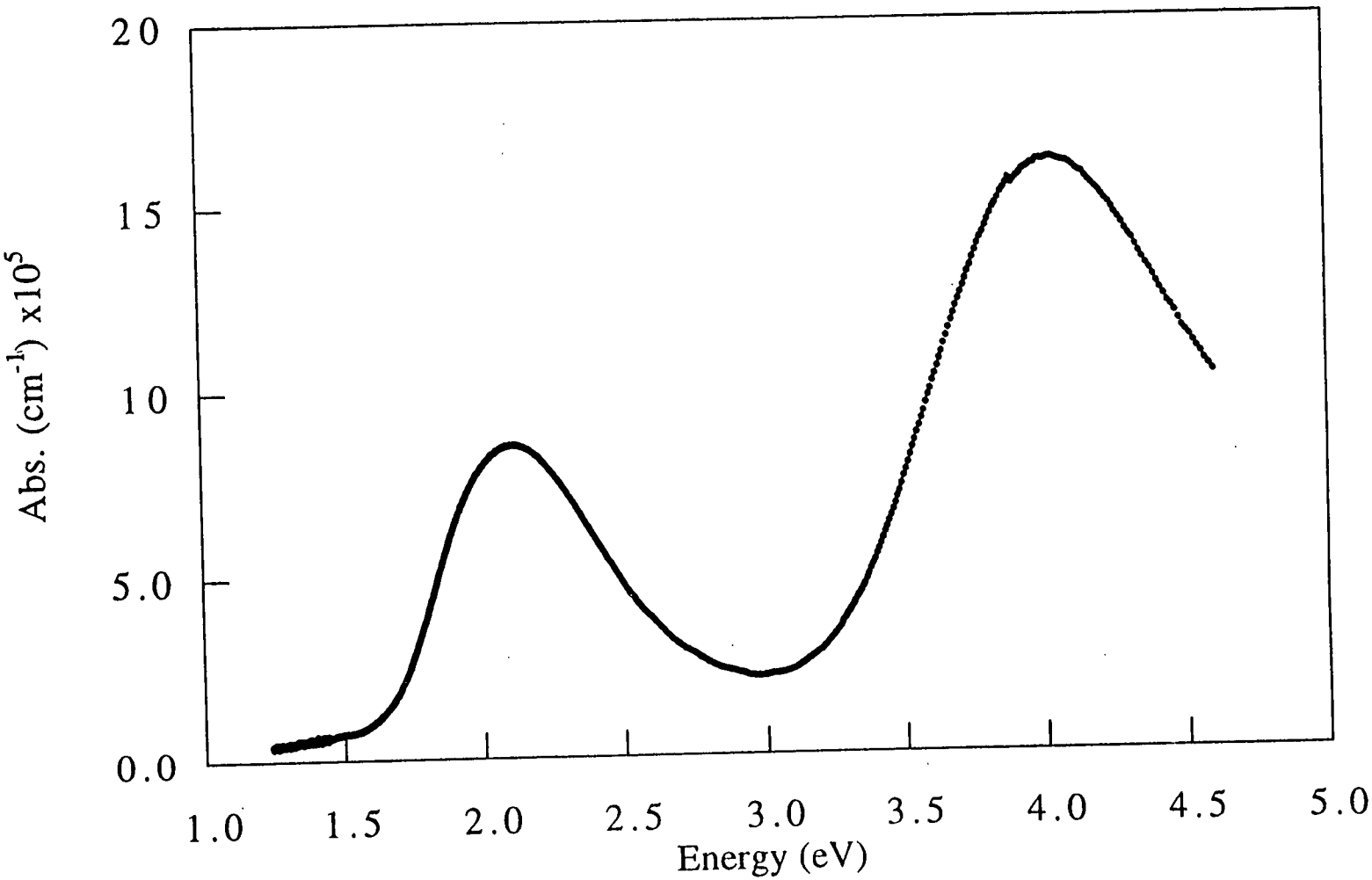

Fig. 6.7. Absorption spectrum of OEB

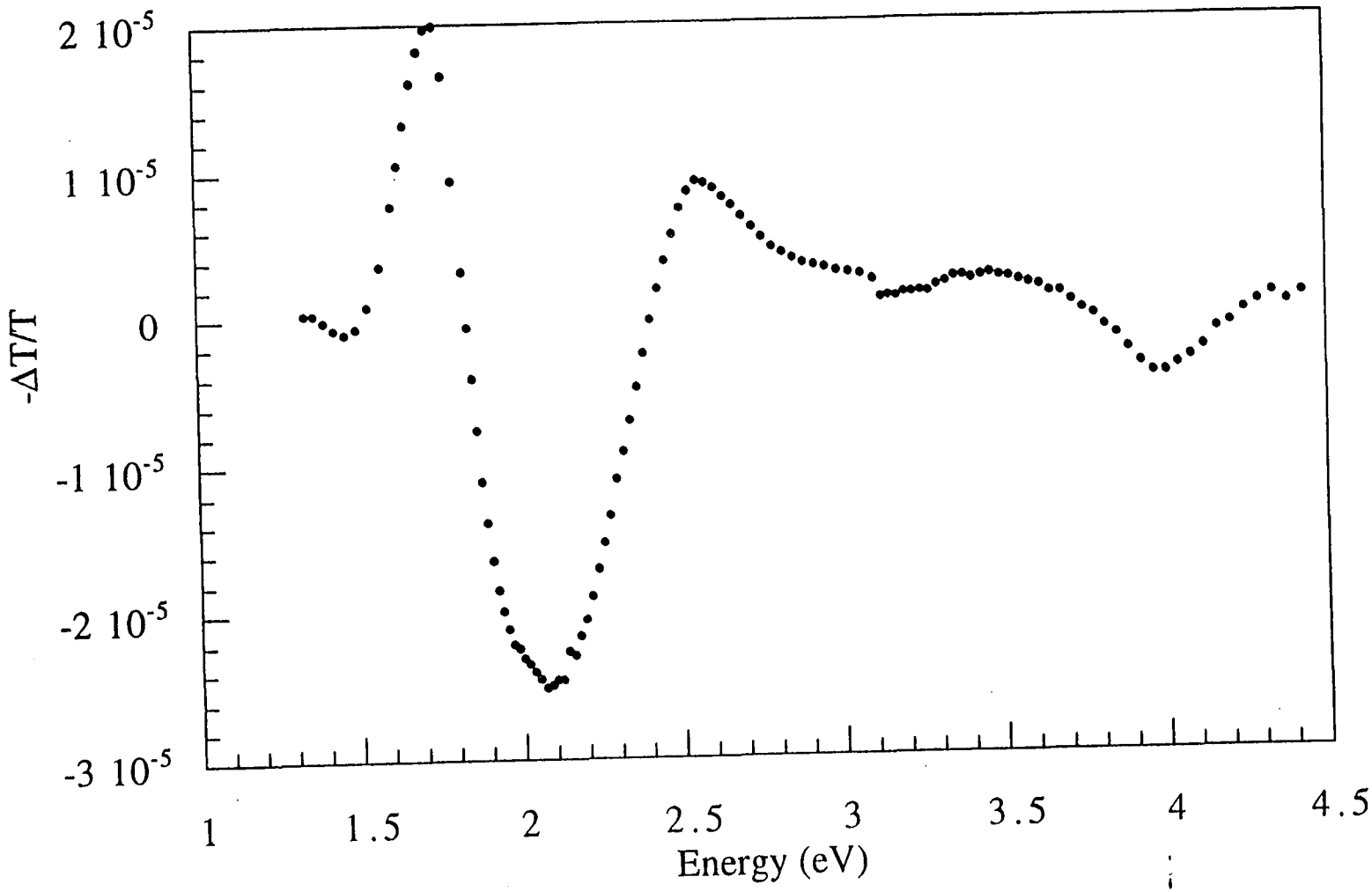

Fig. 6.8 EA of OEB measured at a temperature of 10 K and an applied field of 44 kV/cm.

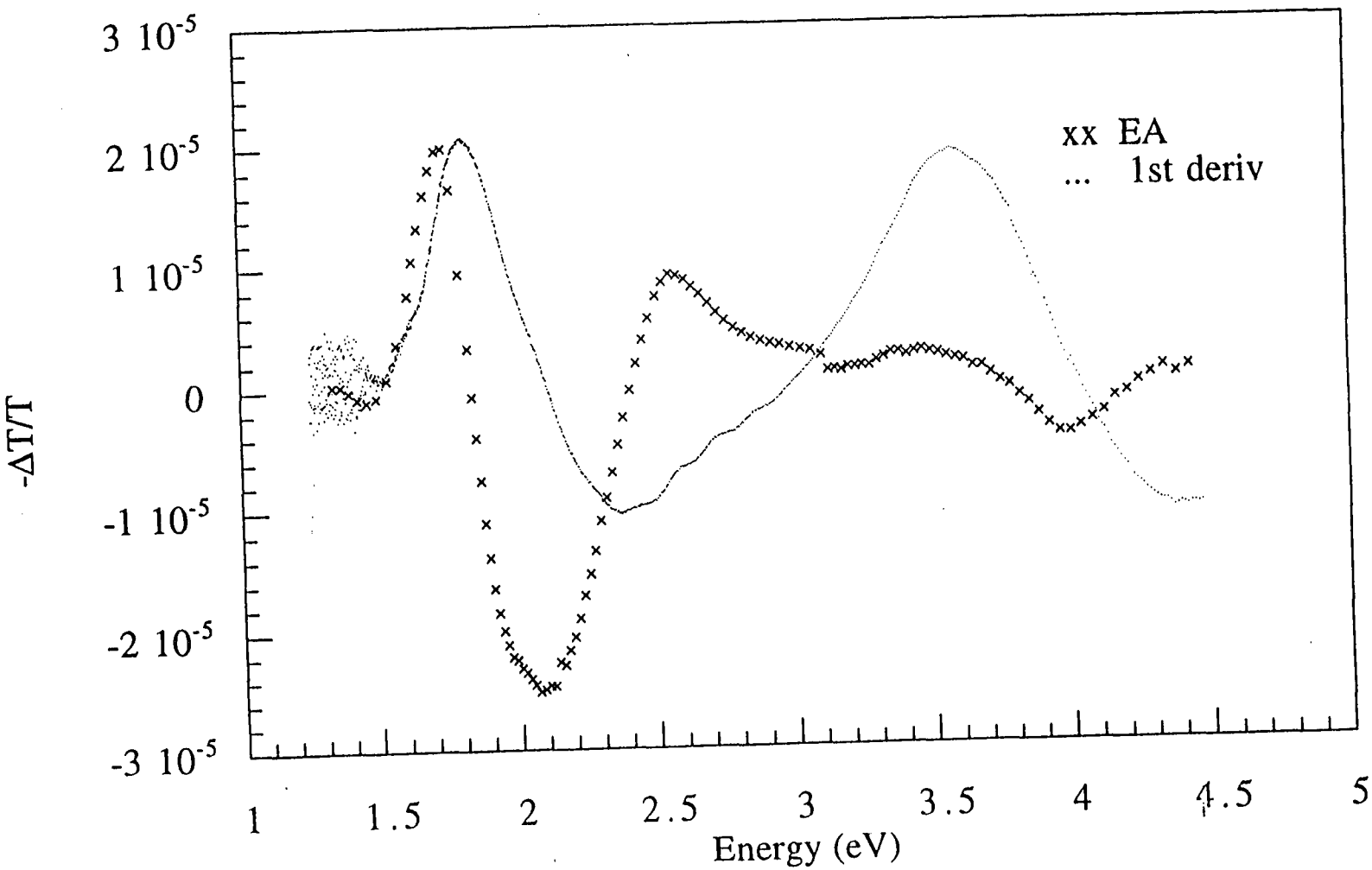

Fig. 6.9. EA of OEB vs. 1st derivative of linear absorption.

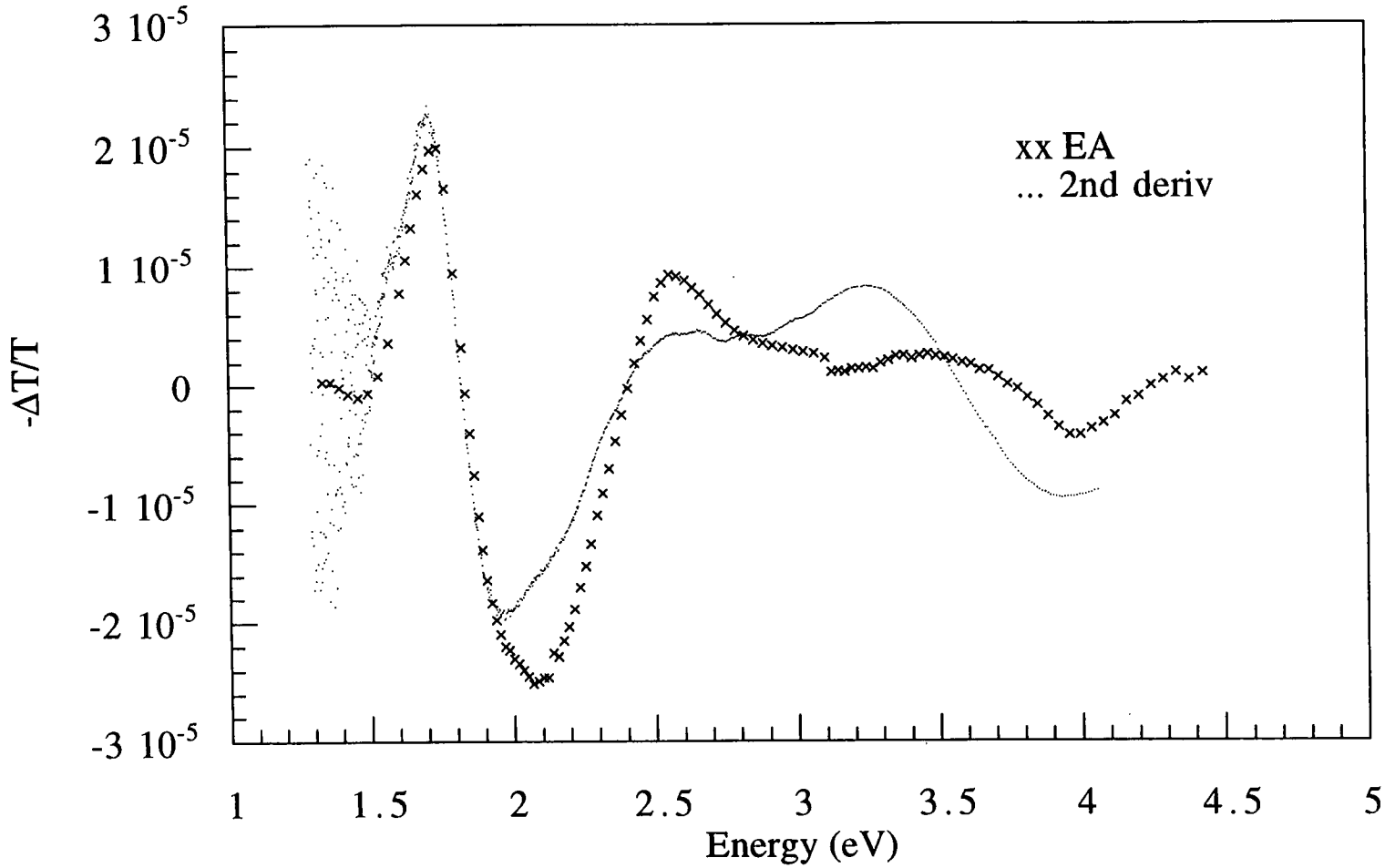

Fig. 6.10. EA of OEB vs. 2nd derivative of linear absorption.

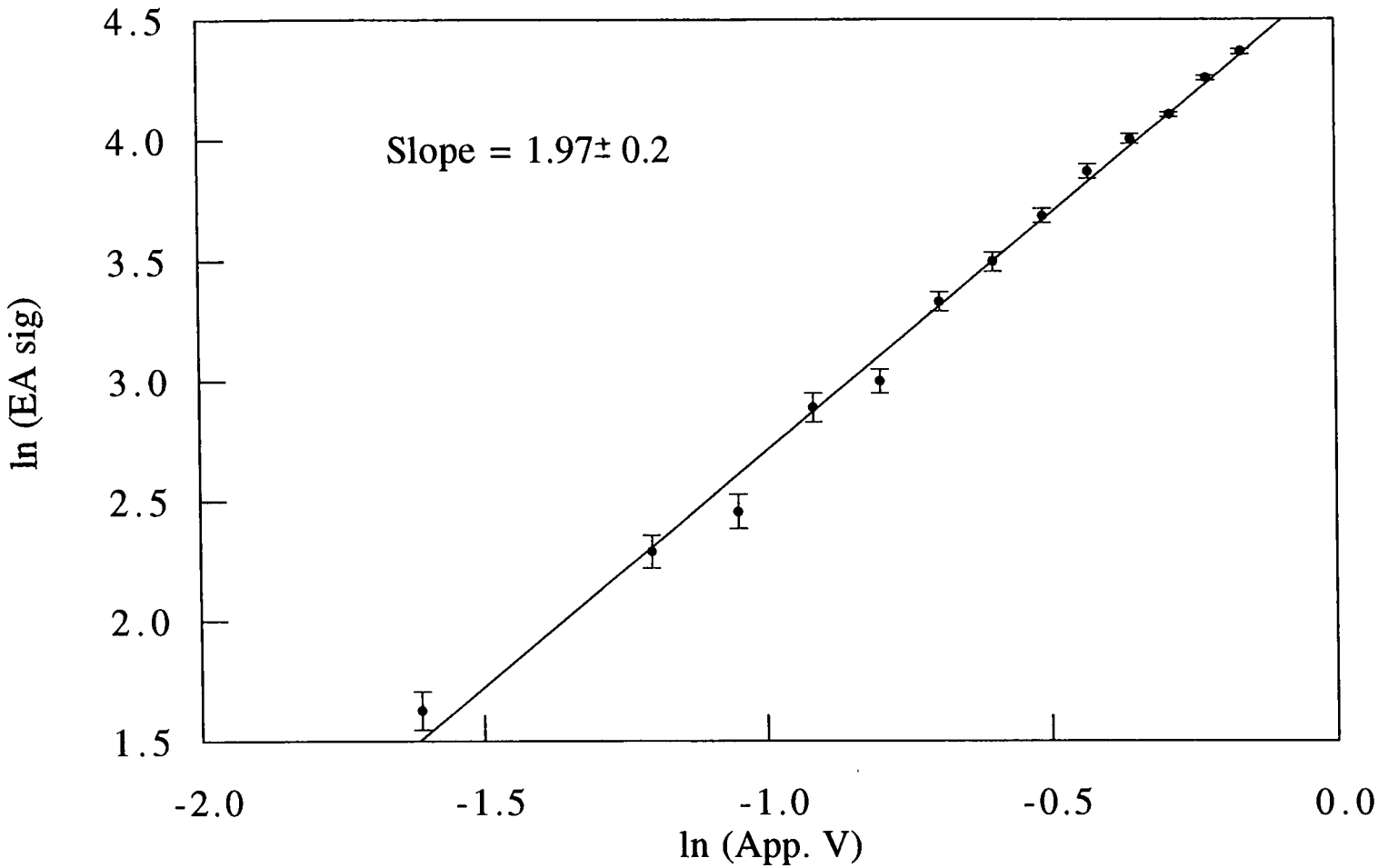

Fig. 6.11. Voltage dependence of EA signal for OEB, measured at 1.6 eV.

dependence was not assertainable due to the error present on such small signals. This feature will be discussed further in the next section.

6.1.3 Comparison of Polymeric and Oligomeric Emeraldine Base

The first point to note in the comparison of the optical properties of EB and OEB is the shift of absorption peaks in linear absorption spectra; the peaks for OEB are ~0.15 eV higher in energy than those of PEB - as can be seen in Figs.6.1 and 6.7. The difference in relative hights of the absorption feactures at 1 eV and 4 eV is also of interest. For EB the ratio is about 1.4, whereas for OEB the ratio is around 2, implying that there are a greater ratio of benzenoid rings to quinoid rings in EB than in OEB. This is consistent with the proposed structures of the two materials - one quarter the rings in EB are quinoidal, compared to only one ring of the five in OEB.

The EA spectra are expanded in terms of $\Delta\alpha$ and are overlaid in Fig.6.12 for ease of comparison. The lineshape of the two spectra are very similar, though the shift seen in the absorption spectra is evident here also - as would be expected.

The fact that the spectra are so similar and that the estimated spatial extent of the excited states coincide, implies that the electronic structure of the chromophores within the two materials are essentially the same. This reinforces the belief that EB is indeed semi-conjugated, and that the theoretical modelling of EB by OEB is a good method.

The absorption and EA spectra of both EB and OEB reveal no vibronic structure, having broad featureless peaks. This type of broad absorption profile is often observed in conjugated polymers and is usually attributed to the distribution of conjugation lengths, and hence of excitation energies, caused by disorder - as mentioned in chapter 2. This cannot be the case for either EB or OEB. EB is semi-conjugated in short conjugated segments, and this negates the possibility of large

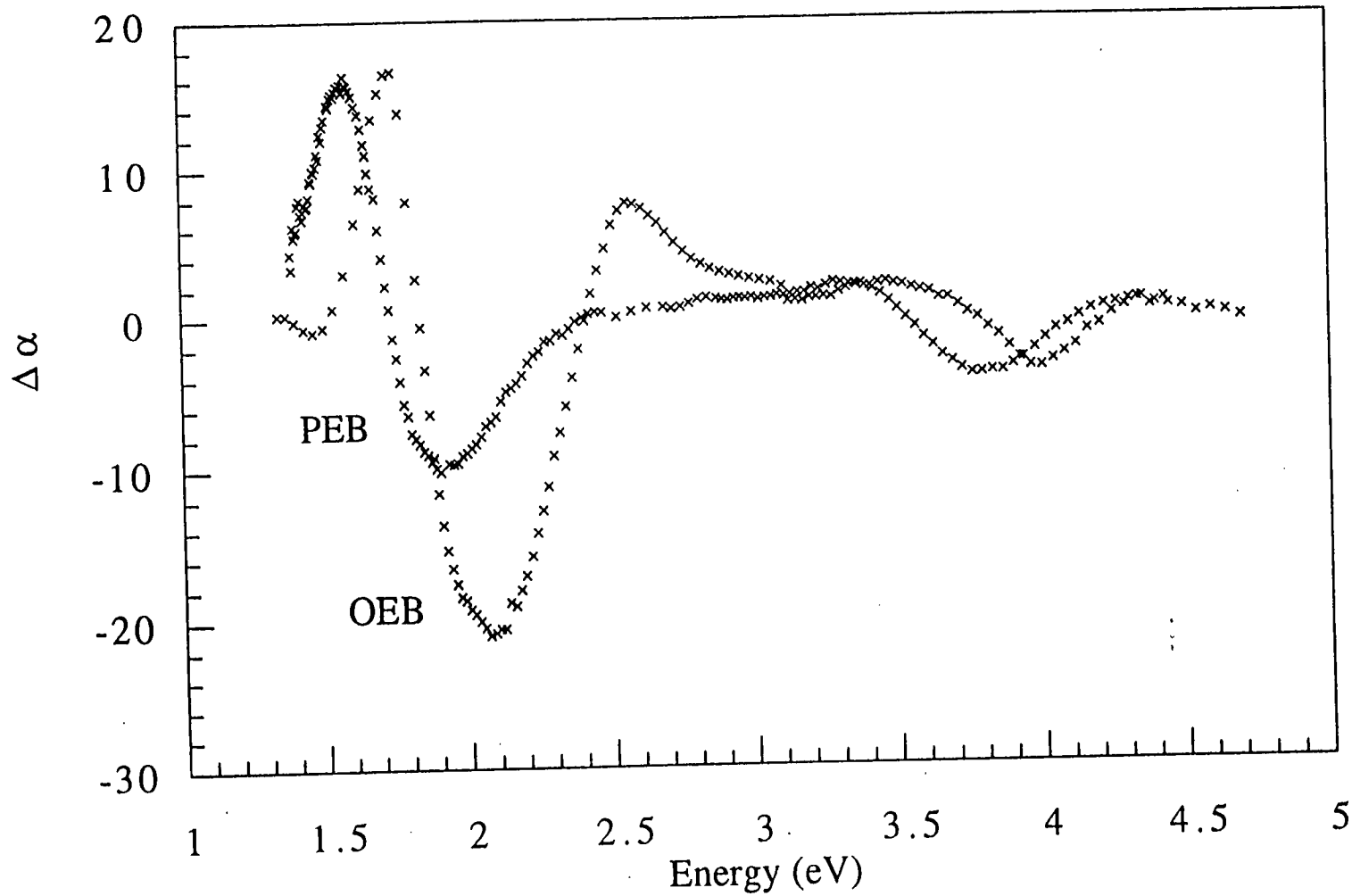

Fig. 6.12. EA of polymeric (PEB) and oligomeric (OEB) emeraldine base: the data have been normalised for applied voltage and film thicknesses.

broadening effects due to changes in conjugation length. OEB also has a broad, featureless absorption peak at 2 eV; variations of conjugation length obviously cannot be predominant in such a short chain oligomer. This implies that there must be some alternative broadening process occuring.

Assuming the photoexcited species produced upon 2 eV photoexcitation is the self-trapped CT exciton suggested by Duke [8], then the broadening of the absorption peak may be related to the separation of the electron and the hole and the exact values of ring torsion angles before excitation. These parameters are also affected by disorder, but the resulting effect is not associated with variations in conjugation length.

The energy of the exciton state suggested by Duke is dependent upon the charge separation involved, and upon the initial degree of delocalisation of the π-electrons across the three ring unit. The degree of electron delocalisation depends upon the torsion angle between the rings; if the rings are nearly planar then there is a high degree of delocalisation, and less energy will be required to excite the electron to the quinoid ring from the benzenoid rings. It is after the photoexcitation process has occurred that the quinoid is predicted to rotate away from the plane thus decreasing the π-electron overlap and trapping the exciton. The presence of disorder within the system may result in a range of torsion angles occurring in the ground state within the three ring conjugated system, and hence in turn result in a spread of excitation energies required to produce the exciton. By the same argument, disorder will also result in a spread in the values of the trapping energies of the excitons after photoexcitation, though due to the nature of the experiment this is not observed in EA investigations.

Another factor that may govern the broadening of the absorption peaks is the exact location of the hole in relation to the electron, as it is of great importance to the final energy of the exciton. The predictions of the probable location of the hole

shown in Fig.4.6 is once again for the case of an ideal system. In addition to the possible ring rotation effects mentioned above, disorder effects such as chain terminations, kinks, and cross linkages will radically effect the local environment of the excitation. The schematics of the conjugated three ring unit presented in Fig.4.2 are an example of the way in which conformational variations may affect the separation distances of the possible electron and hole sites, and at the same time displays the occurrance of varying ring torsion angles. Any resulting spread in effective separation distances of the electron and the hole will result in a spread in the Coulomb energies, and hence broaden the associated absorption feature. This same argument has been used to explain the large broadening of absorption features in such materials as CT glasses and solutions [10].

These effects are not dependent upon the system being fully conjugated, and are hence valid for emeraldine base, both in the polymeric and oligomeric forms. It is possible that such mechanisms may lead to the broadening of the absorption peak to such an extent as to obscure any vibronic structure that may otherwise have been apparent in the 2 eV absorption and EA peak of either material.

There are also some obvious differences between the EA spectra: the trough at 2 eV for OEB is somewhat larger than that for EB, and there is a definite peak evident at 2.5 eV that does not appear for EB. The reason for these differences is, as yet, unclear. One possibility, however, is that the peak at 2.5 eV is due to some energy level that is present in both materials but that does not exhibit the same shift in energy as the other states in going from oligomer to polymer. If this were the case, then an overlap of this peak with the neighbouring trough in the EA signal of the polymer would result in both features being reduced in magnitude. If these features were then separated - i.e. the trough moved to a lower energy, as in the case of the oligomer - the size of the trough and the peak would increase, as is observed.

The EA feature observed at 1.35 eV for OEB is not evident in the EA spectrum of EB. If the feature does exist in EB, it has not been observed only because the feature would occur below the energy range of the experiment. Assuming the same shift as for all the other peaks would place such a feature in PEB at around 1.2 eV.

In this low energy area of the spectrum the second derivative of normal absorption shows merely noise. This is due to the fact that the absorption measured at this point is as small as the error on the spectrometer, and so taking a second derivative of such a signal results the scatter observed in Fig.6.10. Close examination of the absorption spectrum could reveal no feature at this energy, nor has any such feature been reported previously.

This feature could be evidence of a transfer of ocsillator strength, induced by the applied field, to a normally one-photon forbidden state located at 1.35 eV. This suggestion is very tentative; it would require more experimental data, such as the verification that the dependence of signal upon applied field is quadratic and higher resolution absorption spectra, to be confident of such an assignation. It may also be possible that such a feature would be evident in two-photon absorption spectroscopy. EA spectra extending below 1.2 eV for PEB would be necessary to ascertain if a similar feature were present for this material also.

It is interesting to note that recent EA investigations have indicated the existence of such a feature in β-carotene which has also assigned to a normally one-photon forbidden state ($2A_g$) becoming weakly allowed in the presence of an applied field due to the transferal of oscillator strength [11]. The authors have been more confident in this assignation due to the fact that they have been able to characterise the feature to a greater degree - including observing the quadratic dependence of the EA signal on applied field.

6.2 Polysquaraine

6.2.1 Linear Absorption

The spectrum of the linear absorption coefficient of polysquaraine is shown in Fig.6.13. It is consistent with the previously reported absorption spectrum of the material [12, 13], indicating an optical band gap of ~1.3 eV. Vibronic structure with a peak separation of ~150 meV are visible on the higher energy side of the absorption peak, more readily observed in the second derivative of the absorption spectrum shown in Fig.6.16. The thickness of these films was less uniform than those of polyaniline, and so it was decided to take a greater number of measurements of difference spectra, and carry out a slightly more

Sample	Thickness (μm)
S1	0.05 ± 0.03
S2	0.15 ± 0.03
S3	0.30 ± 0.03
S4	0.45 ± 0.03

Table 6.3 Thickness of polysquaraine spun films.

involved averaging process. Table 6.3 lists the thickness measurements of various films. Table 6.4 then lists the absorption per unit thickness taken at 1.4 eV obtained from the difference spectra of various combinations of these films. The absorption value of $3.4.10^4$ cm $^{-1}$ was used to scale the absorption coefficient spectrum of Fig.6.13.

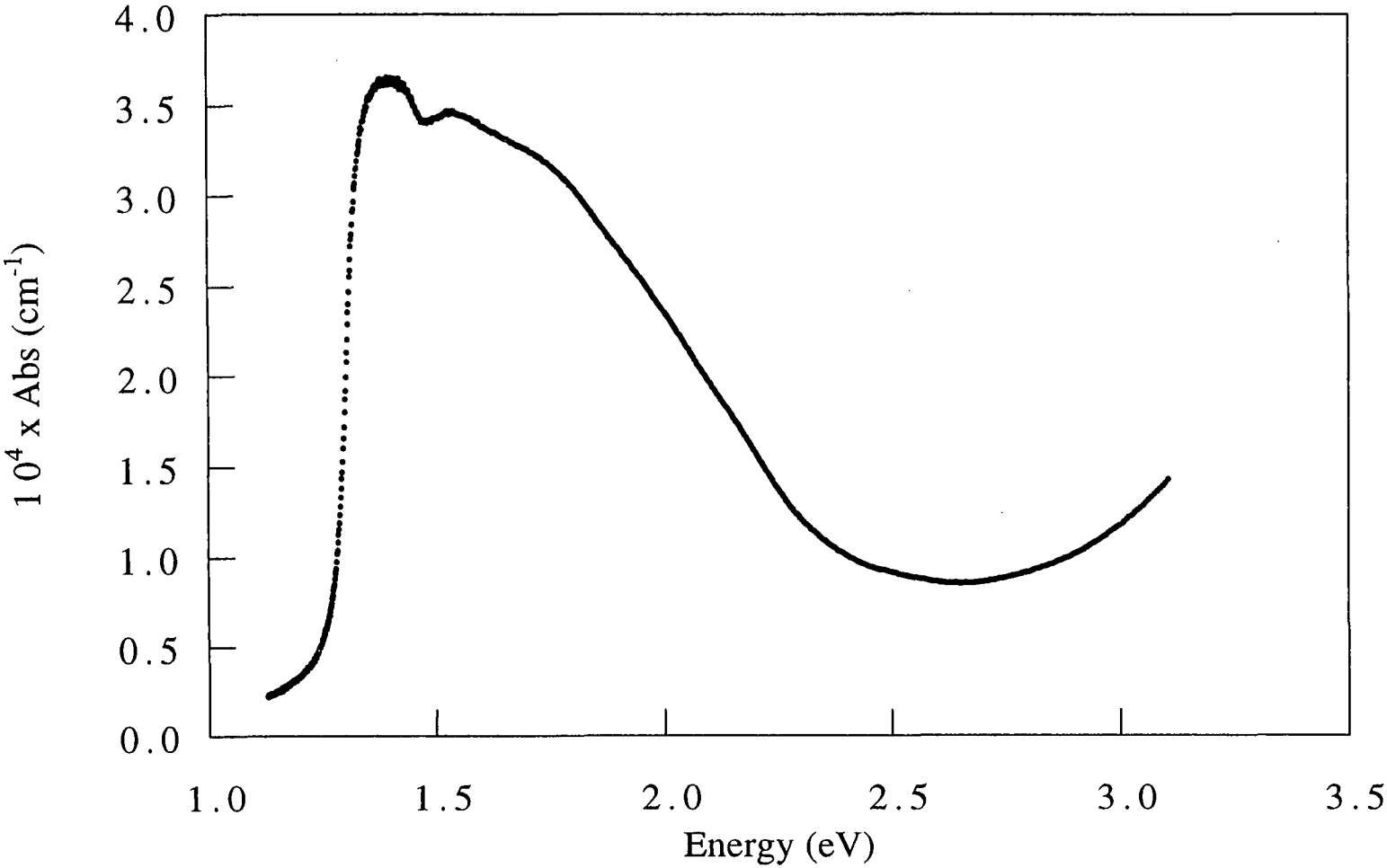

Fig. 6.13. Absorption spectrum of polysquaraine (PS).

Difference taken between samples;	Difference in Absorption at 1.4 eV	Absorption cm^{-1} at 1.4 eV ($x10^4$)
S1 & S2	0.580	5.8
S1 & S3	0.729	2.9
S1 & S4	0.877	2.2
S2 & S4	0.640	2.1
S2 & S3	0.600	4.0

Average: 3.4 (±0.7) $x10^4$ cm^{-1}

Table 6.4. Values of difference in absorption at 1.4 eV for four spun films of polysquaraine.

6.2.2 Electroabsorption

The EA spectrum of polysquaraine at a temperature of 10 K and an applied field of 81 $kVcm^{-1}$ is shown in Fig.6.14. There is a large positive peak at 1.29 eV, a negative peak at 1.35 eV, followed by smaller oscillations returning to zero by 1.9 eV.

Fig.6.15 shows the quadratic dependence of EA signal upon applied field measured at 1.3 eV; the whole spectrum showed the same dependence with no change in lineshape.

6.2.3 Discussion

The EA spectra for polysquaraine shows many similar features to other π and σ conjugated polymers of the form outlined in chapter 3. These include a large

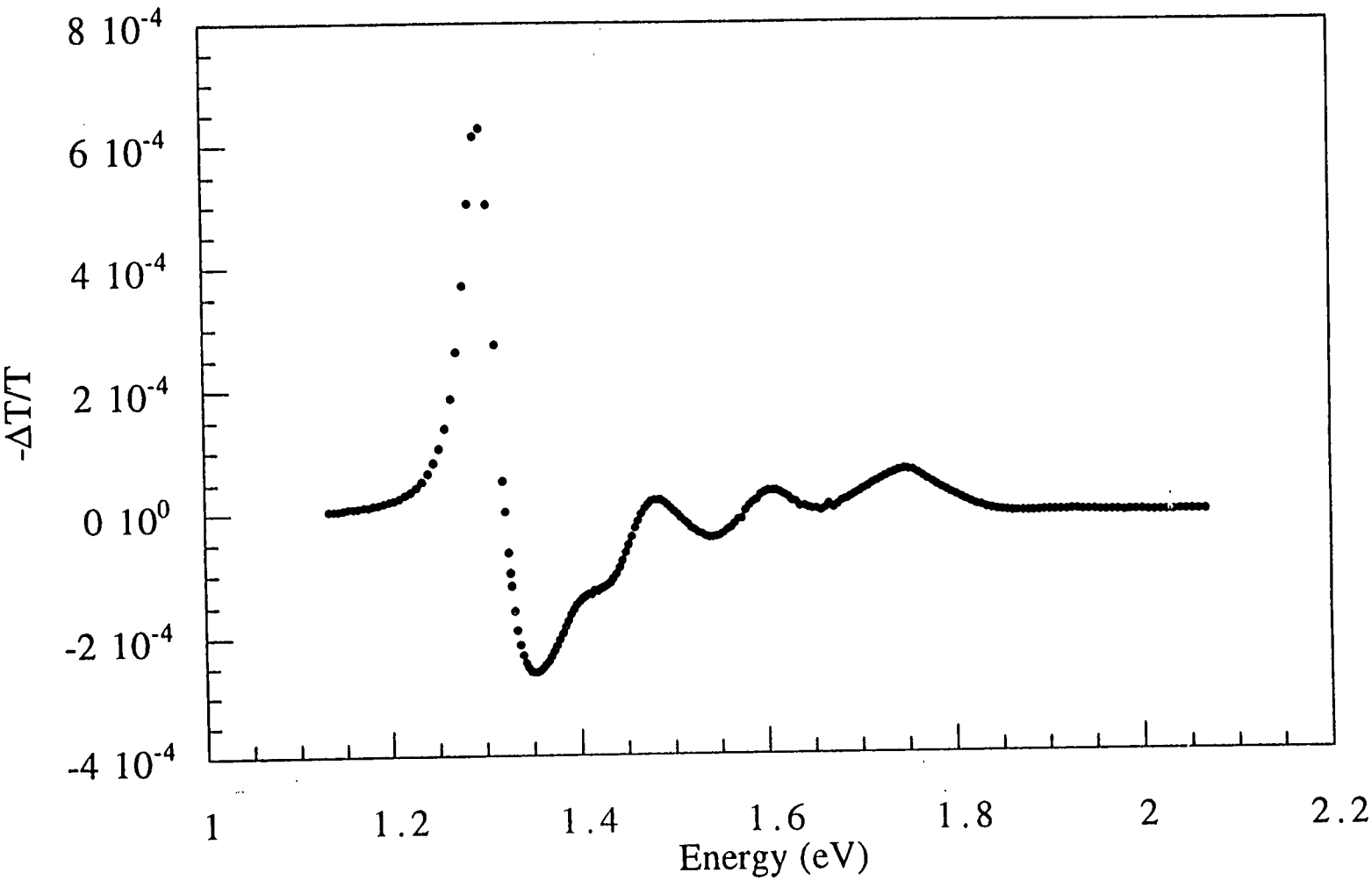

Fig. 6.14. EA signal of PS, measured at a temperature of 10 K and an applied field of 81 kV/cm

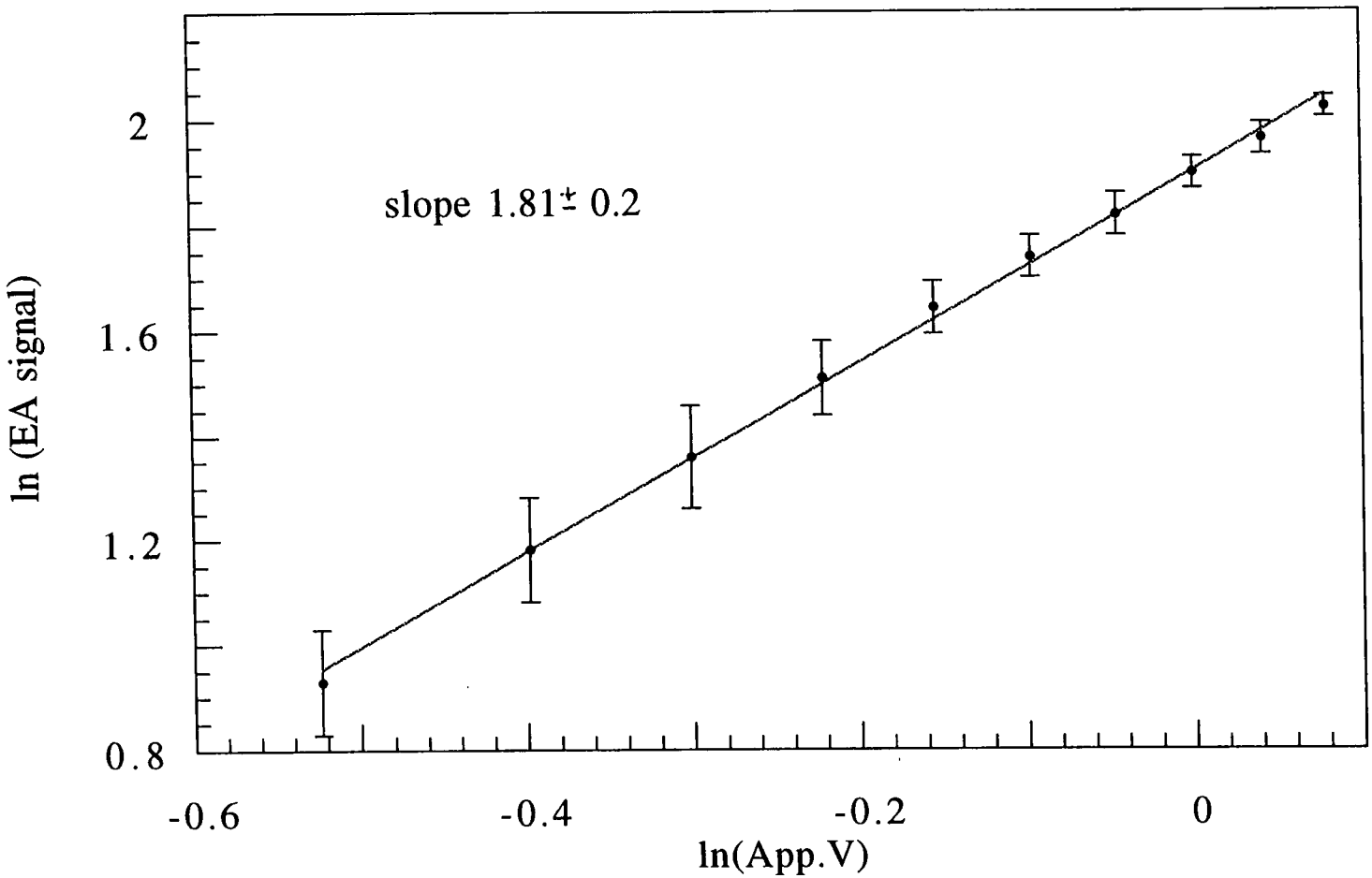

Fig. 6.15. Voltage dependence of EA signal for PS, measured at 1.3 eV

oscillation in $\Delta\alpha$ at or near the absorption band edge, and secondary oscillations that eventually decay to negligible values at higher energies. This leads to a discussion of the EA results of polysquaraine in the manner of Kawabe [14, 15], and Jeglinski [3, 16]- with the energy band structure of the form depicted in Fig.6.16. Only the singlet states will be considered, as there is no data concerning the triplet manifold of states.

This model assumes the system to be best described as a series of short chains of conjugated polymer, separated by topological defects caused by disorder - as described in chapter 3. The first one-photon allowed optical transition is to a $1B_u$ exciton with the 'conduction' band lying at higher energies, and various A_g states - not normally one-photon optically allowed - lying in between. The exact ordering of these states is indeterminate, for example whether the $2A_g$ state lies above or below the $1B_u$ exciton state, especially considering the unusual band curvature predicted for the ground state of this particular polymer. Despite this curvature, it is thought that the energy level scheme of the form shown in Fig.6.16 with the associated model for the origin of the EA signal as desribed in chapter 3 should be applicable in the discussion of the EA signal of polysquaraine.

The EA spectrum is compared with first and second derivatives of the absorption spectrum in Figs.6.17 and 6.18 and a combination of the two in Fig.6.19. The combination of the first and second derivatives (in a ratio 2:3 respectively) is observed to give the best fit. The combination of the derivatives and the EA data correspond closely up to 1.33 eV, encompassing the large peak at 1.3 eV. In the framework of the afore mentioned model this peak corresponds to the Stark shift of the $1B_u$ exciton. At higher energies the curves have the same general shape - though the oscillatory structures due to electron-phonon interactions have been shifted. The reason for this shift is as yet unclear - though, as mentioned in chapter 3, the presence of such a shift has been noted for other materials. Despite this shift the

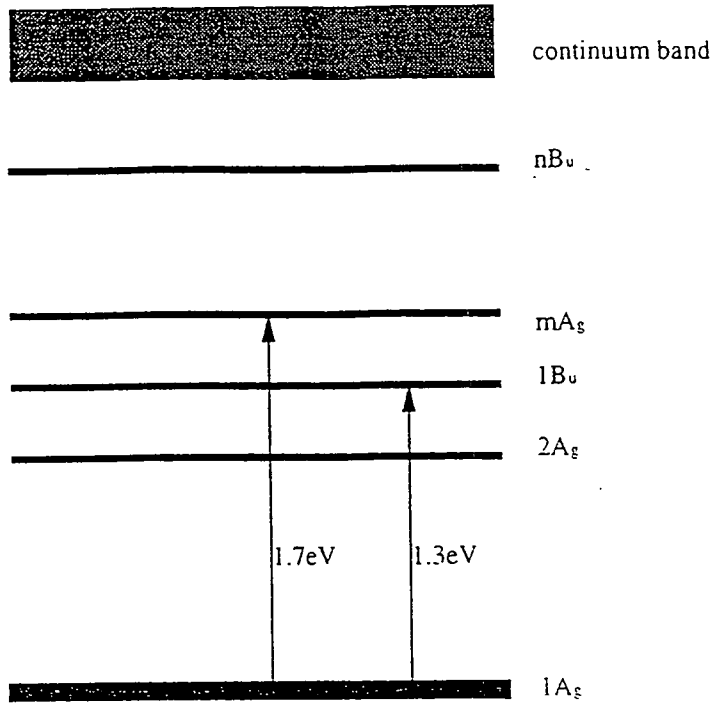

Fig. 6.16 Suggested energy level diagram for polysquaraine.

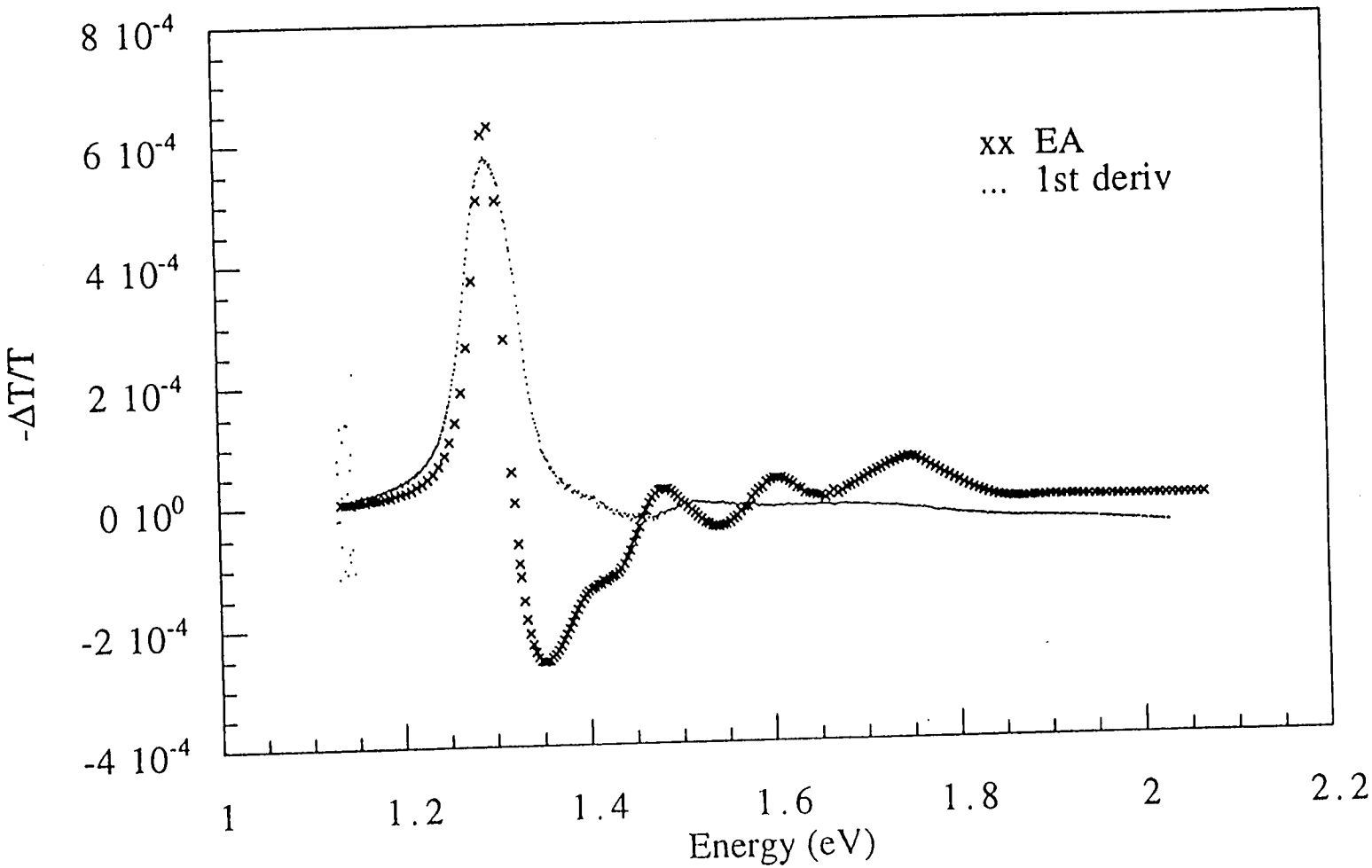

Fig. 6.17. EA of PS vs 1st derivative of linear absorption.

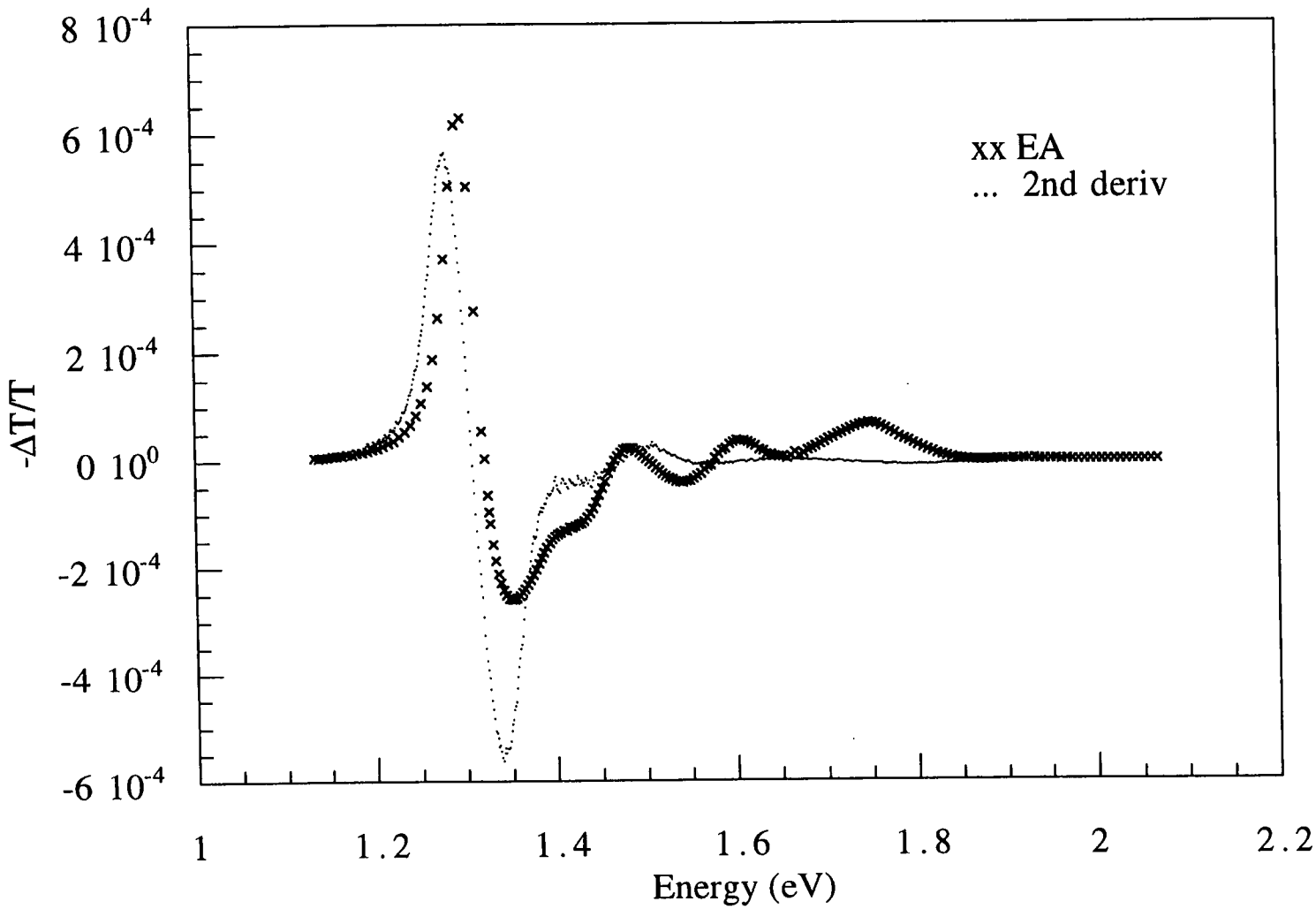

Fig. 6.18 EA PS vs. 2nd derivative of linear absorption.

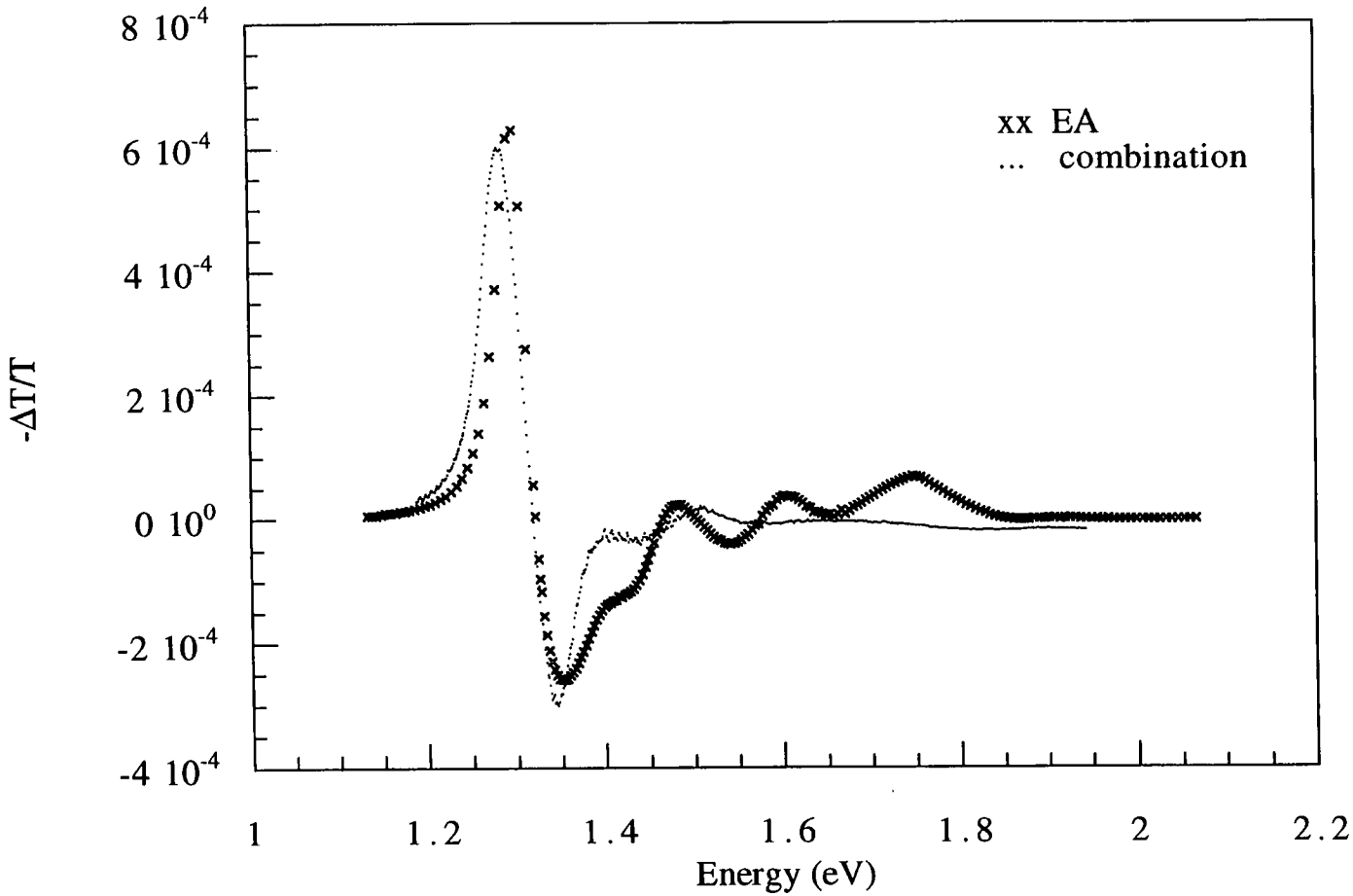

Fig. 6.19 Combination of 1st and 2nd derivatives of absortion spectra compared with EA results for PS.

vibronics are consistently separated by ~130 meV - apart from the broad signal centered at 1.75 eV which does not correspond to any vibronic structure visible in the derivative of the normal absorption spectrum. As was mentioned in chapter 3, this type of feature has been observed previously for other amorphous polymers where it was assigned to a transfer of oscillator strength to a normally one photon forbidden mA_g state that becomes weakly allowed in the presence of a symmetry breaking external field. Considering the similarity of the EA response of polysquaraine with those considered by Jeglinski *et al.* [3], it would seem reasonable to make the same assignation for the 1.75 eV feacture in polysquaraine, and is marked as such on the energy level diagram in Fig.6.16.

Included in chapter 3 was the description of the method of subtracting the EA spectrum from the lineshape of the first derivative of absorption to reveal any deviation of the experimental results from the theoretical prediction. This method allowed the identification of transitions to normally one photon forbidden states. This procedure was employed for the EA spectrum of polysquaraine, but the results showed no meaningful structure. The reason for this probably arises from the main assumption of the method, pointed out in chapter 3, that the features in the EA spectrum must transfer no oscillator strength to or from any energy levels outside the range of the spectrum measurement: there must be conservation of oscillator strength within the spectral range. It has been observed that polysquaraine has many absorption feactures in the UV, above the range of our experimental investigations. It is possible that the application of an external field causes some degree of transferal of oscillator strength from the features investigated in these experiments with those outside the experimental range, thus invalidating the above procedure.

Using the expression

$$\Delta\alpha = \partial^2\alpha / \partial E^2 (\Delta\varepsilon)^2$$

and the data at 1.3 eV for the EA of the $1B_u$ exciton an approximate value of the Stark shift ($\Delta\varepsilon$) may be calculated, though it will be an underestimate due to the neglect of higher order terms in applied field. This gives the result of a Stark shift of ~1 meV, which is comparable with that measured for PDES and *trans*-PA [16], though large in comparison with PDAs . The discrepancy is not well understood, though it has been suggested [16] that it may be due to stronger exciton dipole moment resulting from either stronger internal fields, or the degree of localisation in amorphous polymers.

During the writing of this thesis there have been reports concerning EA investigations of a squaraine monomer [17]. The absorption profile of the material has the same form as the polysquaraine reported here, though shifted to higher energies, as for OEB and EB mentioned previously. The EA response of the material also appears similar to that for PS at energies near those of the onset of absorption, though the responses do differ at higher energies. These differences include a smaller trough above the band edge in the monomer, and the apparent abscence of the peak at higher energies of the form usually ascribed to an mA_g state. These differences may be ascribed to a difference in effective conjugation length with increased chain length, and/or realted to the differences in sidechains attached to the backbone of the two materials.

6.2.4 Summary

These results imply that polysquaraine is a fully conjugated polymer whose EA response may be satisfactorily explained within the generic model of disorder

induced short conjugated segments. The main EA peak at the band edge is proposed to be due to the Stark shift of a $1B_u$ exciton. An EA feacture at 1.75 eV has been assigned to an mA_g state becoming weakly allowed in the presence of an external field. There is no evidence in the experimental data to place the $2A_g$ level below the $1B_u$. It is suggested that the schematic of Fig.6.16 may be used to describe the energy level structure of the polymer.

6.3 Comparison of the Interpretation of the Results of Emeraldine Base and Polysquaraine.

Both EB and polysquaraine have been described as A-B type polymers, as has been discussed in section 4.2 of the 'review of materials'. Emeraldine base may be considered as a regular alternation of [Be-Am-Be-Am-Be] and [Im-Qu-Im] units, where Be represents a benzenoid ring, Qu a quinoid ring, Am an amine group and Im an imine group. EB is proposed to be semi-conjugated, with the conjugation only extending over the [Im-Qu-Im] unit. Polysquaraine, however, is proposed to be fully conjugated over its regular array of donor acceptor units.

Despite this similarity of alternating chemical 'building blocks', the difference in the degree of conjugation has meant that the models used to interpret the data are very different. As mentioned at the end of chapter 3 the choice of model is governed, to some degree, by prior knowledge of the nature of the material. The semi-conjugated nature of EB, and the belief that the 2 eV photoexcitation involves some degree of charge transfer, led to the model of Sebastian and Weiser being employed to interpret the data. The fully conjugated nature of polysquaraine, and the fact that the EA spectrum of the material showed many of the generic feactures of other π-conjugated materials, led to the results being interpreted as being due to mixing of molecular energy levels due to the application of an external field.

References

1. Scully, M.S., *The Characterisation of Thin Films of Polyaniline for Gas Sensing*, M.Sc. Thesis. 1994, University of Durham.
2. Monkman, A.P. and P.N. Adams, Synth. Met, 1991. **40**: p. 87.
3. Jeglinski, S.A., Z.V. Vardeny, Y. Ding, and T. Barton, Mol. Cryst. Liq. Cryst., 1994. **256**: p. 87.
4. Hagler, T., Cem. Phys. Lett., 1994. **218**: p. 195.
5. Sebastian, L., G. Weiser, and H. Bassler, Chem. Phys, 1981. **61**: p. 125.
6. Kim, Y.H., S.D. Phillips, M.J. Nowak, D. Spiegel, C.M. Foster, G. Yu, J.C. Chiang, and A.J. Heeger, Synth. Met., 1989. **29**: p. E291.
7. Kim, Y.H., C. Foster, J. Chiang, and A.J. Heeger, Synth. Met., 1989. **29**: p. E285.
8. Duke, C.B., E.M. Conwel, and A. Paton, Chem. Phys. Lett, 1986. **131**(1-2): p. 82.
9. Phillips, S.D., G. Yu, C. Y, and A.J. Heeger, Phys. Rev. B, 1989. **39**(15): p. 10702.
10. Haarer, D. and M.R. Philpott, *Excitons and Polarons in Organic Weak Charge Transfer Crystals.*, in *Spectroscopy and Excitation Dynamics of Condensed Molecular Systems.*, V.M. Agranovich and R.M. Hochstrasser, Editors. 1983, North-Holland Publishing Company.
11. Rohlfing, F., S.J. Martin, D.D.C. Bradley, A. Eberhardt, K. Mullen, J. Cornil, and J.L. Bredas, To be published in Synthetic Metals.
12. Havinga, E.E., W.T. Hoeve, and H. Wynberg, Synth. Met, 1993. **55**(1): p. 299.

13. Havinga, E.E., W.T. Hoeve, and H. Wynberg, Polym. Bull., 1992. **49**(1-2): p. 119.

14. Kawabe, Y., F. Jarka, N. Peygambarian, D. Guo, S. Mazumdar, S.N. Dixit, and F. Kayzar, 1991. **44**(12): p. 6530.

15. Kawabe, Y., F. Jarka, N. Peyghambrarian, D. Guo, S. Mazumdar, S.N. Dixit, and F. Kajzar, Synth. Met, 1992. **49-50**: p. 517.

16. Jeglinski, S. and Z.V. Vardeny, Synth. Met, 1992. **49-50**: p. 509.

17. Poga, C., Brown, T. M., Kuzyk, M. G. and C. W. Dirk, J. Opt. Am. B., 1994. **24**: p. 531

Chapter 7

Summary

This thesis has reported optical absorption and electroabsorption measurements of three materials: polymeric and oligomeric emeraldine base, and polysquaraine.

To enable the measurements of the electroabsorption response of the materials a purpose built spectrometer was designed and constructed. Due to the small size of the effect a high resolution system was required, and to this end lock-in techniques were used, and the sample kept at low temperatures. The use of these techniques enabled detection of changes in absorption coefficient with a resolution of around $5x10^{-7}$.

The absorption coefficient spectra, necessary for the interpretation of the electroabsorption data, have been measured for each material and are in agreement with previously reported results.

The electroabsorption results for polymeric and oligomeric emeraldine base have been presented and are seen to closely resemble each other - both in magnitude and lineshape. This indicates that the photoexcitation processes occurring in the two materials have the same origin, and hence that the modelling of the polymer on the oligomer is a valid extrapolation.

A feature has been observed at 1.35 eV in the electroabsorption spectrum of the oligomeric emeraldine base. This feature is tentatively assigned to a transfer of oscillator strength to a normally one photon forbidden transition due to the application of an external field. This feature has not been observed in the polymeric emeraldine base, though if it were to occur, extrapolation of other absorption and

electroabsorption features would place the feature at 1.2 eV - below the spectral range of the apparatus.

Previous theoretical and experimental investagations of emeraldine base have suggested that the 2 eV photoexcitation produces an excited state that possess some degree of charge transfer characteristics. Taking this into account the electroabsorption spectra have been interpreted in the context of the relevant model, and an approximate value of the charge separation distance of the excited state calculated. For the 2 eV excited state this yields a separation distance of ~0.4 nm. This implies that the 2 eV photoexcitation results in the formation of an excited state that is spatialy extended over a distance greater than just one ring repeat unit. Though the results cannot conclusively be used to differentiate between the competing theories, they do imply that the photoexcitation is that of the charge transfer exciton suggested by Duke.

Using the same model for the 4 eV transition gives a charge separation distance of ~0.25 nm, which would imply the formation of an intra-ring exciton. It may be, however, that this may be the wrong method of interpreting the data, with the possibility of another perturbation mechanism, such as line broadening or transferal of oscillator strength, dominating.

The electroabsorption data for polysquaraine have also been presented. Polysquaraine is proposed to be a fully conjugated polymer, and as such the results have been interpreted in the framework of a different model. The electroabsorption spectrum shows many generic feactures of spectra of other conjugated polymers, such as a large peak at the absorption edge, followed by a trough, returning to zero with smaller oscillations on the high energy side of the peak. This has led to the spectrum being interpreted in a similar manner to that of other such polymers. An energy level diagram of the material has been proposed, which includes the

possibility of a normally one photon transition occurring at 1.75 eV. It is suggested that this transition becomes allowed due to the mixing of energy levels due to the application of an external field, resulting in a transfer of oscillator strength to this normally forbidden transition.